DEVELOPMENT OF HIGH-SPEED INTERNAL FINISHING AND CLEANING OF FLEXIBLE CAPILLARY TUBES BY MAGNETIC ABRASIVE FINISHING

By

JUNMO KANG

A DISSERTATION PRESENTED TO THE GRADUATE SCHOOL
OF THE UNIVERSITY OF FLORIDA IN PARTIAL FULFILLMENT
OF THE REQUIREMENTS FOR THE DEGREE OF
DOCTOR OF PHILOSOPHY

UNIVERSITY OF FLORIDA

2012

I dedicate this to my family.

ACKNOWLEDGMENTS

I would like to thank my family for giving me the chance to study in the US and I would like to thank my advisor, Dr. Hitomi Yamaguchi Greenslet, for her great research guidance and total support. Moreover, this work would not have been possible without her and all the members of the MTRC (Machine Tool Research Center). Therefore, I really would like to thank them with sincerity. I would also like to thank the Creganna-Tactx Medical Company for providing the workpieces, the University of Florida Research Foundation (Gatorade), the Office of Research at the University of Florida for travel grants, and the 2011-2012 Society of Manufacturing Engineers (SME) Education Foundation (E. Wayne Kay Graduate Scholarship) for their support and encouragement. Special thanks to Mr. John Greenslet for his kind assistance with my written work.

TABLE OF CONTENTS

page

LIST OF TABLES

LIST OF FIGURES

Abstract of Dissertation Presented to the Graduate School
of the University of Florida in Partial Fulfillment of the
Requirements for the Degree of Doctor of Philosophy

DEVELOPMENT OF HIGH-SPEED INTERNAL FINISHING AND CLEANING OF FLEXIBLE CAPILLARY TUBES BY MAGNETIC ABRASIVE FINISHING

By

Junmo Kang

December 2012

Chair: Hitomi Yamaguchi Greenslet
Major: Mechanical Engineering

Tube-shaped medical components such as catheter shafts, coronary stents, and biopsy needles should be precisely designed and manufactured, since surface imperfections can cause severe—possibly lethal—implications for patients. Therefore, internal machining (surface and edge finishing) is increasingly in demand for these devices, but as the tube diameter decreases, the more difficult the internal finishing becomes.

Magnetic abrasive finishing (MAF) has been studied to accomplish the internal finishing of capillary tubes. The MAF process can produce a smoothly finished inner surface of tubes by means of relative motion between magnetic abrasive and tube inner surface. To achieve successful internal finishing of capillaries, controlling the magnetic abrasive motion and lubricant inside the tube is critical. The magnetic abrasive is suspended in magnetic field generated by the magnet located outside the tube. The magnetic field is controlled by the geometry and arrangement of the magnets as well as the geometry of pole tip attached to the magnets. In the case of flexible capillary tubes, deburring the edges of laser-machined slots and removing the re-solidified material caused by laser machining process on the inner surface are required in addition to the

internal surface finishing. The burrs are obstacles to magnetic abrasive, hindering the generation of smooth relative motion against the tube inner surface. The tube also easily deforms during the finishing process due to its flexibility. These factors increase the difficulty of achieving a smooth internal finish on flexible capillary tubes.

This research develops a new finishing method featuring the use of a multiple (double) pole-tip system with a special magnetic tool. This method produces smooth inner surfaces of capillary tubes and finishes multiple areas simultaneously to improve finishing efficiency. This study explains the processing principles of newly developed finishing method and describes the surface finishing characteristics. The finishing mechanism is also thoroughly investigated and described in both straight and flexible capillary tubes.

CHAPTER 1
INTRODUCTION

1.1 Background

1.1.1 Introduction of Flexible Capillary Tubes and Necessity of Internal Cleaning

Capillary tubes are used for refrigerant conduction in industrial refrigerators [1], in needles for biopsy procedures, and in precision analytical instruments. Flexible capillary tubes are widely used for medical applications such as coronary stents and catheter shafts. The components for medical applications are remarkably precise and sensitive, but can be fatal to patients when manufactured with any defects or misalignment during installation [2, 3]. Medical stents are implanted into arteries in order to expand blood vessels and guarantee blood flow, and catheter shafts guide other medical components into the human body. Currently, these devices are made of 304 and 304L stainless steels, which are widely available, cost efficient, have good corrosion resistance, and have high machinability and weldability, which allows them to be drawn and formed into the required long, fine tubes. (304L is good for welding because it has 0.03 % (max) carbon content, which eliminates carbide precipitation due to welding [4], whereas 304 has a higher of carbon level (0.08 % max)). The minimum tube size for medical usage is 0.005” (0.127 mm) outer diameter (OD) and 0.00325” (0.082 mm) inner diameter (ID). To fit into the human body, the components must have inherent flexibility, which is accomplished by numerous laser-etched slits into the tube wall by laser micromachining processes [5, 6].

A hypotube, a critical component of the balloon catheter, is a long metal tube with micro-engineered features along its length. This tube enables a cardiologist to navigate the vascular anatomy to the site of the clogged artery and ensure accurate placement of

the balloon and stent. To achieve optimal performance, the factors pushability, torqueability, kink, and trackability of the tube need to be considered during design. Pushability is the ability of the shaft to transmit energy from one end of the catheter to the other, and this can be improved by increasing the wall thickness of tube, reducing its overall length, or increasing the stiffness of the material. Torqueability is the ability of the shaft to transmit a rotational displacement along the length of the shaft, and it can be improved by increasing the wall thickness or shear stiffness of the material. A measure of a shaft's ability to maintain its cross-sectional profile during deformation is known as kink. A bending or compressive force on shaft causes kink failure. Trackability is the ability of a shaft to travel or track through tortuous anatomical structures. Trackability is influenced by the flexibility of the shaft and can be improved by reducing the shaft's outer diameter or decreasing the material's elastic modulus. These factors are controlled by patterns of multiple slits made in the tube walls by the laser micromachining process [7].

Laser micromachining processes are generally used for cutting, drilling, marking, texturing, welding, and developing for medical (stents, shafts), optical (micro-lens), automotive (fuel injector nozzle, high-pressure fuel filter), aerospace (nano-satellite) and microelectronics industry (silicon micromachining) applications. Laser micromachining processes cut material by melting the workpiece with thermal energy and are capable of making small holes and slits in capillary tubes [8, 9]. These multiple slits in the tube wall increase the flexibility of the tube, as is desired in components such as catheter shaft.

During the laser machining process, some molten material splashes inside the tube, solidifies, and adheres to the inner surface or cut edges and re-solidified material

forms hard heat-affected burrs [10]. The burrs cause serious problems in manufacturing, and the quality of precision parts can be evaluated by the surface and edge quality; therefore, they must be removed completely in a subsequent process to allow the proper operation of components. The existence of burrs in parts deteriorates the accuracy and the performance of the products. However, it is difficult to use existing conventional techniques to remove the hard heat-affected burrs and re-solidified material that project inside the capillary tubes.

1.1.2 Current Techniques for Internal Machining of Tubes and Magnetic Abrasive Finishing

For internal deburring of flexible capillary tubes, conventional deburring tools cannot be easily introduced or adequately controlled inside flexible capillary tubes that have inner diameters around 1 mm and incorporate micro machined multiple slits. Chemical and micro-abrasive blasting processes are commonly used for deburring flexible tubes [11-13]. However, it is difficult to drag deburring tools, including chemical reagents and abrasive media, inside long flexible capillary tubes. It is difficult to remove the burrs completely even using these nontraditional techniques. Moreover, the removal of solidified material adhered to inner tube surfaces and cut edges necessitates machining harder material, which is a result of the laser-induced heat-affected zones. In the case of internal surface finishing, the variations in the as-received peak-to-valley surface roughness can be several micrometers. In contrast, the burr height can be up to 100 μm, and therefore the deburring process requires greater material removal than the internal surface finishing [14].

In surface finishing, traditional machining process leaves impurities such as rust spots, scale, and non-metallic inclusions on the grooves of the machined surface, which

are unacceptable for proper performance [15]. To reduce these defects, nontraditional finishing methods such as electropolishing [16-19], known as electrochemical polishing or electrolytic polishing, has been considered and developed.

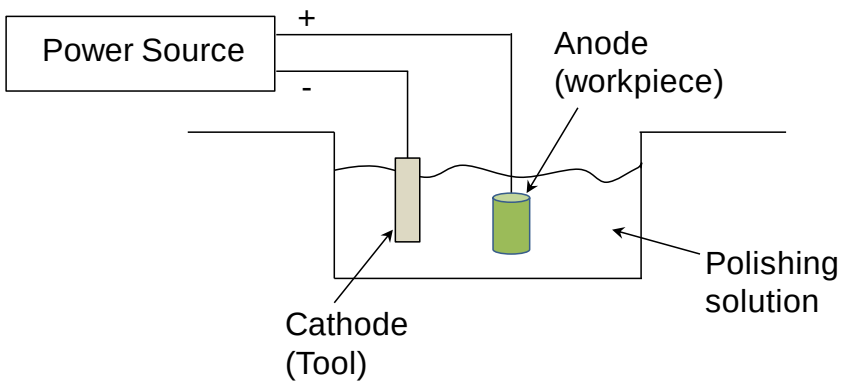

Figure 1-1. Schematic of electropolishing process

Electropolishing is a chemical surface finishing technique applied to clean metallic surfaces to reduce micro-roughness. The process depends on electrolysis, which uses a flow of current and a solution comprised mostly of sulphuric and orthophosphoric acids as an electrolyte. This process removes metal from a submerged workpiece by passing an electric current through the electrolyte. It can produce a smooth, bright, and reflective surface that exhibits superior corrosion resistance when the workpiece (anode) and tool electrode (cathode) are electrically charged (Figure 1-1). Electropolishing is suitable for the polishing of both complex shapes and hardened materials, which are difficult to machine mechanically because the electrode and the workpiece are not in contact with each other [15, 20]. Electropolishing produces mirror-like surfaces on metals as well as being used for deburring by electrolyte which removes material from peaks and raised area faster than lower areas. However, disposal of the chemical reagents after the process can contribute to the destruction of

the environment. In the case of capillary tubes, it is difficult to introduce the electrolyte into the tubes. Therefore, an alternative process is desired. Recent developments in nonconventional machining process technology have enabled automated micro deburring and surface finishing for precision parts. They include ultrasonic vibratory finishing [21], ultrasonic cavitation deburring [22], thermal energy deburring [23, 24], abrasive flow machining [25-27], laser deburring [28], magnetic barreling [29], and magnetic abrasive finishing [30-33]. However, for finishing the inner surfaces of capillary tubes, only abrasive flow machining and magnetic abrasive finishing are potentially viable processes.

Abrasive flow machining performs deburring of the small holes of diesel injection nozzles made by drilling, electrodischarge machining, or laser machining. The pressurized media (a mixture of a polymer carrier, lubricant, and abrasive) pass through the holes and finish the inner surfaces, as well as remove the burrs. However, as long as the abrasive behavior is controlled by media pressure at the end of the hole, the pressure drop along the length of the hole will impede the expansion of the process application [25-27]. Although this process is proper for surface finishing of capillary tubes, it may cause difficulties for internal deburring of flexible capillary tubes due to the significant pressure leakage from the slits.

In internal finishing by magnetic abrasive finishing, the abrasive mixed with ferrous particles is introduced into a tube and pushed against the inner surface of the tube by magnetic force in the presence of a magnetic field. The smooth relative motion of the magnetic abrasive against the inner surface results in material removal and successful surface finishing when the tube rotates. Manipulating the magnetic field

along the tube axis direction drags the magnetic abrasive to target finishing area and achieves the internal finishing of long tubes [33]. A study of the internal finishing of straight capillary tubes has demonstrated successful surface finishing of tubes with inner diameters down to 400 μm [34]; however, the machining rate of this process was low. The internal deburring and finishing efficiency of flexible capillary tubes have yet to be investigated.

1.2 Development of Internal Cleaning and Finishing Process for Flexible Capillary Tubes using Magnetic Abrasive Finishing

The objectives of this study are to develop a new internal surface and edge finishing method using the magnetic abrasive finishing process and to apply the process to flexible capillary tubes. In order to achieve these goals, three specific aims are proposed:

1. Determine fundamental finishing characteristics and mechanism of flexible capillary tubes in magnetic abrasive finishing.
2. Develop a new finishing method using a heat-treated metastable austenitic stainless steel tool in combination with multiple pole tips.
3. Design and develop a high-speed finishing machine, and determine finishing characteristics and mechanisms of both straight and flexible capillary tubes using the multiple pole-tip system.

To achieve successful finishing of capillaries by magnetic abrasive finishing, controlling the magnetic abrasive and lubricant at the finishing area inside the capillary tube is critical. This can be accomplished by controlling the magnetic field generated by the permanent magnets through the modification of the magnetic pole-tip geometry. When the tube diameter decreases, the width of pole tip along the tube axial direction is shortened. This causes a shortened default finishing length and results in increased processing time. Moreover, in deburring of flexible capillaries, the burrs on the edge

impede the movement in the tube axial direction of the particles introduced into the tube. This limits the pole feed length and reduces finishing efficiency. Moreover, to remove the hard material on the machined edge (the areas hard to reach by conventional methods), a large-sized diamond abrasive is required to enhance the material removal rate [14], and magnetic tools are applied inside the tube to strengthen the magnetic force using the volume of ferrous tool and to keep the flexible tube straight during the process at the finishing area [33]. Based on these methods, a new finishing process to have multiple processing areas for a single tube and to process multiple tubes simultaneously has been considered to improve the processing rate per tube [35-38]. It is called a multiple pole-tip system. To realize this concept, a partially heat-treated metastable austenitic stainless steel tool has been fabricated. The roles of ferrous tools, the effects of their geometric and magnetic properties, and the dynamic behaviors on finishing characteristic for capillary tube finishing are studied.

Another key factor for improving the processing rate is to increase the tube rotational speed. Preston introduced an empirical formula for determining how quickly material is removed from a surface [39]. According to Preston's equation, the material removal rate is a function of the finishing pressure or force per unit area, relative speed between the tube and abrasive, and the Preston coefficient, which is determined by the finishing system (e.g., by the abrasive type and size, and friction coefficient between the abrasive and tube). The magnetic force is the main parameter determining the finishing pressure. The relative speed between the tube and abrasive is controlled by the combination of tube rotational speed and pole reciprocation speed in the direction of the tube axis. The higher the relative speed, the longer the theoretical sliding distance of the

abrasive against the tube surface. A previous study has shown the feasibility of high-speed finishing machine that can rotate the tube up to 30000 min^{-1} [34]. A new high-speed machine has been designed and manufactured with a spindle speed up to 30000 min^{-1}. The developed machine has shown its finishing capability successfully, and the effects of tube rotational speed on abrasive motion and finishing characteristics using capillary tubes are studied. For further improvement of finishing efficiency, the multiple pole-tip system for the high-speed machine is proposed and implemented.

Based on high-speed finishing experimental results, the finishing characteristics and mechanism using a high-speed multiple pole-tip system for straight and flexible capillary tubes will be studied and clarified.

CHAPTER 2
INTERNAL FINISHING PROCESS USING MAGNETIC ABRASIVE FINISHING

2.1 Magnetic Abrasive Finishing

Magnetic abrasive finishing is defined as a finishing process that removes material in the presence of a magnetic field. This process was invented during the 1930s but not further developed until after the 1960s [31, 40], and it has been developed as a new finishing technology in the last decade and still a useful and viable finishing method. In the last decade, the magnetic field-assisted finishing process has garnered much attention; it is widely used in the field of precise and sensitive instrument manufacturing such as for medical, optics, electrical and engine components [41-45].

The magnetic field-assisted finishing process is based on the use of slurry consisting of ferrous particles mixed with fine abrasive particles (diamond, aluminum oxide (Al_2O_3), silicon carbide (SiC), cubic boron nitride (CBN), etc.). These non-metallic abrasives have hard sharp edges with irregular shapes. This mixture combines along the lines of the magnetic field (generated by poles attached to magnets) and forms a flexible magnetic abrasive brush. The flexibility of the brush can be altered by adjusting the magnetic field generated by a permanent or alternating magnet system, the brush performs like a multi-point cutting tool for finishing process because it has the ability to modify itself according to surface contours [46,47]. In a magnetic field strong enough to overcome the inherent friction between the abrasive and a target surface, the motions of the abrasive brush finish the surface. In this process, ferromagnetic particles sintered with abovementioned non-metallic abrasives (diamond, Al_2O_3, SiC,or CBN) and such particles are called magnetic abrasive.

In a magnetic field, magnetic flux flows unimpeded through nonferrous workpiece material, and ferrous material—a component of the magnetic tool—is suspended by magnetic force. It is possible to influence the magnetic tool motion by controlling the magnetic field, thus enabling the finishing operation to be performed not only on easily accessible surfaces but also on areas that are hard to reach by conventional mechanical techniques.

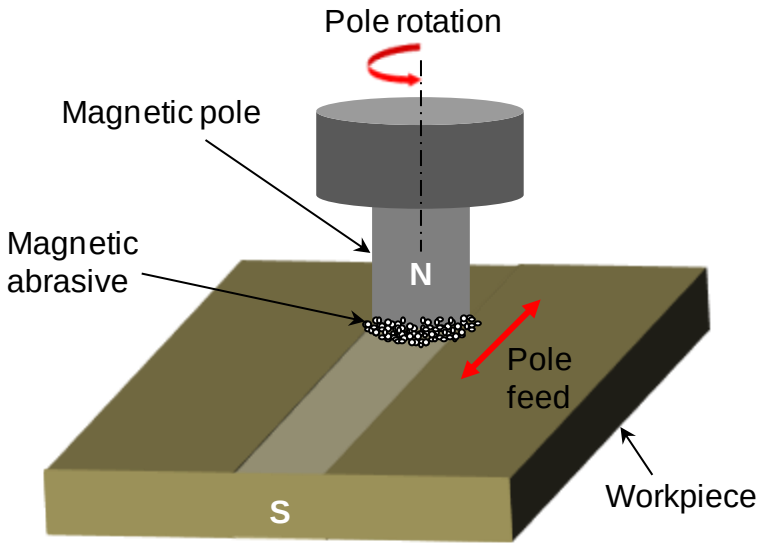

Figure 2-1. Schematic of the processing principle for planar magnetic abrasive finishing

Figure 2-1 shows a schematic of the processing principle for planar magnetic abrasive finishing process where the finishing action is generated by application of a magnetic field across the gap between the surface of the workpiece and a rotating magnetic pole. The magnetic field generated by the magnetic pole forms the (self-adaptive) magnetic abrasive brush, and the normal force acting on the workpiece surface, in combination with pole rotation, causes material removal (in the form of chips) and gradually improves the surface roughness with pole feed.

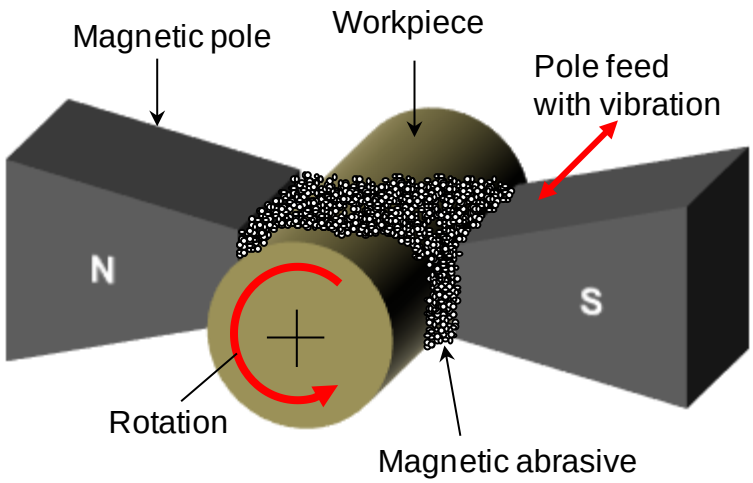

Figure 2-2. Schematic of the processing principle for cylindrical magnetic abrasive finishing

Figure 2-2 shows a schematic of the processing principle for a cylindrical magnetic abrasive finishing process. The magnetic abrasives are joined magnetically between magnetic poles (N and S) along the lines of magnetic force and form flexible magnetic brush. When the rotating cylindrical workpiece is introduced into the magnetic field between the poles, surface and edge finishing are performed by the magnetic abrasive brush [31].

The magnetic abrasive finishing process has certain advantages which make it an efficient process:

1. The abrasive brush is flexible to conform to workpiece surface and hence complex surfaces can be finished.
2. The finishing pressure can be controlled by varying the magnetic field (current in the case of electromagnet and air gap in the case of permanent magnet).
3. The finishing tool is independent.
4. In electromagnet system, the disposal of used abrasive is automatic and new abrasive is fed to the finishing area by turning the current in the coils on and off.
5. No scattering of abrasives due to the magnetic field.
6. Less consumption of abrasive.

2.2 Processing Principle and Parameters of Internal Finishing of Straight Tube

Internal finishing by MAF has two system configurations. One is the rotating-tube-stationary-pole system [33], and the other is the rotating-pole-stationary-tube system [41]. These systems are chosen to suit the workpiece geometry. The former system is suitable for short workpieces that are rotatable at high speeds. The latter system was developed for non-rotatable workpieces, which have long, large or non-rotationally-symmetric geometry, such as elbows, bent tubes, and slender tubes [48]. Since the workpieces provided for this study were relatively short (approx. 100 mm long) and rotatable at high speeds, the rotating-tube-stationary-pole system was selected.

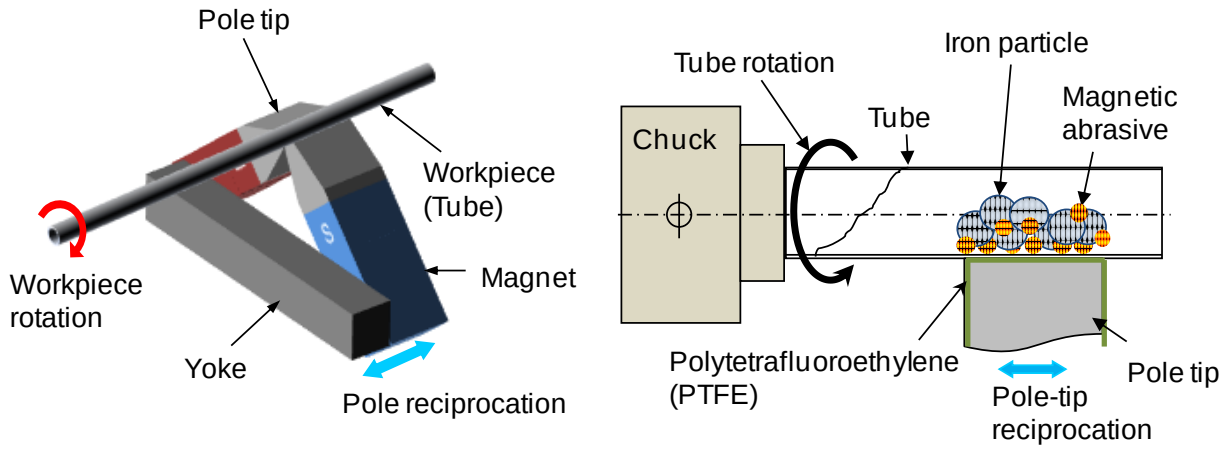

Figure 2-3. Schematic of processing principle of internal finishing of straight tube using rotating-tube-stationary-pole system

Figure 2-3 shows a schematic of the internal finishing process using the rotating-tube-stationary-pole system for tubes. The desired magnetic field in the finishing area is generated by permanent magnets attached to a steel yoke. In the case of capillary tubes, to concentrate the magnetic field in specific area, a tapered steel pole-tip is used. In the presence of a magnetic field, magnetic abrasive introduced inside the workpiece

is magnetized, and it is pushed against the workpiece inner surface by magnetic force. In a non-uniform magnetic field, the magnetic force *F* acting on magnetic abrasive can be described using following equation [36],

$$\vec{F} = V\chi H \cdot \mathrm{grad}\, H \qquad (2\text{-}1)$$

where *V* is the volume of the magnetic abrasive, χ is the susceptibility, and *H* and grad *H* are the intensity and gradient of the magnetic field, respectively.

If the tangential component of the magnetic force acting on the magnetic abrasive is larger than the friction force between the magnetic abrasive and the inner surface of the workpiece, the magnetic abrasive shows smooth relative motion against the inner surface when the workpiece is rotated at high speed [34]. Manipulating the poles along the workpiece axis causes the magnetic abrasive to move in the axial direction following the pole motion, effectively finishing the inner surface and removing burrs in the case of flexible capillary tubes.

The clearance between the pole tip and tube should be set at approximately 0.1 mm; this can be accomplished by using polytetrafluoroethylene (PTFE) tape on the pole-tip surface. In the case of capillary tube case, magnetic force attracts the tube towards pole tips, and they are always contacted each other. This tape also prevents damage to the outer surface of workpiece from the pole tip during rotation. In addition, in the case of flexible capillary tubes which have spiral slits, rotating the tube in the direction in which the motion itself acts to close spiral slit is chosen. This helps not to lose the abrasive and lubricant from the slits. As the tube is rotated, the mixture of ferrous particles exhibits relative motion against the tube inner surface, and thus material is removed from the tube surface. The default finished length (the finished

length without pole-tip motion) is determined by the pole-tip width in the tube axial direction; motion of the pole along the tube axis extends the finished area.

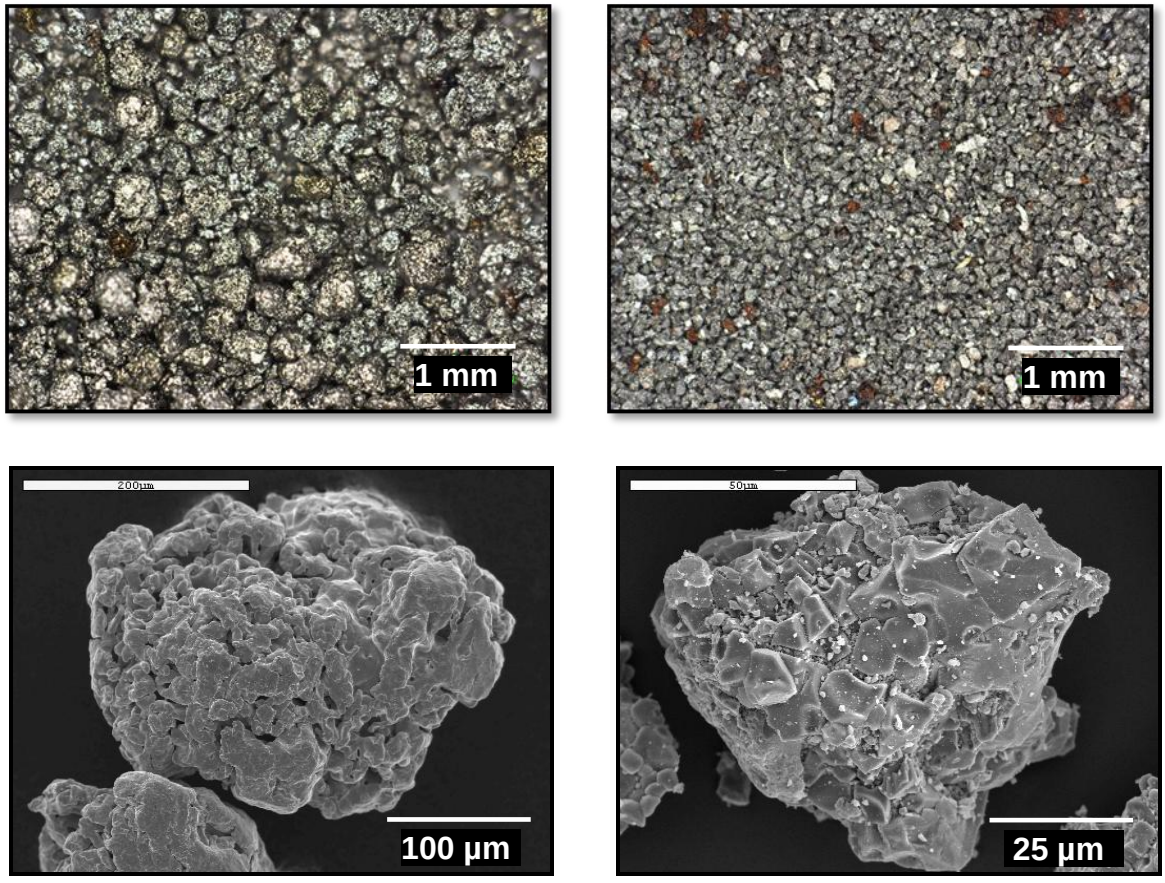

A Iron particle B White alumina magnetic abrasive

Figure 2-4. Microscopy and scanning electron microscopy of A) iron particle (dia. 150~300 µm) and B) white alumina (WA) magnetic abrasive (mean dia. 80 µm, aluminum oxide (Al_2O_3): ≤10 µm).

This process controls magnetic abrasive chains where the abrasive mixtures conform to the contour of the surface to be finished. The mixture of iron particles (Figure 2-4(A)) and aluminum oxide magnetic abrasive (Figure 2-4(B)) is called mixed-type magnetic abrasive and is introduced into the tube. The magnetic abrasive is pushed by iron particles and held firmly against the inner surface of workpiece while short reciprocating motions are applied in the workpiece axial direction. The mixed-type

magnetic abrasive contacts and acts upon the surface. When removing the surface defects such as scratches, lay lines, and other disparities, these defects on the surface are corrected to a limited depth of few microns [49]. The material removal rate depends on the relative motion of magnetic abrasive, which depends on the magnetic force, workpiece rotational speed, abrasive size and type, working clearance, workpiece material, feed rate, and lubricant.

To achieve smooth relative motion of the mixed-type magnetic abrasive, it requires that the mixed-type magnetic abrasive must be kept in a stable configuration during rotation in the finishing area against the inner surface of the tube. This relative motion determines the material removal and results in successful surface finishing. To keep the mixed-type magnetic abrasive in the finishing area, a strong magnetic force is required, which is determined by the magnetic field generated by magnet. Based on the magnetic force equation (2-1), magnetic force acting on the abrasive depends on the volume of ferrous particles. Due to the limited inner space in capillary tubes, the size of iron particles has a maximum constraint and the volume of mixed-type magnetic abrasive must be close to 43 vol% of the tube for efficient finishing [34].

The tube rotational speed also affects smooth relative motion of the magnetic abrasive against the inner surface. Preston’s equation predicts that material removal increases with increased rotational speed. However, at high rotational speeds, lubricant can be easily spun out from the finishing area due to centrifugal and frictional forces. The lubricant encourages the mixed-type magnetic abrasive to congregate uniformly on the inner surface of the tube at the beginning of the finishing process. Moreover, lubricant helps smooth relative motion of particles against the inner surface and

removes the heat, chips, grain fragments, and dislodged grains from the surface during the finishing process. Therefore, a lack of lubricant deteriorates the relative motion and material removal.

The overall finishing efficiency of the process is dependent on the default finishing length, which is determined by the width of the pole tip along the tube axis direction. The magnetic flux density is stronger at the edges of pole tip because of edge effects. This condition causes powder to be distributed non-uniformly on the finishing area because it gives ferrous mixtures a higher tendency to collect towards one edge (usually the edge closest to where the mixture is introduced) instead of uniform distribution in the finishing area. As a result, the abrasive relative motion is obstructed and this results in unsuccessful surface finishing. This causes the pole-tip width to be shortened in capillary tube finishing and increases the processing time.

Compared to a surface finishing process, an internal deburring process requires a higher material removal rate. This requirement is met by increasing the intensity of the magnetic force acting on the magnetic abrasive or employing larger abrasive sizes. In this study, in order to increase material removal with a strengthened magnetic force, (non-ferrous) diamond abrasive is used, and a solid ferrous rod is substituted for a portion of the ferrous particles.

CHAPTER 3
PARAMETERS AFFECTING ON FINSIHNG CHARACTERISTICS IN FLEXIBLE CAPILLARY TUBE FINISHING USING A SINGLE POLE-TIP SYSTEM

3.1 Processing Principle of Flexible Tube Finishing

A schematic of internal machining process of flexible capillary tubes using a rotating-tube-stationary-pole system is shown in Figure 3-1. The desired magnetic field in the finishing area is generated by permanent magnets attached to the steel yoke (Figure 2-2). Since laser-machined burrs have various shapes and heat-affected zones, sharp and hard cutting edges combined with strong magnetic force are required to remove the burrs. Increased magnetic force using large-sized ferrous tool contributes to the removal of material adhered to the tube inner surface and burrs along the slits (shown in Figure 3-2(A) and (B), burr heights: up to 90 μm). The internal volume of the capillary tube is limited, so there is an upper constraint to the size of the introduced ferrous materials. In an attempt to encourage the cutting action, large-sized diamond abrasive (4-8, 20-40, 50-70 μm diameter) was introduced. A mixture of iron particles, magnetic abrasive, and diamond abrasive is attracted to the finishing area by the magnetic field generated by permanent magnets. The sizes of these particles must be greater than the slit widths to prevent leakage. Manipulating the poles along the tube axis causes the mixture to follow the pole motion and move in the axial direction, finishing the inner surface and removing the burrs. The methods without the modification of finishing unit to adjust the magnetic field are to change magnetic properties or geometry of the magnetic abrasive [44,46,50,51], or to change magnetic properties, geometry, or concentration of magnetic tools (such as ferrous particles, a ferrous rod, or permanent magnet) inserted with magnetic abrasive or conventional abrasive slurry [52-57].

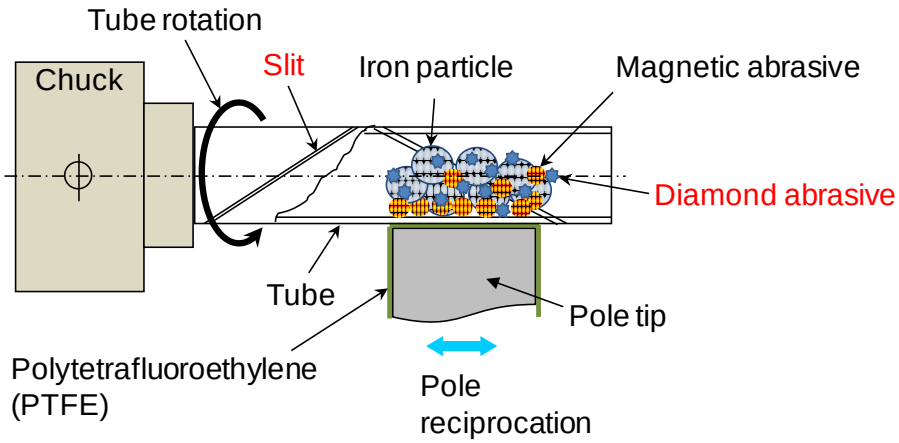

Figure 3-1. Schematic of processing principle of internal finishing of flexible tube

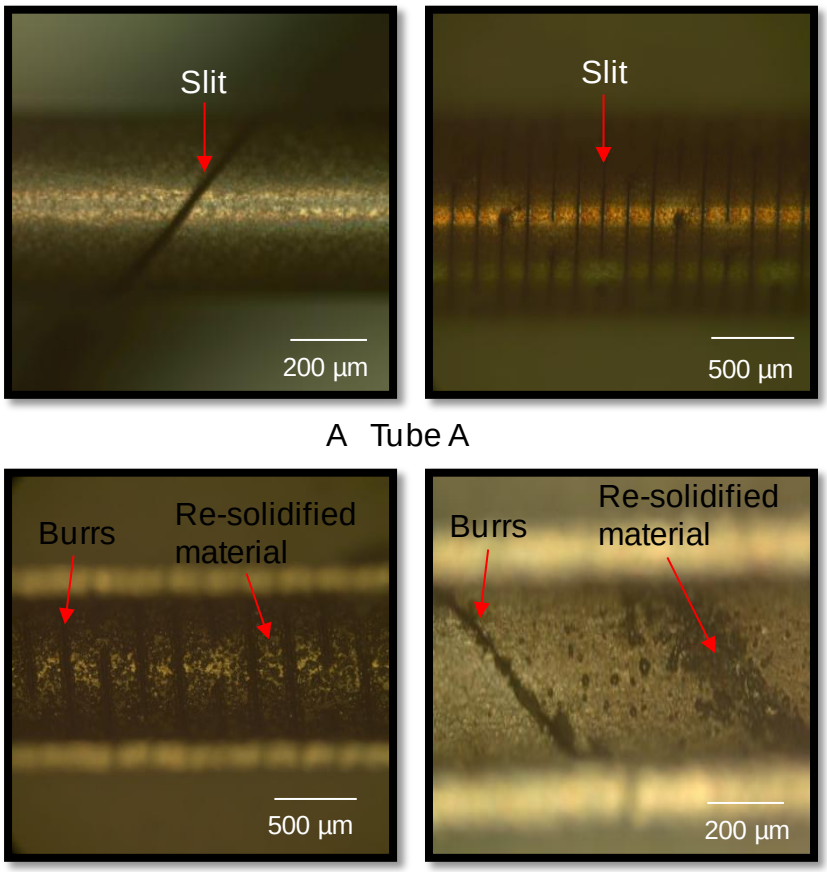

Figure 3-2. Exterior and interior microscopy of laser-machined flexible capillary tubes, Tubes A and B

In this study, two different flexible capillaries are prepared. In Figure 3-2, exterior and interior microscopy of tube A and B which have different diameters and slit patterns

machined with laser on the body are shown. Tube A has 0.58 mm OD, 0.42 mm ID and spiral slit pattern on it. The slit has 12 μm distances and this can be wider or narrower according to the tube rotational direction and it affects total tube length. Tube B has a 1.36 mm OD and 1.02 mm ID, it has more numbers of slit which make the tube more flexible than tube A. In Figure 3-2, the edges have burrs; moreover re-solidified material caused by thermal energy during laser machining exists between the slits.

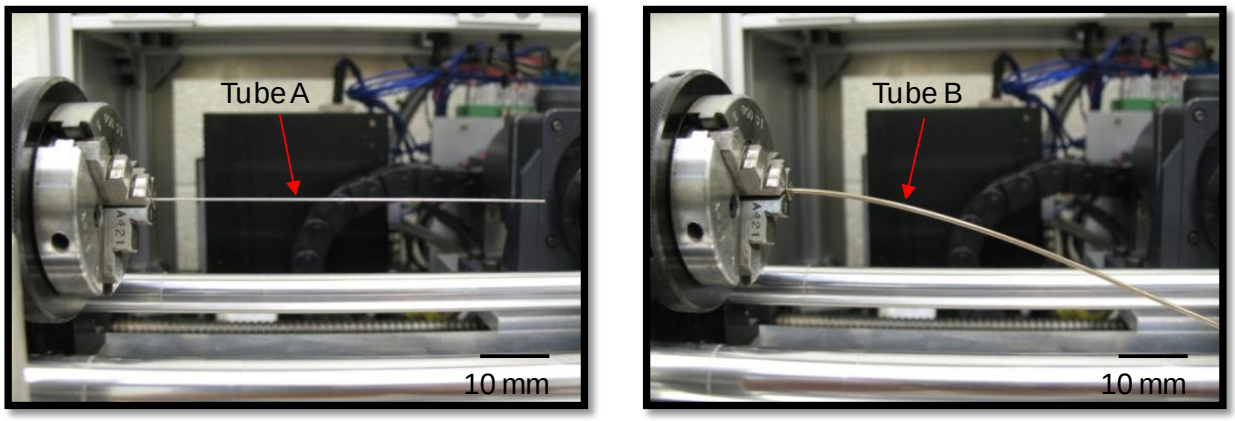

A Tube A B Tube B

Figure 3-3. Photographs of tubes chucked on the finishing spindle with different slit patterns, Tubes A and B (Photograph courtesy of Junmo Kang)

Figure 3-3 is photographs of tube A and B chucked on the finishing spindle respectively. One end of tubes is chucked on finishing unit while other end is free. Tube A with a few slits can be treated as a rigid tube as shown in Figure 3-3(A), and more slits encourage the tube flexibility as shown in Figure 3-3(B), it becomes no longer to treat it as a straight rigid tube. Even the other end is supported flexible jig, tube fluctuates during it rotates at high speed when the tube length gets longer. Moreover, abrasive and lubricant can leak easily from the slits. Without critical control of magnetic abrasive and lubricant at the finishing area, it is unfeasible to produce the smoothly finished surface and the deburred edges.

The internal surface and edge finishing experiments with tube A (Figure 3-2(A)) have been conducted focusing on mostly diamond abrasive size and processing time. Due to small (less than 10 μm) cutting edges embedded in magnetic abrasive, it has difficulties to remove material of the burrs inside the tube which is not suitable. To remove large-sized burr (50-90 μm height), diamond abrasives are introduced during the finishing process. In case of tube B (Figure 3-2(B)), even the tube is allowed to introduce more ferrous particles inside, the laser-machined slits are closer each other, and they are formed along to cutting direction (same as tube rotational direction), which makes the difficulties to be removed. Therefore, two kinds of magnetic tools (steel rod and stainless steel rod) have been considered to increase the magnetic force acting on the magnetic abrasive to go over the burrs. Using single pole-tip system, the factors effects on surface and edge finishing of flexible capillary tubes, and the roles and behaviors of magnetic tools inside the tubes will be discussed.

3.2 Effects of Finishing Time, Tube Rotation, Slits, and Abrasive Size on Edge and Surface Finishing

3.2.1 Experimental Setup and Conditions

An external view of the experimental setup for flexible capillary tube finishing is shown in Figure 3-4. The stainless steel capillary tube with spiral slits (Tube A) is held by the chuck. While the tube is rotated, centrifugal force acts inside the tube. Depending on the direction of the tube rotation, the tube either elongates or shortens by changing the slit widths because of its spiral slits. The rotational direction is determined with the direction make the tube shortened to keep the abrasive and lubricant inside the tube. To diminish the run-out of the capillary tube beyond the finishing area, the other end of tube is held by a flexible jig, which also can react to the changes in the tube length.

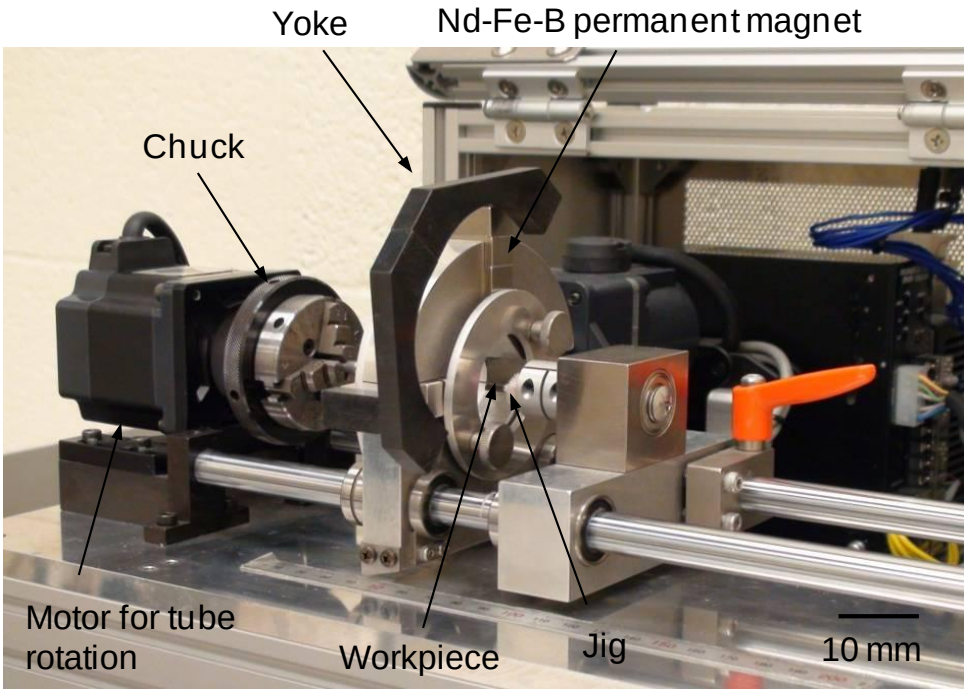

Figure 3-4. External view of finishing equipment for flexible capillary tube finishing (Photograph courtesy of Junmo Kang)

Three neodymium-iron-boron (Nd-Fe-B) permanent magnets (10×12×18 mm, residual flux density 1284 mT, coercive force 1440 kA/m) generate the magnetic field needed for attracting the magnetic abrasive to the finishing area. The magnets can be oscillated in the axial direction by a crank mechanism connected to the motor, and also fed in the axial direction of the tube with or without oscillation. The pole-tip geometry shown in Table 3-1 was determined based on the previous study of capillary tube finishing [34], and the pole-tip surface was covered by 0.11 mm thick polytetrafluoroethylene (PTFE) tape. The tube was in contact with the pole-tip surface during finishing. This minimized the clearance between the pole tip and finishing area to maintain a strong magnetic field at the finishing area and contributed to diminishing the run-out of the tube during finishing. The tape also protects both pole tip and the tube from rubbing against each other.

The previous research [34] reported that the key to achieve finishing of capillary tubes was the combination of the methods that a) Control the magnetic field at the finishing area, b) Determine the appropriate amount of mixed-type magnetic abrasive, and c) Support the capillary at three points. The finishing setup and conditions were refined to satisfy the abovementioned requirements.

Table 3-1 shows the experimental conditions. 304 stainless steel tubes (0.42 mm ID, 0.58 mm OD, and 55 mm length) with spiral slits were provided as workpieces for this study. The undeformed slit width was measured at about 12 µm. The tube was chucked 12.5 mm from one end. Since laser-machined burrs have various irregular shapes and heat affected zones, sharp and hard cutting edges combined with strong magnetic force are required to remove the burrs. Conventionally, used for 304 stainless steel tube finishing, mixed-type magnetic abrasive—a mixture of relatively large-sized iron powders and white alumina magnetic abrasive (mean diameter 80 µm and comprising iron particles and Al_2O_3 abrasive grains under 10 µm in diameter)—could not remove the heat-affected hard burrs. Diamond abrasive in a paste form was, thus, added to the mixed-type magnetic abrasive with lubricant. The WA magnetic abrasive has irregular microasperities on the surface produced during the manufacturing process. These microasperities allow the WA magnetic abrasive to hold the nonferrous diamond abrasives through the lubricant at the finishing area. One of the important properties of the lubricant must be the viscosity, which must be high enough to prevent leaking through the slits and to encourage the lubrication between the abrasive cutting edges and target surface but low enough to be introduced into the capillary tube.

Table 3-1. Experimental conditions for internal deburring of flexible capillary tube with laser machined slits: Tube A

Workpiece	Tube A 304 stainless steel tube (∅0.58×∅0.42×55 mm)
Workpiece revolution	2500 min^{-1}
Ferrous particle	Iron particles (-50/+100 mesh, 150-300 μm dia.): 80 wt% + Aluminum oxide (WA) particles (80 μm mean dia.) in magnetic abrasive (<10 μm): 20 wt%
Amount of ferrous particle	0.5 mg
Diamond abrasive	4-8, 20-40, 50-70 μm diameter
Lubricant	Soluble-type barrel finishing compound: 4.53 μL
Permanent magnet	Nd-Fe-B permanent magnet: 10×12×18 mm
Pole reciprocating motion	Amplitude: 4 mm, Speed: 0.69 mm/s
Workpiece-Pole clearance	0.11 mm
Pole tip	1080 carbon steel 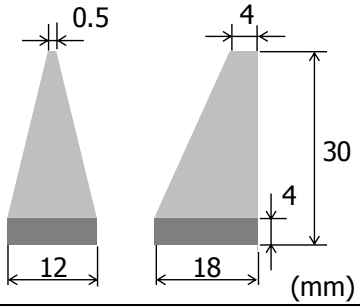

The necessary amount of the magnetic abrasive can be determined according to the ratio of the volume of the magnetic abrasive to the overall volume inside the tube (in a length corresponding to the width of the pole tip). There exists a threshold of the supplied abrasive amount between 43 and 55 vol%; a supplied amount less than the threshold is required for efficient finishing [34]. The mixture of 0.1 mg WA magnetic abrasive and 0.4 mg iron particles—which results in 47 vol% taken up by the iron powder and WA magnetic abrasive—was supplied for the experiments.

Under the conditions with high speed tube rotation, the mixture of the magnetic abrasive and iron particles shows difficulties to follow the poles feed in the tube axis

direction because the friction force becomes much larger than the magnetic force. The burrs also obstruct the mixture to follow the poles feed. Therefore, the feed speed was set at the lowest of the experimental setup, 0.69 mm/s. The crossing angle θ of the cutting marks generated by the diamond abrasive is calculated as $2\times\tan^{-1}(v_f/v_r)$, where v_f is the pole feed velocity, and v_r is the tube rotational speed. Under the experimental conditions, θ was calculated to be 1.4°.

The effects of the diamond abrasive size on the processing characteristics were examined. Three sizes of diamond abrasive were prepared: 4-8, 20-40, and 50-70 μm, which are smaller, slightly larger, and much larger than the slit width, respectively. The finishing unit was reciprocated over 4 mm at 0.69 mm/s, finishing an 8 mm length located 3 mm from the end opposite the chuck.

The stylus of the surface roughness profilometer, which is the device most commonly used for surface roughness measurement, could not be inserted inside the 0.42 mm ID capillary because of the small tube diameter. This created difficulty in measuring and tracking the changes in the surface roughness and burr heights with finishing time. The tube was cleaned using ethanol (200 proof) in an ultrasonic cleaner every 6 min, and the changes in the material removal with finishing time were tracked only by measuring the weight reduction by the process with a micro-balance (10 μg resolution). Following replenishment of the mixture of the ferrous powders and abrasive every 6 min, the finishing experiments were continued. After the finishing for a certain period, the tube was sectioned along the tube axis, and the surface was evaluated using an optical profilometer and microscope.

3.2.2 Effects of Diamond Abrasive Size on Deburring Flexible Capillary Tube

The time sufficient for finishing was initially determined by examining the changes in the finishing characteristics with finishing time using the 50-70 μm diameter abrasive. The diamond abrasive is larger than the undeformed slit width, measured to be 12 μm. Figure 3-5 shows the micrographs of the unfinished surface and the surface finished for 30 min and 60 min. Although areas damaged by the laser machining process are observed between the slits, the initial surface burrs adjacent to the slits are the target of this study. The initial heights of the burrs generated by laser machining were measured by an optical profiler to be in the range between 8 μm and 50 μm.

During the process, the tube was deformed such that the slits were narrowed due to the tube rotation. When the diamond abrasive encounters the slit during the process, the abrasive momentarily loses contact with the surface, but contacts the surface again on the other side. According to the cutting marks, the reengagement of the abrasive must be smooth. The diamond abrasive must gradually remove material from the peaks of the burrs and the microasperities of the tube surface. The conditions for 30 min were found to be insufficient for effective deburring. By increasing the finishing time, however, the edge and surface finishing were both smoothly performed.

Figure 3-6 shows the changes in the material removal with finishing time. The variation of the material removal at the beginning was due to the variation in the initial burr conditions. This indicated that about 0.3 mg of material removal might be necessary for both edge and surface finishing of the tubes for 8 mm finishing length. Accordingly, it was shown that MAF is applicable for inner surface finishing and removal of laser-machined spiral burrs projected inside flexible capillary tubes. Next, the effects

of the diamond abrasive size on the deburring characteristics were examined with three sizes of diamond abrasives: 4-8, 20-40, and 50-70 µm diameter.

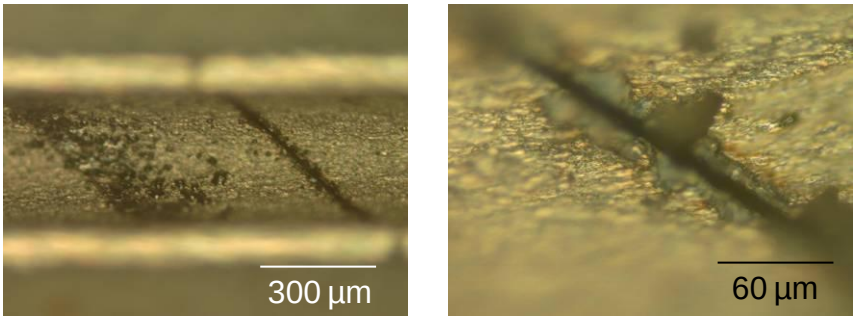

A Unfinished surface

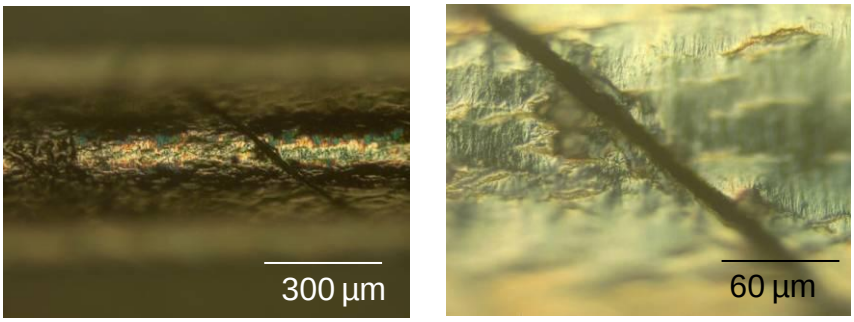

B Surface finished for 30 min

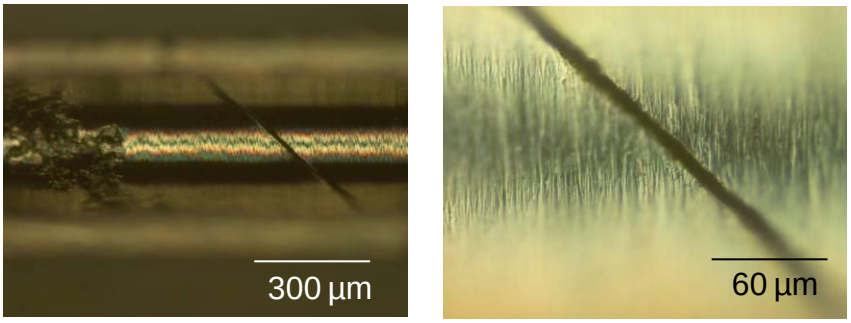

C Surface finished for 60 min

Figure 3-5. Micrographs of unfinished surface, and surfaces finished for 30 and 60 min with 50-70 µm diamond abrasive

Figure 3-7 shows micrographs of the surfaces finished with 20-40 and 4-8 µm diamond abrasive for 60 min. In the case with 20-40 µm diamond abrasive, shown in Figure 3-7(A), the burrs and the initial surface unevenness remain due to a lack of material removal. This is because of the smaller cutting edges of the diamond

compared to the 50-70 μm diamond abrasive. In the case of the 4-8 μm diamond abrasive, shown in Figure 3-7(B), no burrs remain, but deep, irregular undulations are observed on the finished surface. During the process, the magnetic force pushes the iron particles, which push the WA magnetic abrasive, which, in turn, push the diamond abrasive against the inner surface of the tube. Some 4-8 μm diamond abrasive must agglomerate between the WA magnetic abrasives and tube surface. The mass of the diamond abrasive pushed by the WA magnetic abrasive and ferrous particles must participate in the finishing performance, resulting in the deep scratches. This also led to the removal of the burrs and surface finishing with irregular undulations.

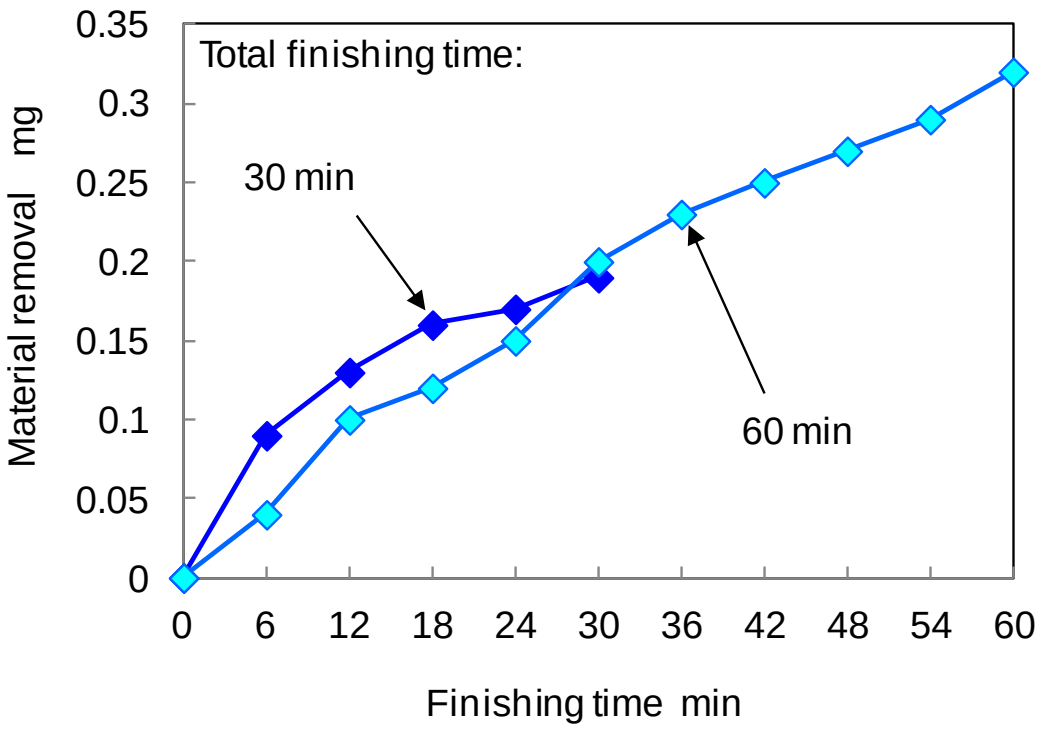

Figure 3-6. Changes in material removal with finishing time

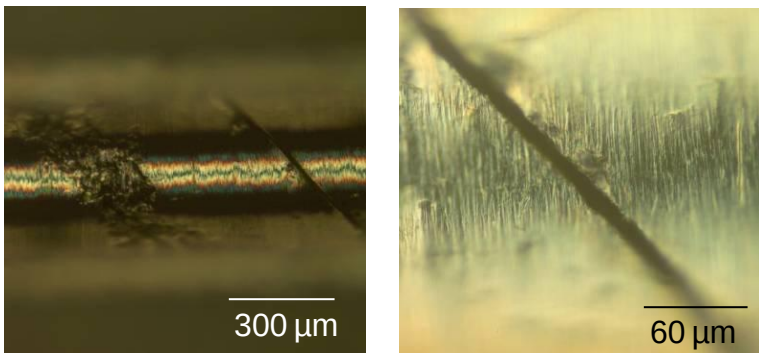

A Surface finished with 20-40 µm diamond abrasive

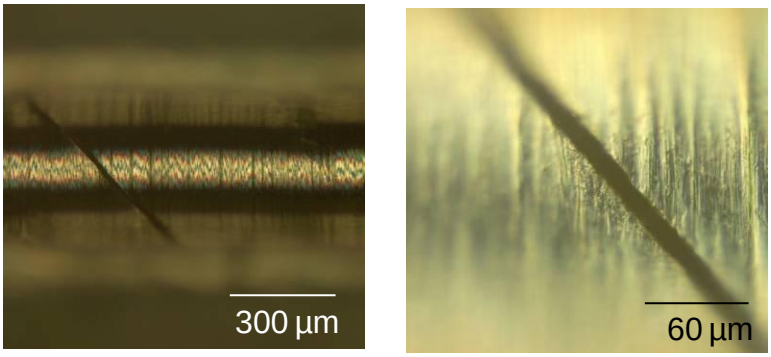

B Surface finished with 4-8 µm diamond abrasive

Figure 3-7. Micrographs of surface finished with 20-40 µm diamond abrasive and 4-8 µm diamond abrasive

Figures 3-8 and 3-9 show the three-dimensional shapes (measured by an optical profiler) of the unfinished inner surface and the inner surfaces finished with three sizes of diamond abrasives for 60 min. In Figure 3-8, the surface data in the area of a slit is passed through a low-pass filter so that the burr shapes can be examined. The irregularity of the surface brought about measurement difficulties, resulting in the discontinuity of the surface seen in Figure 3-8. However, the surface is continuous except for the slit. The abovementioned burr heights were obtained as peak-to-valley values of lines drawn perpendicular to the slit from several observations. To examine the surface roughness, Figure 3-9 shows the unfiltered area between slits. As shown in Figure 3-8(A) and 3-9(A), the case with 50-70 µm diamond abrasive demonstrated the

burr removal and surface finishing. The surface was modified from 0.67 to 0.12 μm *Ra*. In the case of the 20-40 μm diamond abrasive, the initial burrs remained after 60 min, as shown in Figure 3-8(B). This condition must have merely removed material from the peaks of the surface irregularities and left the 5-7 μm high burrs. Although the three-dimensional surface shape observation barely shows the initial micro-unevenness remaining, the small material removal resulted in slowed surface roughness improvement, from 0.65 μm 0.21 μm *Ra* (Figure 3-9(B)). However, the 4-8 μm diamond abrasive removed burrs successfully, as shown in Figure 3-8(C). The surface finished by the 4-8 μm diamond abrasive consists of the accumulation of shallow cutting marks on the deep undulations with relatively longer wavelength, which must be caused by the agglomerated diamond abrasive. This generated the surface roughness value to 0.35 μm *Ra* (Figure 3-9(C)).

The cases with 4-8 and 20-40 μm diamond abrasives show another trend, as well. After finishing, a mixture of lubricant, diamond abrasive, and chips was observed outside the tube, and cutting marks were observed on the outer surface of the tube, as shown in Figure 3-10. The heat generated during the finishing process must decrease the viscosity of the lubricant, and the 4-8 μm diamond abrasives, which are smaller than the slits, must have leaked through the slits. The diamond abrasive became sandwiched between the rotating tube and pole tip, and achieved external surface finishing of the tube. The unagglomerated 4-8 μm diamond abrasive must pass easily through the slits, and a large number of abrasive must participate in finishing of the outer surface. On the other hand, the 20-40 μm diamond abrasive could have been larger than the slit widths. In practice, a distribution including smaller-sized diamond abrasive results from the

manufacturing process. Alternatively, the diamond abrasive could be crushed during the process, and some abrasive would thus be reduced in size. The diamond abrasive that was able to migrate from the internal finishing area must have caused the scratches on the outer surface and slightly removed the material from outer surface.

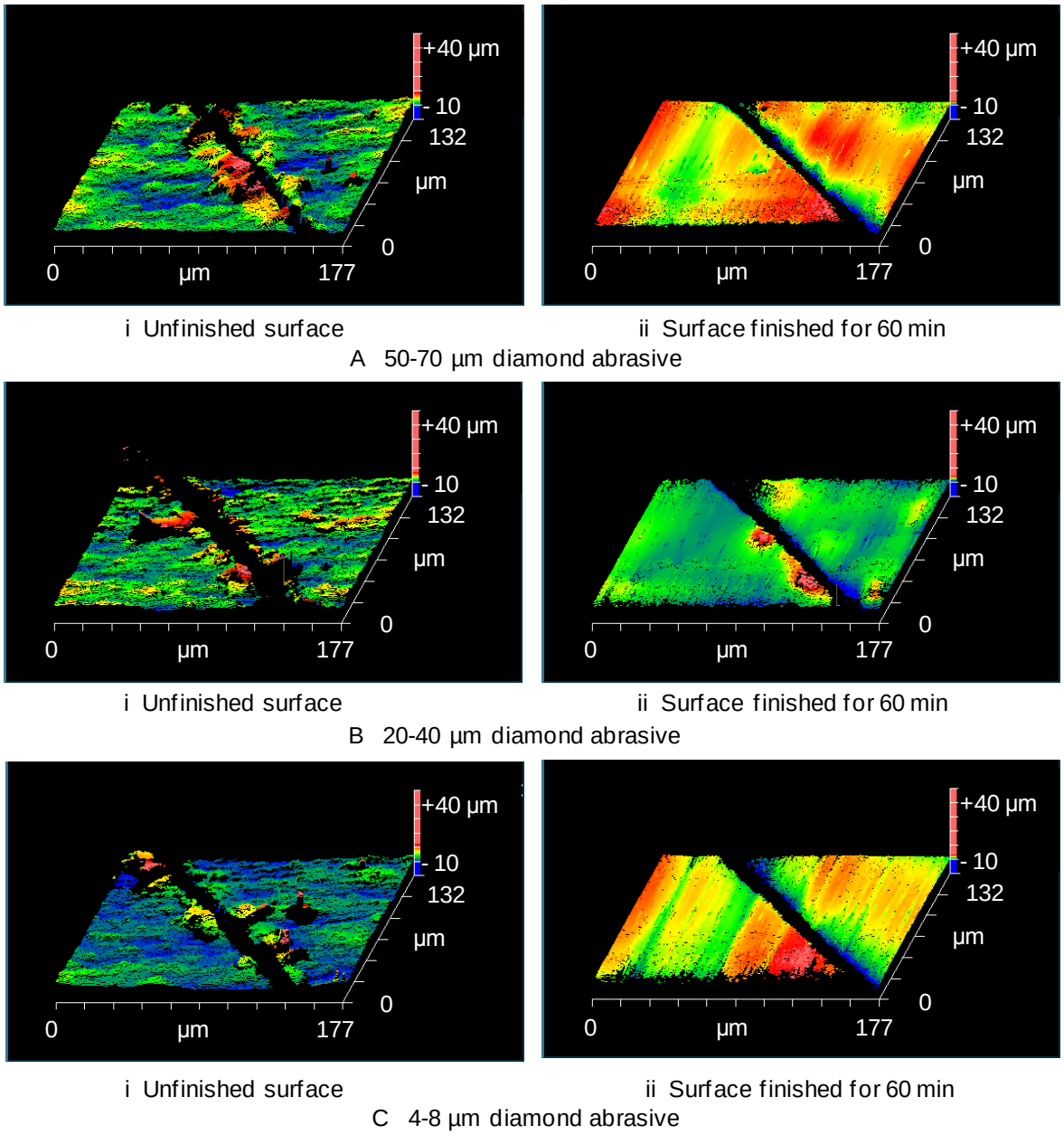

Figure 3-8. Three-dimensional burr shapes measured by optical profiler; A) edge finished by 50-70 µm diamond abrasive, B) edge finished by 20-40 µm diamond abrasive, and C) edge finished by 4-8 µm diamond abrasive

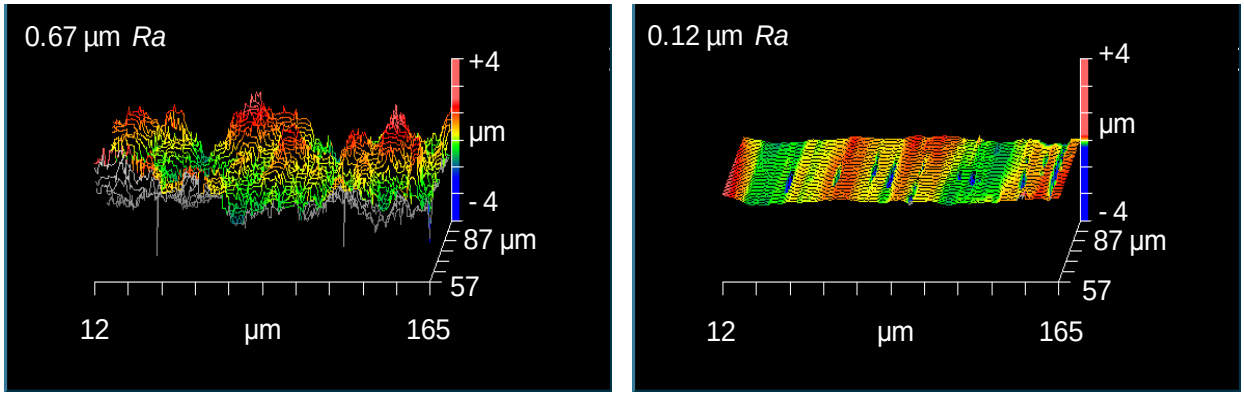

i Unfinished surface ii Surface finished for 60 min

A 50-70 µm diamond abrasive

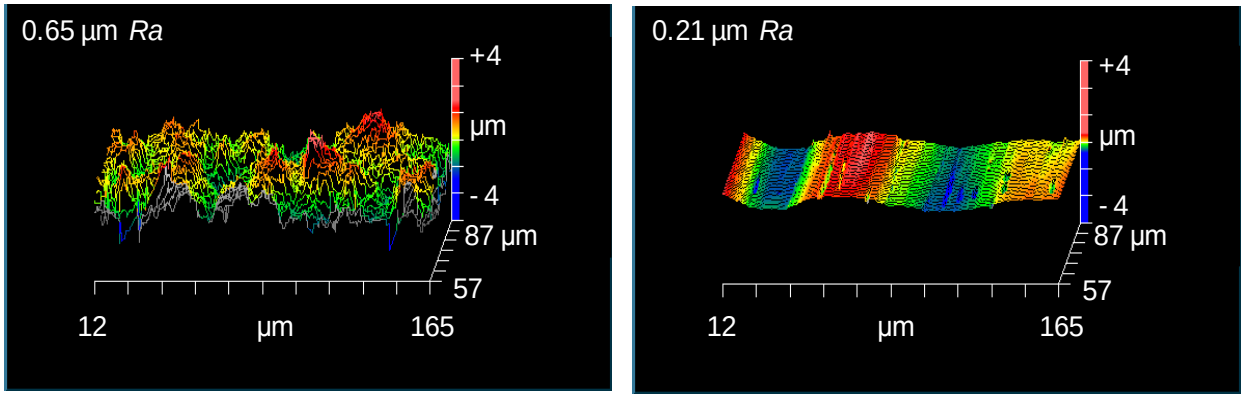

i Unfinished surface ii Surface finished for 60 min

B 20-40 µm diamond abrasive

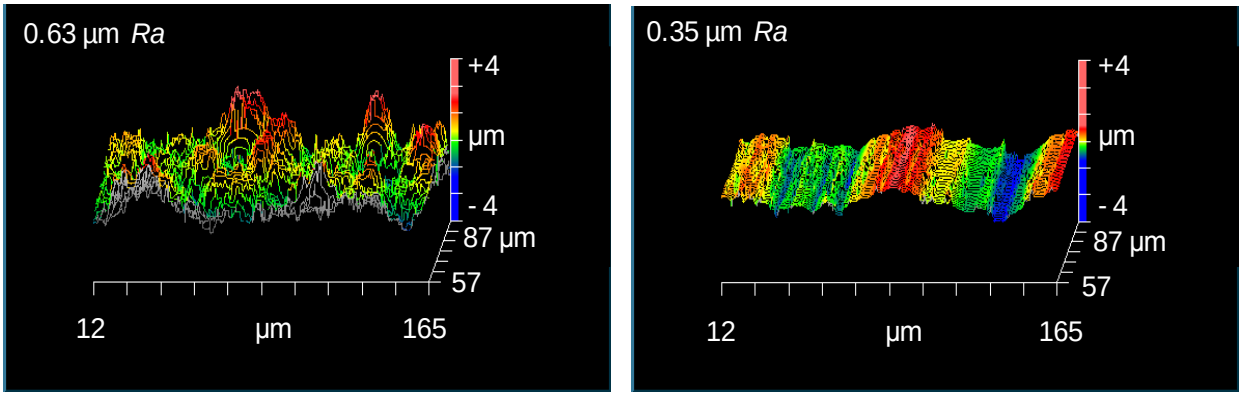

I Unfinished surface ii Surface finished for 60 min

C 4-8 µm diamond abrasive

Figure 3-9. Three-dimensional surface shapes measured by optical profiler; A) surface finished by 50-70 µm diamond abrasive, B) surface finished by 20-40 µm diamond abrasive, and C) surface finished by 4-8 µm diamond abrasive

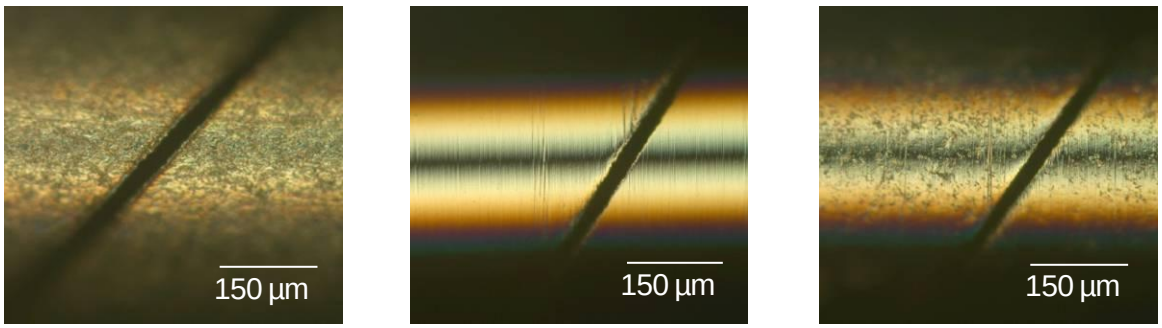

A As received surface

B Surface finished with 4-8 µm diamond abrasive

C Surface finished with 20-40 µm diamond abrasive

Figure 3-10. Micrographs of outer surface of tube; A) as received surface, B) surface finished with 4-8 µm diamond abrasive, and C) surface finished with 20-40 µm diamond abrasive

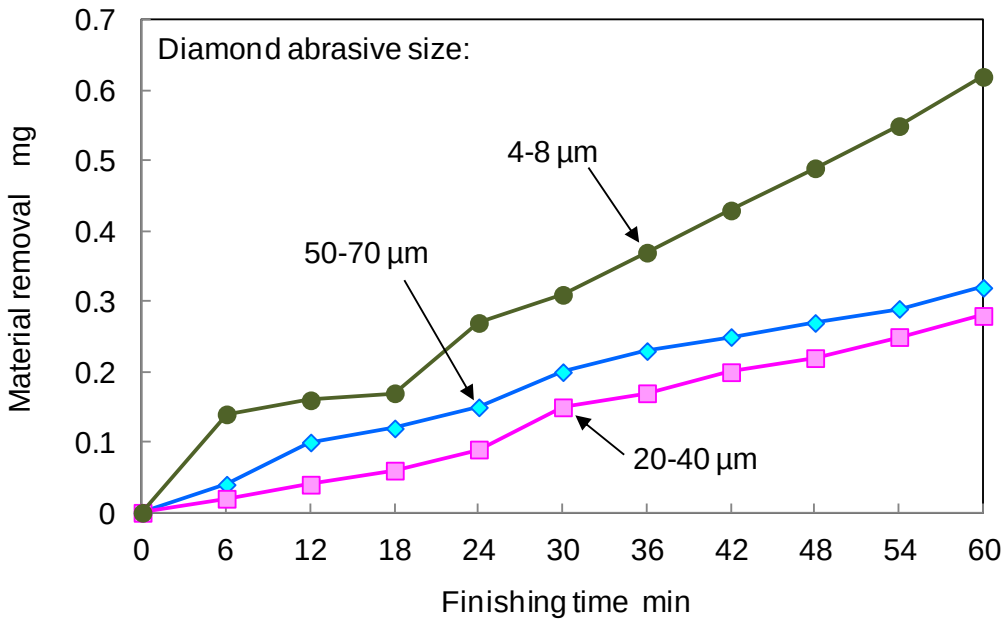

Figure 3-11. Changes in material removal with finishing time according to diamond abrasive size

Figure 3-11 shows changes in the material removal with finishing time. The material removal in the 20-40 µm diamond abrasive case is lowest of the three conditions. It is noted that the material removal in the 4-8 and 20-40 µm diamond

abrasive cases are the results of finishing of both the inner and outer surfaces. In the case with 20-40 μm diamond abrasive, the lack of large cutting edges of the abrasive resulted in the smallest material removal. Regardless of the fact of being the smallest abrasive of the three, the effects of the agglomeration of the 4-8 μm diamond abrasive in the internal finishing and the leakage of the diamond abrasive from the slit for the outer finishing led to the greatest material removal.

3.3 Roles and Behaviors of Magnetic Tools

In an attempt to encourage the material removal rate for flexible capillary tubes, diamond abrasive was introduced to have large cutting edges. This method was successful for tube A with less number of slits and small burrs (up to 50 μm). However, it was unsuccessful in finishing trial for tube B with more number of slits and large burrs (up to 90 μm), because the abrasive size is smaller than the burr height, that is, abrasives cannot go over the burr when the magnet moves along the tube axis (Figure 3-12). Therefore, stronger magnetic force to overcome these difficulties is required. Based on the magnetic force equation (Eqn. 2-1), change the volume of ferrous particle is considered.

Increasing the diameter of the iron particles is not the only method for increasing the volume of included ferrous tools. Increasing the length of the ferrous tool along the tube axis direction, that is, replacing the some ferrous particle with a rod is another method to increase the volume and thus increase the magnetic force acting on magnetic abrasive (Figure 3-13). The geometric, as well as magnetic, properties of the ferrous tools play important roles in realizing the MAF process in the limited space, especially capillary tubes.

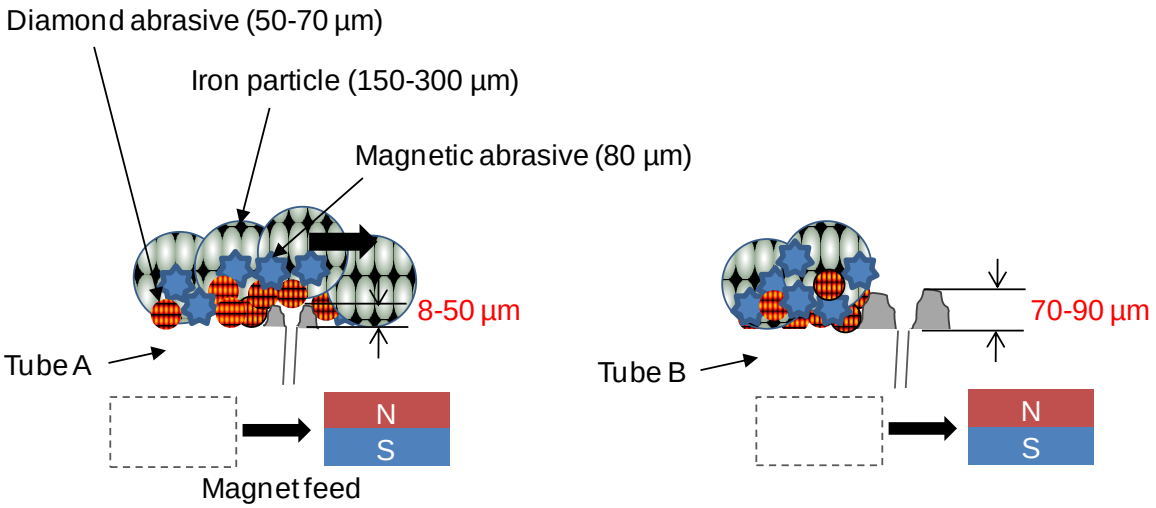

Figure 3-12. Schematic of iron particle, magnetic abrasive, and diamond abrasive behavior inside the flexible capillary tube with magnet feed

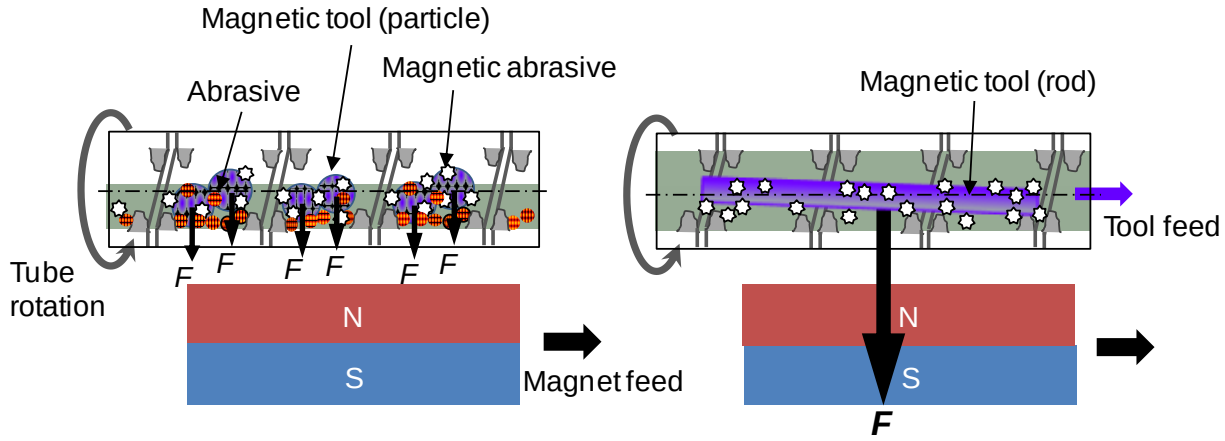

Figure 3-13. Schematics of processing principle with different magnetic tools (switching the iron particle to rod)

Previously, carbon steel (JIS designation: S48C (0.48 wt% C)) and austenitic stainless steel rods or pins replaced iron particles for the surface finishing of 18 mm ID tube [58]. The carbon steel is ferromagnetic and exhibits high magnetic susceptibility. Austenitic 304 stainless steel is paramagnetic but becomes ferromagnetic when plastic deformation causes the face-centered cubic (austenitic, nonferrous) structure to be transformed into a body-centered cubic (martensitic, ferrous) structure. Moreover, its

magnetic anisotropy is attributed to the shape of martensite formed in the austenitic matrix during the plastic deformation [59-63]. When the same mass of stainless steel rods, carbon steel rods, or iron particles is subjected to the same magnetic field, the magnetic force generated with the stainless steel rods is about three to four times lower than the force with carbon steel rods and about half of that with iron particles [54].

Introducing the carbon steel rods into the finishing area generated higher magnetic force than the iron particles. In the magnetic field, the steel rods (Figure 3-14(A), ∅0.5×5 mm) are magnetized in line with the magnetic flux (i.e., perpendicular to the tube surface), but they also cling to one another and agglomerate. In this configuration, the steel rods pushed the magnetic abrasive against the tube inner surface, and the finished surface consisted of the accumulation of deep scratches. In the case of stainless steel rods (Figure 3-14(B)), the axes of the magnetized rods are generally aligned with the magnetic flux, but there is repulsion between the individual rod chains, so a differently configured mass pushed the magnetic abrasive against the tube surface. When subjected to the unevenness of the tube surface, the rods show instability, e.g., relocating and impacting the surface because of the magnetic anisotropy and reduced magnetic force. The magnetic abrasive was pushed by unstable rods and showed discontinuous contacts against the tube surface. This enhanced the material removal but hardly resulted in continuous surface finishing.

In contrast, the interior volume of capillary tubes is limited, so the rods must be introduced into the tube with their axes parallel to the tube axis. Consequently, the rods in capillary finishing behave differently from those in the cases of large-sized tube finishing. Moreover, the rods may help to keep the flexible capillary tube straight at the

finishing area, allowing a flexible tube to be treated as a straight tube. Before applying the ferrous rods to the finishing experiments, the motion of the rods was observed using a transparent nonferrous polymer tube. To facilitate the observation, large-sized iron particles (150-300 μm) were introduced in place of magnetic abrasive.

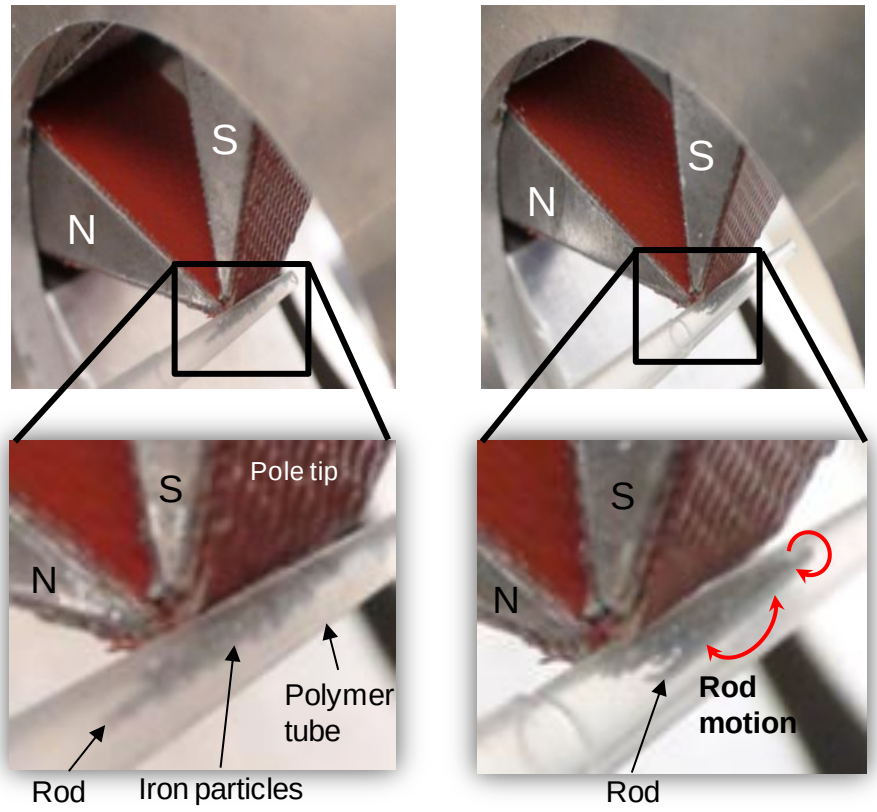

A Carbon steel rod (∅0.50×4 mm)

B 304 stainless steel rod (∅0.51×4 mm)

Figure 3-14. Photographs of carbon steel rod and 304 stainless steel rod inside nonferrous polymer tube (Photograph courtesy of Junmo Kang)

Figure 3-14 shows photographs of carbon steel (0.80-0.90 wt% C) and stainless steel rods and iron particles inside nonferrous polymer tube while the tube is rotated at 200 min^{-1} to facilitate visual observation. Tube rotation is measured by tachometer. The magnetic flux flows from one pole tip to another, and the ferrous rod and iron particles are magnetized following the magnetic flux. In the case of the carbon steel rod, magnetic force causes the iron particles to gather as a mass around the rod (Figure 3-

14(A)) due to the ferromagnetism of both the carbon steel rod and the iron particles. The mass pushes the inner surface of the rotating plastic tube with strong magnetic force, and, when the pole tips are reciprocated in the axial direction, the mass follows the pole tips stably and produces scratches on the tube surface.

In the case of the stainless steel rod (Figure 3-14(B)), the iron particles are attracted by the magnetic field more than the rod is, and, in the restricted area inside the tube, the stainless steel rod settles into a position over the iron particles while slightly leaning toward the line of magnetic force. At the contact area between the iron particles and the rod, there is no interaction by magnetic force between them. Only one end of the rod pushes the iron particles against the tube surface and participates in the finishing action. As the carbon steel rod does, the stainless steel rod (with the iron particles) follows the motion of the pole tips when the pole tips are fed in the axial direction. However, the weak magnetic force acting on the rod causes unstable conditions, and the rod occasionally shows rotation about its axis over the iron particles.

When the pole tips change direction during reciprocation, the stainless steel rod does not immediately change direction to follow the pole tip motion in the same way that the carbon steel rod does. Because of the magnetic anisotropy and low magnetic susceptibility, the stainless steel rod requires a strong magnetic field to be attracted to the pole tips. Regardless of the pole motion, the rod is stationary until the magnetic field becomes strong enough to attract the rod, and it was observed that one end of the rod needs to be close to the pole tip edges. After the rod is attracted by the field, it follows the motion of pole tips. As a result, the reciprocating stroke of the rod is shorter than the stroke of the pole tip reciprocation. Occasionally, the rod moves so that the other end of

the rod pushes the iron particles against the inner surface of the tube. Considering these effects, the finishing area for the stainless steel rod is typically shorter than the area when using the carbon steel rod.

In Section 3.3.1, the effects of the tool behavior (due to the geometric and magnetic properties) on the internal finishing characteristics will be experimentally studied with straight capillary tubes. Iron particles and rods of carbon steel and stainless steel are prepared for the tests.

3.3.1 Experimental Setup and Conditions

Table 3-2 shows the experimental conditions, for this study, 304 stainless steel tubes (straight, OD 0.64 mm, ID 0.48 mm, length 100 mm, initial surface average roughness ~1 µm *Ra*) and flexible capillary (Tube B) were used as workpieces. In each test, the tube was chucked 12.5 mm from one end. Centrifugal force acts on the capillary tube when it is rotated at high speed, and to diminish the run-out of the tube beyond the finishing area, the opposite end of tube was held by a flexible jig, which can accommodate changes in the tube length during the rotation. The tube rotational speed was set at 2500 min^{-1}. The reciprocating stroke of the 4 mm wide pole was set at 4 mm in the axial direction, and the pole feed rate was set at 0.69 mm/s, which has been found to be appropriate for deburring.

Because of the small tube diameter, the stylus of a surface roughness profilometer, the device most commonly used for surface roughness measurement, could not be inserted inside the capillary. This created difficulty in measuring and tracking the changes in the surface roughness and burr heights with finishing time. Instead, the finishing tests were performed for a certain period, then the tube was cleaned using ethanol in an ultrasonic cleaner, sectioned along the tube axis, and the

inner surface was evaluated using an optical profilometer and microscope. The changes in the material removal were tracked by measuring the weight with a micro-balance (10 μg resolution).

Table 3-2. Experimental conditions of internal finishing of straight capillary tube

Workpiece	Straight tube: 304 stainless steel tube (∅0.64×∅0.48×100 mm),
Workpiece revolution	2500 min^{-1}
Magnetic abrasive	Aluminum oxide (WA) particles (80 μm mean dia.) in magnetic abrasive (<10 μm)
Magnetic tool	Iron particles (-50/+100 mesh, 150-300 μm diameter), Carbon steel rod (∅0.25×4 mm), 304 Stainless steel rod (∅0.24×4 mm)
Lubricant	Soluble-type barrel finishing compound
Permanent magnet	Nd-Fe-B permanent magnet: 10×12×18 mm
Pole reciprocating motion	Amplitude: 4 mm, Speed: 0.69 mm/s
Workpiece- Pole clearance	0.11 mm
Pole tip	Table 3-1

3.3.2 Effects of Material Properties of Magnetic Tools

Initially, the relationship between the finishing time and surface roughness improvement was evaluated to determine the duration of experiments using mixed-type magnetic abrasive (a mixture of 80 μm mean diameter magnetic abrasive and iron particles in the 150-300 μm range, which was the largest range that could be introduced into the tube without clogging) [52]. To determine the appropriate amount of the mixed-type magnetic abrasive, the volume of the mixture was compared to the total volume inside a length of tube equal to the width of the pole tip. A mixture of 0.13 mg magnetic abrasive and 0.49 mg iron particles - which results in 41.1 vol% occupied by the mixed-type magnetic abrasive - was supplied for the experiments. After 117 cycles (22.5 min), the roughness improvement slowed down, and this became the index used for the

subsequent experiments. The finishing experiments were repeated under each set of conditions at least three times to confirm the repeatability of the results.

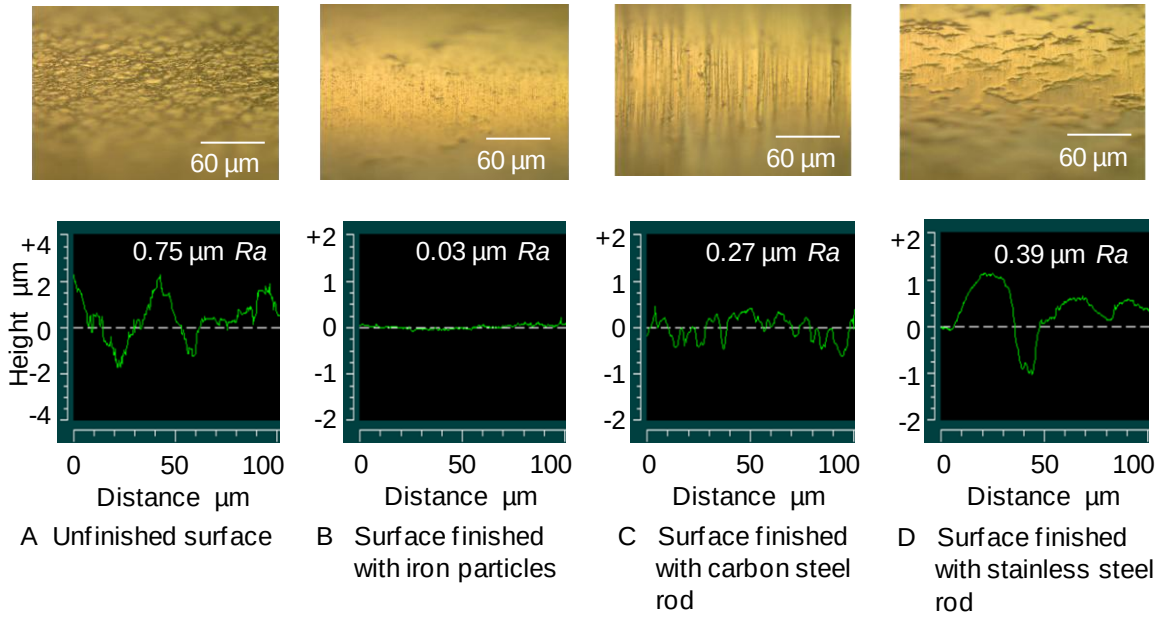

Figure 3-15. Photographs and surface roughness profiles of tube interior before finishing, surface finished with iron particles, surface finished with carbon steel rod, and surface finished with stainless steel rod for 22.5 min

Figures 3-15 show (A) photographs of tube interiors and (B) representative surface roughness profiles measured by an optical profiler. Figure 3-16 shows the three dimensional surface of Figure 3-15. With a mixture of magnetic abrasive and iron particles, the mass of the mixture nearly followed the motion of the pole tips, and the finished length was 5-6 mm, although the pole tips covered 8 mm (4 mm pole tip width and 4 mm stroke) in the tube axis direction. This was a result of the friction between the mass and tube surface, which caused a delay in the following motion of the abrasive. The chains of iron particles and magnetic abrasive conform to the shape of the tube interior. This enables uniform internal finishing of capillary tubes. Within the finished area, the surface was almost uniformly finished from 0.75 µm *Ra* to 0.03 µm *Ra* (Figure 3-15(A) and (B)).

When a carbon steel rod was inserted with the magnetic abrasive, the finished length of the surface was about 7 mm. The steel rod and magnetic abrasive (0.25 mg) occupied 43.7 vol% at the finishing area. The rod and magnetic abrasive were both strongly attracted by the pole tips and more closely followed the pole motion. The representative finished surfaces are shown in Figure 3-15(C), and a representative surface roughness value was 0.27 μm *Ra*. With strong magnetic force, the steel rod pushed the magnetic abrasive sandwiched between it and the tube surface. Depending on the configuration of the magnetic abrasive pushed by the rod, the magnetic abrasive irregularly generated deep scratches on the tube surface. This resulted in the larger surface roughness than that in the case with iron particles (no rod). Moreover, the material removal with the steel rod (0.18 mg) was nearly twice as high as the case with iron particles (0.1 mg).

In the conditions with the stainless steel rod, the material removal (0.02 mg) was not enough to completely remove the initial surface texture. The magnetic abrasive (0.25 mg) and rod occupied 41.6 vol% at the finishing area; however, due to the tilted position of the rod, only one end of the rod participated in the finishing action. Figures 3-15(d) show that the initial texture partially remained on the finished surface, and the roughness was measured to be 0.39 μm *Ra*. The finished length was measured to be only about 1.5-2 mm along the tube axis. This is attributed to the irregular rod motion due to the weak magnetic force and the anisotropic magnetic properties.

Accordingly, the effects of the ferrous tools on the finishing characteristics can be summarized: (1) The chains of iron particles and magnetic abrasive conform to the shape of the tube interior. This enables uniform internal finishing of capillary tubes. This

method is sufficient for operations that require small material removal, such as tube surface finishing, (2) The carbon steel rod pushes the magnetic abrasive against the tube surface with strong magnetic force, generating high material removal. This method is appropriate for conditions that require large material removal (such as deburring) but not for surface finishing, and (3) The stainless steel rod generates weak magnetic force with its magnetic anisotropy. This results in the slow material removal rate and relatively shorter finished area. This method is insufficient for performing either surface finishing or deburring in a timely manner.

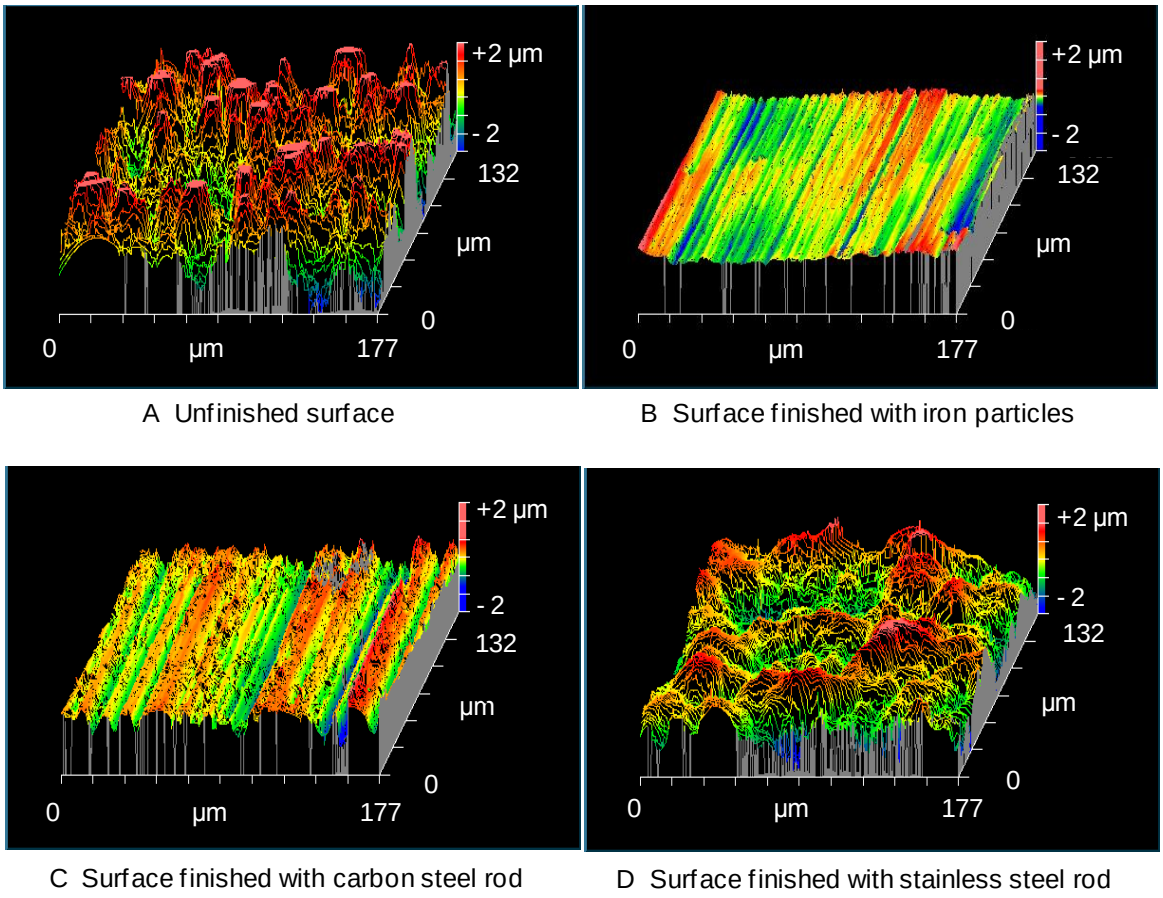

Figure 3-16. Three-dimensional surface shapes of tube interior before finishing, surface finished with iron particles, surface finished with carbon steel rod, and surface finished with stainless steel rod for 22.5 min

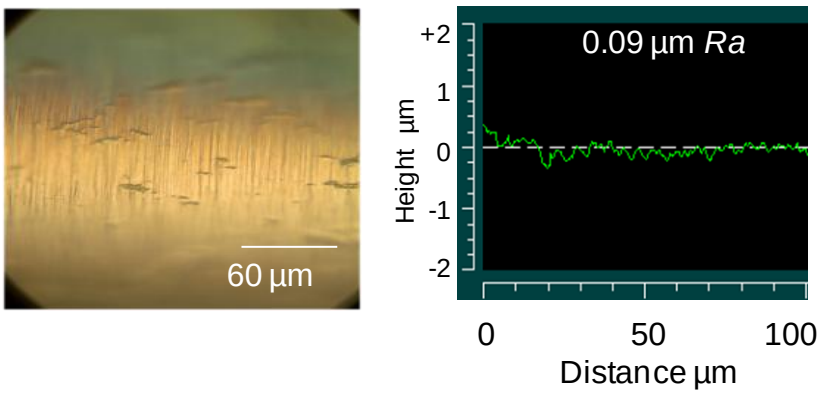

A Photograph B Roughness profile

Figure 3-17. Photograph and roughness profile of surface finished with stainless steel rod, magnetic abrasive, and iron particles

For the internal finishing of flexible capillary tubes, it is necessary to introduce a rod inside the capillary tube to make it straight for processing. While the carbon steel rod is a promising ferrous tool for deburring purposes, it is not appropriate for surface finishing purposes. If the material removal rate using the stainless steel tool rod could be improved, this method may be another potential method for both deburring and surface finishing. The lack of relative motion between the tube surface and the magnetic abrasive pushed by the stainless steel rod can be overcome by extending the stroke of the rod reciprocation. For example, increasing the stroke of the pole tip from 4 to 8 mm resulted in a finished length of about 11 mm instead of 12 mm. Furthermore, a part of magnetic abrasive can be replaced with iron particles, since some of the magnetic abrasive did not directly participate in the material removal. The mixed-type magnetic abrasive will increase the magnetic force. Accordingly, a portion of the magnetic abrasive (65 wt%) was replaced by iron particles, and the finishing experiments were performed for 51.3 min (the pole tips were reciprocated for 8 mm in 117 times at 0.6 mm/s).

Figure 3-17 shows surface roughness profiles of the finished surface as measured by the optical profilometer. The material removal increased from a previous value of 0.02 mg to 0.10 mg, and the surface consisted of an accumulation of almost evenly generated scratches (the roughness value was 0.09 μm *Ra*). The micro-asperities left from the initial surface must be removed by the extending the finishing period. In the hybrid conditions (stainless steel rod and iron particles), the role of the rod is to drive both the iron particles and magnetic abrasive in the axial direction, and the role of the iron particles is to form the mixed-type magnetic abrasive, increase the magnetic force acting on the magnetic abrasive, and encourage the material removal. This hybrid method is applicable for simultaneous surface finishing and deburring.

In magnetic abrasive finishing, magnetic force acting on magnetic abrasive determines the finishing force as well as the magnetic abrasive behaviors. To clarify the finishing mechanism of capillary tube finishing using the magnetic tools, the measurement of magnetic force acting on magnetic abrasive was measured.

The system for magnetic force measurement using strain gauge has been designed (Figure 3-18) and implemented. Two strain gages (Half-bridge method, gage factor: 2.09±1.0%, gage resistance (24°C, 50%RH): 119.8±0.2Ω) were attached on the aluminum plate (14.6x3.11x150 mm), and a magnetic tool with particles was located in the groove on the plate for preventing the dispersion of particles. The plate located on the 3-axis micrometer stage. In order to avoid the contact between the bottom of plate and the top of pole-tip, the clearance between the plate and pole tip was set at 0.1 mm. Each measurement was repeated three times, and the standard errors were indicated on the each bar in Figure 3-19 and Figure 3-20.

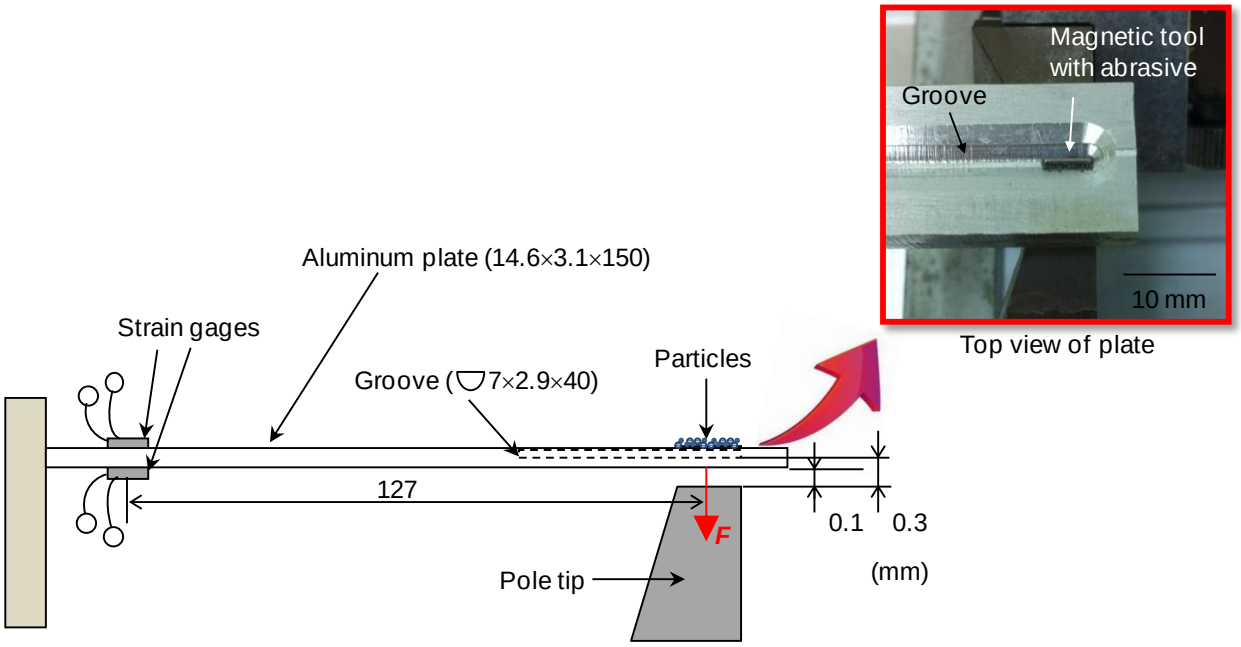

Figure 3-18. Schematic of magnetic force measurement system for single pole-tip system and photograph for top view of plate (Photograph courtesy of Junmo Kang)

Each ferrous particles (carbons steel tool, 304 stainless steel tool, iron particle and magnetic abrasives) are prepared in same volume percent (21 vol%) and the magnetic force are measured. The iron particle has twice magnetic force than that of magnetic abrasive (Figure 3-19), and this has been shown in previous study [50]. Within 21 volume percent of ferrous tools in flexible capillary tube (Tube B), carbon steel tool (∅0.5×4 mm, 6.71 mg) is 3.7 times stronger than the iron particles (150-300 μm diameter,1.5 mg) and has 2.5 times stronger force than 304 stainless steel tool itself (∅0.51×4 mm, 6.75 mg). Using the 304 stainless steel tool instead of iron particle shows 50 percent incensement of magnetic force. This helps the magnetic abrasive follow the pole along the tube axis and enhances the material removal rate during the process. Only mixed-type magnetic abrasive could not achieve the internal finishing of

flexible capillary tube due to its both small particle size and less magnetic force. The magnetic tools (carbon steel and 304 stainless steel rods) can increase the magnetic force acting on magnetic abrasive. Moreover the substitution of magnetic abrasive to iron particles assists the flexible chain forms on the surface strongly.

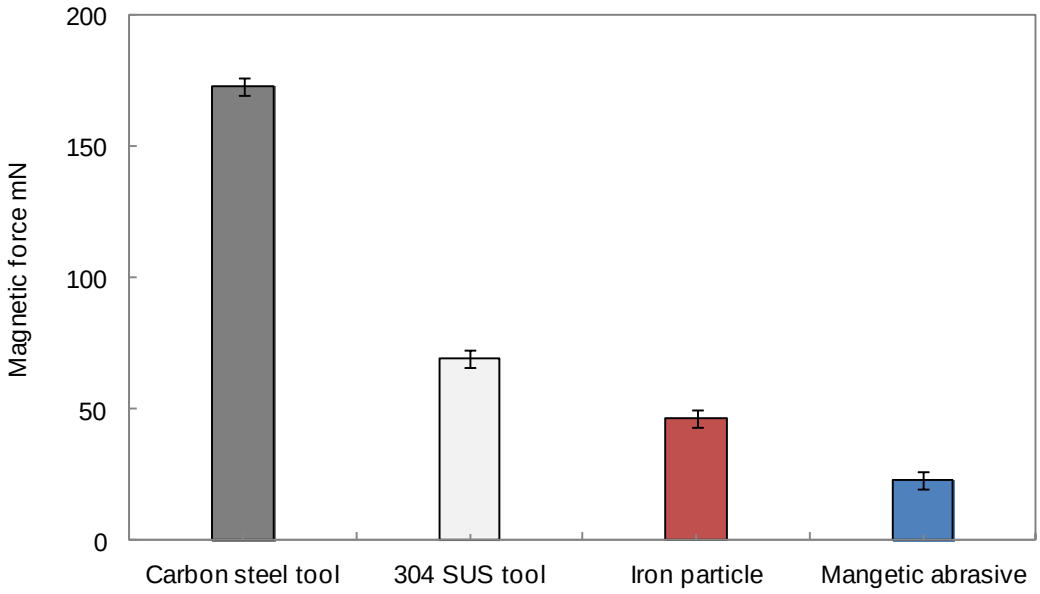

Figure 3-19. Relationship between finishing force and magnetic tool in same volume percent

The case of carbon steel tool (∅0.25×4 mm, 1.54 mg) and magnetic abrasive (0.25 mg) showed the strongest magnetic force due to its high susceptibility. This made the highest material removal as well as deep scratches on the surface. This force was 1.6 times stronger than the mixed-type magnetic abrasive (0.6 mg) and 2.6 times stronger than that of 304 stainless steel case. The case of 304 stainless steel tool (∅0.24×4 mm, 1.55 mg) and magnetic abrasive (0.25 mg) exhibited the weakest magnetic force as expected due to its magnetic properties. With the tool instable motion during process, this case resulted in insufficient material removal. In order to increase the magnetic force, some portions of magnetic abrasive were substituted with iron

particle (hybrid method). The mixture of 304 stainless steel tool, iron particle (0.24 mg), and magnetic abrasive (0.06 mg) were applied and showed stronger magnetic force than the mixed-type magnetic abrasive case. Even though the force of hybrid method is weaker than the case of carbons steel tool, the method produces smoother surface with uniform surface asperities as well as with increased material removal. This can allow the method is applicable for the internal deburring of flexible capillary tubes.

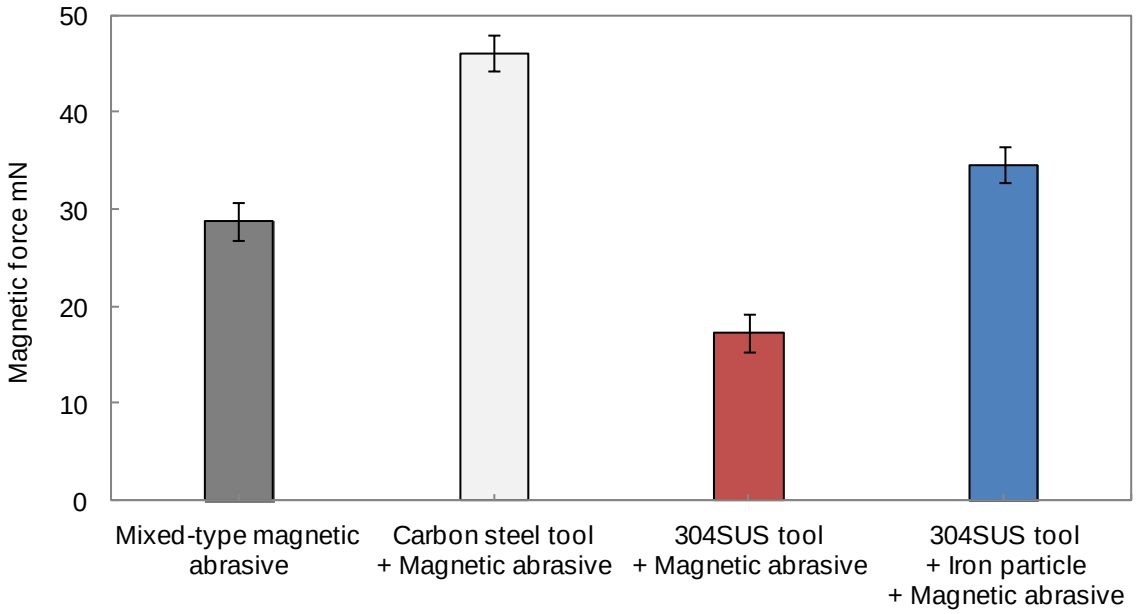

Figure 3-19. Relationship between finishing force and experimental condition

3.3.3 Hybrid Finishing Methods for Flexible Capillary Tube

Based on the fundamental understanding of the ferrous tools, the hybrid method was applied to the internal finishing of flexible capillary tubes. Experiments were conducted using 304 stainless steel flexible capillary tubes (Tube B: OD 1.36 mm, ID 1.02 mm, Figure 3-1(B)). During the micro laser machining process, molten material re-solidified and adhered all over the surface; burr heights were measured by an optical

profilometer to be in a range between 70 and 90 μm. The slit pitch (distance between slits) was about 400 μm, as shown in Figure 3-21(A).

At first, mixed-type magnetic abrasive, a mixture of 1.20 mg iron particles and 0.33 mg magnetic abrasive, was inserted into the tube with a carbon steel rod (∅0.50×4 mm). The abrasive mixture and the rod occupied 46.8 vol% of the finishing area of the tube. The finishing experiments were performed for 30 min, during which time the poles made a total of 155 four-millimeter reciprocating strokes at 0.69 mm/s. As shown in Figure 3-21(B), the re-solidified material adhered to the surface and edges were clearly removed after finishing. The surface was not finely finished (0.24 μm *Ra*, 0.2 mg/mm), which was previously shown to be a trend of the process using a carbon steel rod.

Table 3-3. Experimental conditions of internal deburring of flexible capillary tube with laser machined slits: Tube B

Workpiece	Tube B: 304 stainless steel tube (∅1.36×∅1.02×100 mm)
Workpiece revolution	2500 min^{-1}
Magnetic abrasive	Aluminum oxide (WA) particles (80 μm mean dia.) in magnetic abrasive (<10 μm)
Magnetic tool	Iron particles (-50/+100 mesh, 150 -300 μm diameter), Carbon steel rod (∅0.5×4 mm), 304 Stainless steel rod (∅0.51×4 mm)
Lubricant	Soluble-type barrel finishing compound
Permanent magnet	Nd-Fe-B permanent magnet: 10×12×18 mm
Pole reciprocating motion	Amplitude: 4 mm, Speed: 0.69 mm/s
Workpiece- Pole clearance	0.11 mm
Pole tip	Table 3-1

The experiments were also performed with stainless steel rod (∅0.51×4 mm). The finished edge and surface retained the burrs and re-solidified materials (0.19 μm *Ra*, 0.11 mg/mm) in Figure 3-21(C). The pole reciprocation stroke was extended from 4

to 8 mm, and the pole reciprocation was set for 312 strokes in 120 min. The abrasive mixture, 1.25 mg iron particles and 0.36 mg magnetic abrasive, and the rod occupied 48.8 vol% of the finishing area. Lubricant was added after every 78 pole strokes. As shown in Figure 3-21(D), the burrs were completely removed, and the inner surface was finished to 0.05 µm *Ra* with the rate of 0.27 mg/mm.

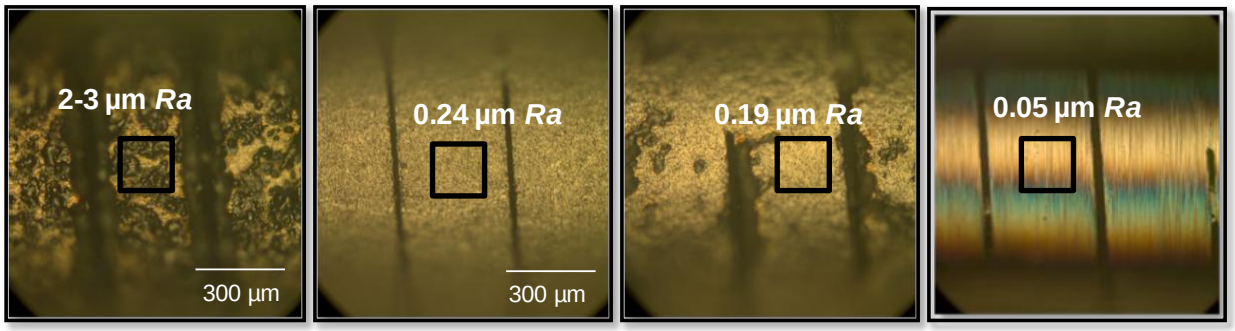

A As-received surface

B Surface machined with carbon steel rod, magnetic abrasive, and iron particles (30 min)

C Surface machined with stainless steel rod, magnetic abrasive, and iron particles (30 min)

D Surface machined with stainless steel rod, magnetic abrasive, and iron particles (120 min)

Figure 3-21. Photographs of tube interior before and after finishing; As-received surface, surface finished with carbon steel rod, magnetic abrasive, and iron particles for 30 min, surface finished with stainless steel rod, magnetic abrasive, and iron particles for 30 min, and surface finished with stainless steel rod, magnetic abrasive, and iron particles for 120 min

In the carbon steel tool, strong magnetic force acting on magnetic abrasive allows removing the burrs completely in short period with high material removal. However, the force caused by 304 stainless steel tool, even though the magnetic force is stronger than that of iron particles, still shows insufficient material removal and requires more processing time for successful surface and edge finishing of flexible capillary tube.

CHAPTER 4
MULTIPLE POLE-TIP SYSTEM USING A METASTABLE AUSTENITIC STAINLESS STEEL TOOL

4.1 Introduction of Multiple Pole-tip System

Use of a magnetic tool facilitates finishing efficiency (reduces processing time) by control of magnetic force. The roles of magnetic tool are to increase magnetic force and to straighten the tube. However, it still requires long finishing time due to limitation in the numbers of finishing spot. To resolve this problem, it is desired to finish multiple areas simultaneously. In order to satisfy this demand, a new method which uses a metastable austenitic stainless steel tool has been proposed.

A metastable austenitic stainless steel rod alternating magnetic and nonmagnetic regions in a body can be fabricated through selective heat treatment. Magnetic abrasive is attracted to the borders of the magnetic regions of the developed tool to create additional finishing points when it magnetized. In combination with a multiple pole-tip system, this unique magnetic property facilitates simultaneous finishing of multiple regions for shortening finishing time. Chapter 4 describes the fabrication, the crystalline structure, and the resulting magnetic properties of the heat-treated metastable austenitic stainless steel tool. The magnetic abrasive behavior, the finishing characteristics, and a mechanism to extend the finished length are clarified for internal finishing of capillaries.

A new system is proposed to improve the finishing efficiency by increasing the number of finishing points and by shortening the length of the pole stroke, and it is used in combination with a partially heat-treated stainless steel tool. This system is called a multiple pole-tip system.

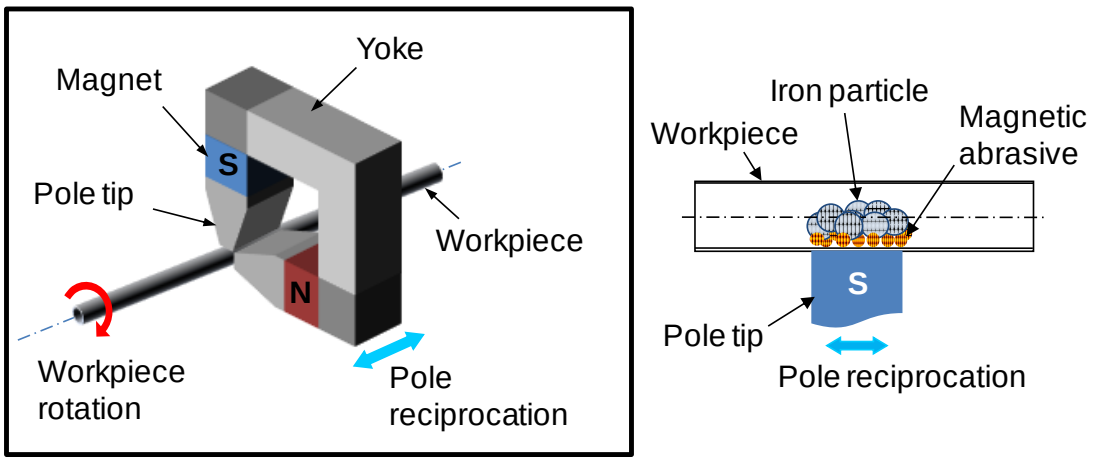

A Single pole-tip system

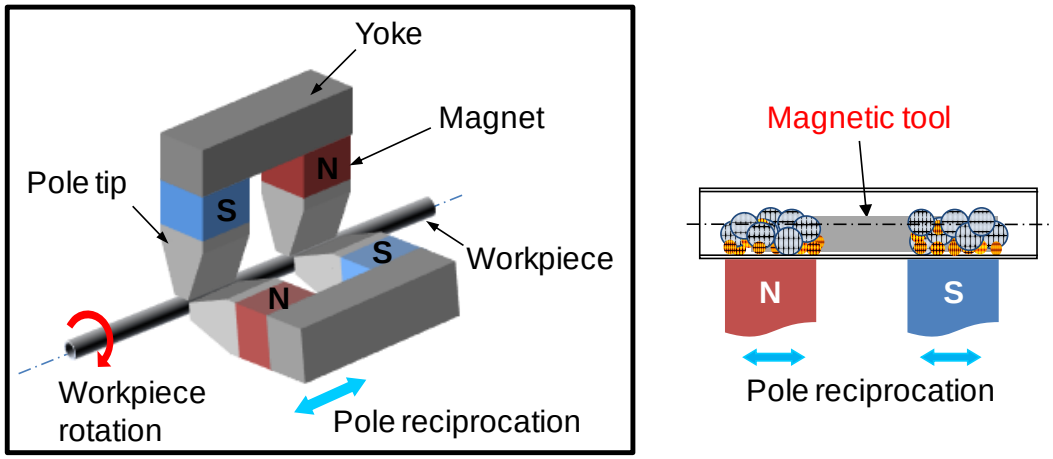

B Multiple pole-tip system

Figure 4-1. Schematics of single pole-tip system and multiple pole-tip system

Figure 4-1(A) shows a schematic of a typical magnetic abrasive finishing setup with a single pair of pole tip which called as a single pole-tip system. The desired magnetic field at the finishing area is generated by two permanent magnets attached to a steel yoke. A mixed-type magnetic abrasive introduced into the tube is pushed by magnetic force against the tube surface and finishes the tube when the tube is rotated at high speed. The pole-tip width is the default finished length, and the accumulation of multiple short-length finishing passes is needed for long tube finishing.

Figure 4-1(B) conceptually shows the proposed method to extend the default finished length. An additional pair of pole tips is added (yoked together as shown Fig. 4-1(B)) and a long magnetic tool is placed inside the tube. The mixed-type magnetic abrasive is introduced into two sections inside the tube; this doubles the default finished length and, thus, doubles the finishing efficiency. A tool with alternating magnetic and non-magnetic sections is introduced inside the tube with a mixture of magnetic abrasive and iron particles. The length of the magnetic section of the tool corresponds to the pole-tip width. The magnetic abrasive follows the lines of magnetic force and accumulates at the borders of the magnetic sections of the tool, thereby creating multiple finishing areas. The magnetic abrasive pushes the inner surface of the tube, and, when the tube is rotated at high speed, it exhibits relative motion against the tube surface and removes material. By feeding the magnetic pole-tip assembly along the tube axis, the magnetic abrasive and the tool are both dragged by magnetic force, and the finished area is extended.

4.2 Magnetic Properties of Metastable Austenitic Stainless Steel Tool

The key to realizing the multiple pole-tip system is the use of a tool that has alternating magnetic and non-magnetic sections; this is accomplished by using a metastable austenitic stainless steel tool, 304 stainless steel is used for this study. Once the stainless steel has undergone cold working or strain hardening by plastic deformation, it experiences a martensitic transformation and exhibits ferromagnetism. However, the austenitic phase can be retrieved (and thus exhibit nonmagnetic properties) by heat treatment beyond the Curie temperature (at least 600 °C) [60,61]. This treatment can make multiple alternations in the magnetic property of a single tool. In this study, the tool was partially heat treated using the flame of butane lighter in

ambient conditions for 30 s. After the heat treatment, the tool was cooled in air to room temperature.

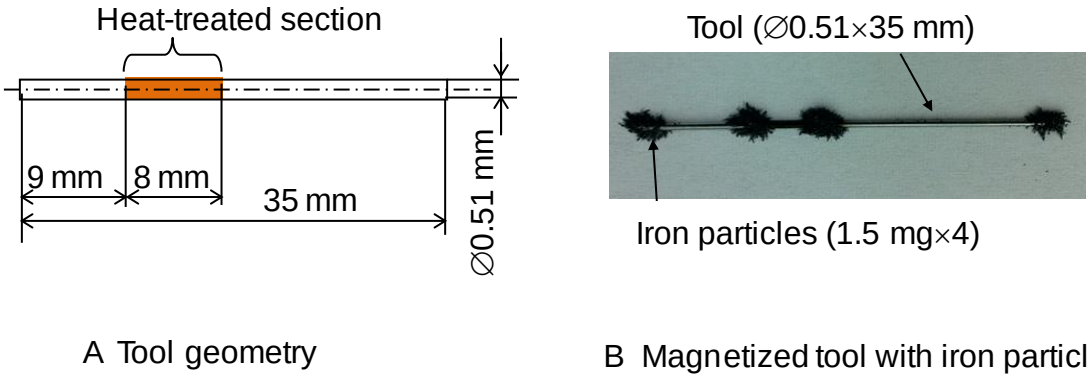

Figure 4-2. Tool geometry and photograph of partially heat-treated stainless steel tool with iron particles (Photograph courtesy of Junmo Kang)

Figure 4-2 shows the geometry and a photograph of partially heat-treated stainless steel tool with iron particles. The untreated sections of the tool exhibit magnetic anisotropy due to the plastic deformation of the manufacturing process, and the heat-treated section exhibits paramagnetism due to fully austenitic condition. The iron particles are attracted to the borders of the ferromagnetic sections. The crystal structures of the tool were characterized using an X-ray diffractometer (XRD: Copper anode (Cu Kα wavelength: 1.54 Å)) at room temperature. The X-ray beam penetrates 5 μm from the surface. Figure 4-3 shows XRD patterns of the untreated and the heat-treated sections of the stainless steel tool. Both body-centered cubic (bcc) and face-centered cubic (fcc) structures are observed in the untreated section. The bcc structure must have been generated during the previous tube drawing process. In the heat-treated section, only an fcc structure is observed. This confirms that the applied treatment locally retrieved the fcc structure (austenitic phase) in the surface layer.

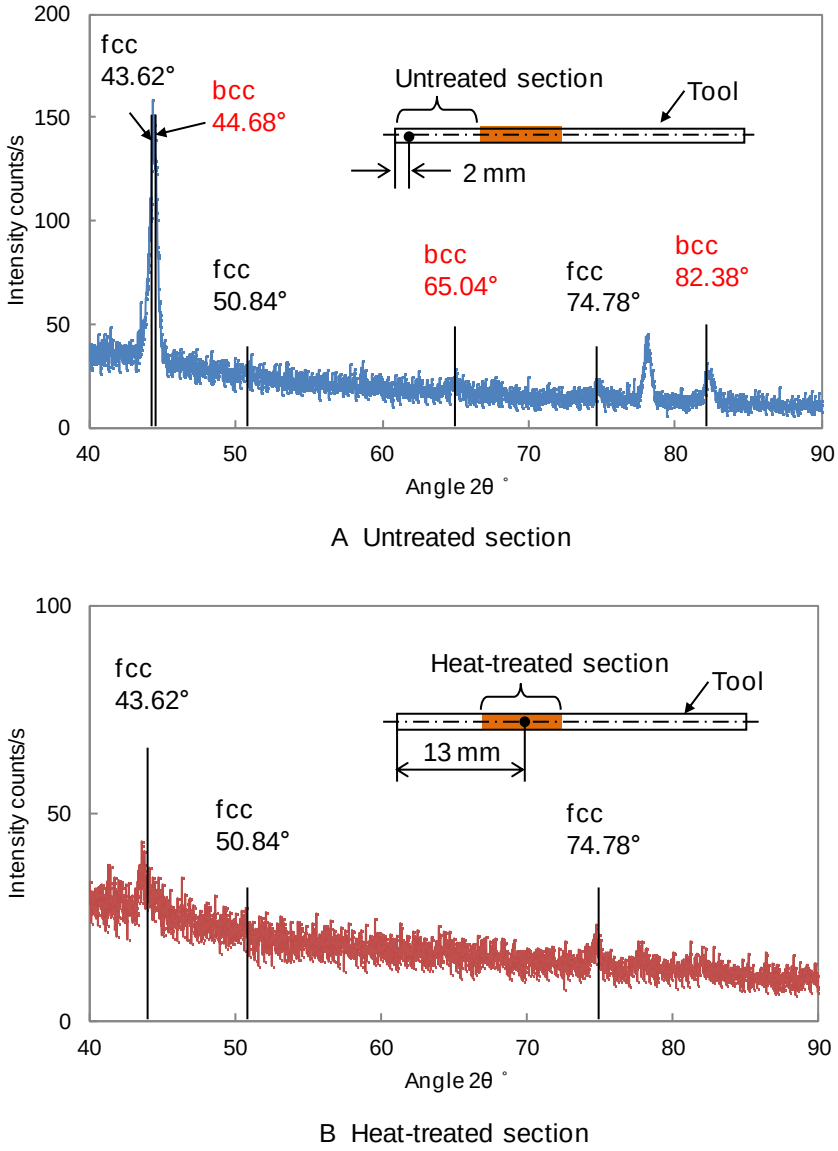

Figure 4-3. Partially heat-treated stainless steel tool and X-ray diffraction patterns; Untreated section and Heat-treated section

4.3 Finishing Characteristics in Multiple Pole-tip System

4.3.1 A Method to Deliver Magnetic Abrasive Deeper into Capillary Tube

For capillary tube finishing, the finished surface quality obtained using the stainless steel tool has not reached the level of the single pole-tip (pair) system [35]. Moreover, it was observed that unstable tool motion occasionally creates a poorly

finished surface. Practically, the finishing area corresponding to the pole tip farthest from the open end of the tube (i.e., toward the machine chuck) tends to show a poorly finished surface. Using magnetic pole tips placed outside the tube, magnetic abrasive can be introduced into the tube by means of magnetic force; however, some magnetic abrasive typically remains on the inner surface of the tube instead of being dragged by the magnet. This is because of friction against the tube inner surface and is unavoidable. To alleviate this situation, the magnetic force acting on the magnetic abrasive must be increased enough to overcome the friction.

The force can be controlled by the magnetic field, and adjusting the pole-tip geometry is a simple way to control the magnetic field [65]. Two kinds of pole tips were prepared (as shown in Figure 4-4(A)) to examine the effects of the magnetic field on the delivery of the magnetic abrasive into the area corresponding to the chuck-end pole tip: straight and tapered in the axial direction.

Figure 4-4(B) shows the relationship between the magnetic flux density (measured by a hall sensor (∅1.0 mm sensing area)) of the pole-tip set and the distance *X*. The condition in which the center of the sensing area is placed over the pole edge was *X*=0 mm. A higher magnetic flux density and a larger gradient were obtained above the tapered pole tip B, compared to the values measured above the straight pole tip A [66]. This indicates that the tapered pole tip B generates greater magnetic force acting on the magnetic abrasive. The interaction of the pole tips increased the magnetic flux density between the pole tips. The magnetic abrasive tends to be attracted by these inward edges more than outward edges.

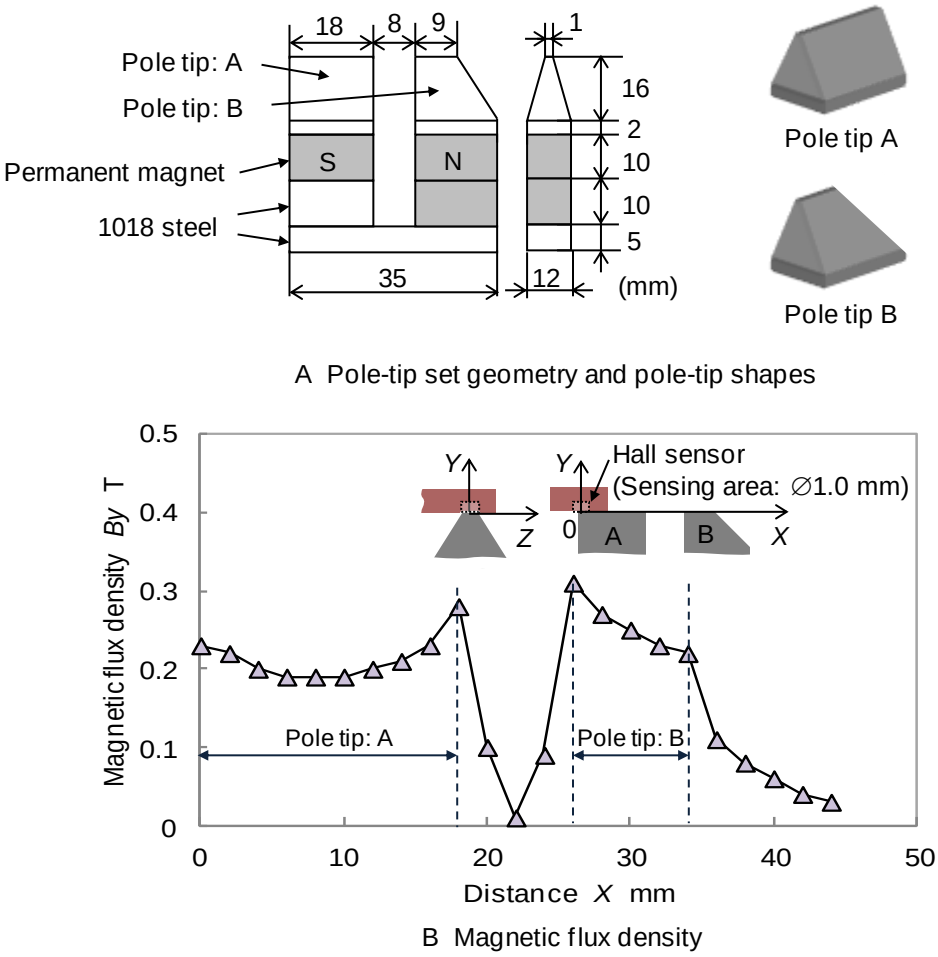

Figure 4-4. Geometry of pole-tip set geometry and pole-tip shapes and changes in magnetic flux density

Photograph of finishing unit is shown in Figure 4-5 and the finishing conditions are listed in Table 4-1. The case where pole tip A is mounted close to the free end of the tube is called the 18-8-9 pole-tip set, and the opposite configuration is called the 9-8-18 pole-tip set. In the both cases, the two pole-tip sets were mounted at an angle of 90º, as illustrated in Figure 4-1(B). The supplied amount of magnetic abrasive was determined based on the space inside the tube corresponding to the pole tip, and 47 % of the volume was occupied by the magnetic abrasive.

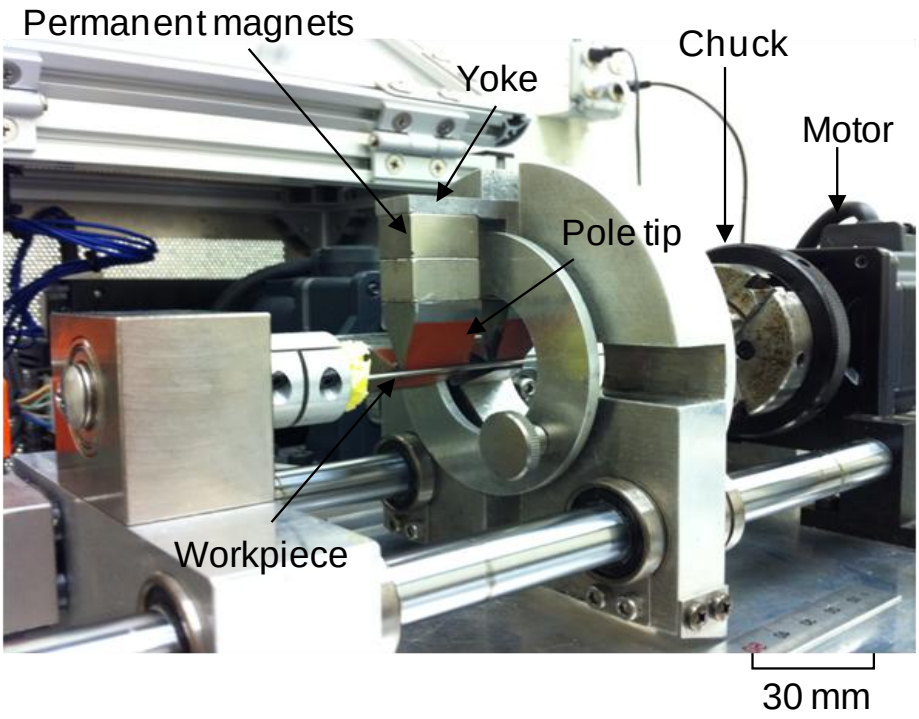

Figure 4-5. External view of multiple pole-tip system (9-8-18 pole-tip set) (Photograph courtesy of Junmo Kang)

As Table 4-1 shows, 8 mg for pole tip A and 4 mg for pole tip B were initially supplied into the tube. When the pole tip is fed toward the chuck end of the tube, the magnetic abrasive suspended at the area corresponding to the other end of pole tip A moves toward the chuck end, but some of the magnetic abrasive particles adhere to the surface of the tube due to friction. When the pole tip returns to its original position, the chuck-end pole tip attracts some magnetic abrasive and drags it along the tube surface. This back-and-forth motion can be used as a mechanism to convey the magnetic abrasive into areas deeper in the tube. The pole stroke was initially set at 26 mm, which is the length that causes the inner edge of pole tip B to reach the farthest edge of pole tip A in the 9-8-18 case.

Table 4-1. Experimental conditions for 9-8-18 and 18-8-9 pole-tip set

Workpiece	304 stainless steel tube (∅1.27×∅1.06×100 mm)	
Pole-tip type	9-8-18 pole-tip set (18 mm inside) 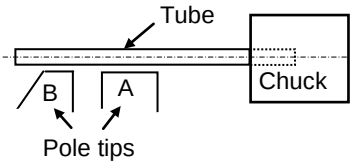	18-8-9 pole-tip set (9 mm inside) 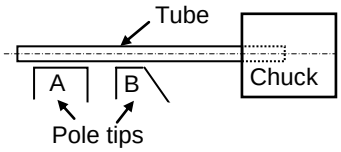
Workpiece revolution	2500 min^{-1}	
Ferrous particle	Iron particles (-50/+100 mesh, 150-300 μm dia.): 80 wt% + Aluminum oxide (WA) particles (80 μm mean dia.) in magnetic abrasive (<10 μm): 20 wt%	
Amount of ferrous particle	Pole tip A: 8 mg, Pole tip B: 4 mg	
Magnetic tool	Heat-treated 304 Stainless steel rod: ∅0.51×35 mm	
Lubricant	Soluble-type barrel finishing compound (pH 9.5, 755 mPa·s at 30°C)	
Pole reciprocating motion	Speed: 0.59 mm/s, Stroke length: 26 mm Number of strokes: 117	
Workpiece- Pole clearance	0.11 mm	
Processing time	174 min	

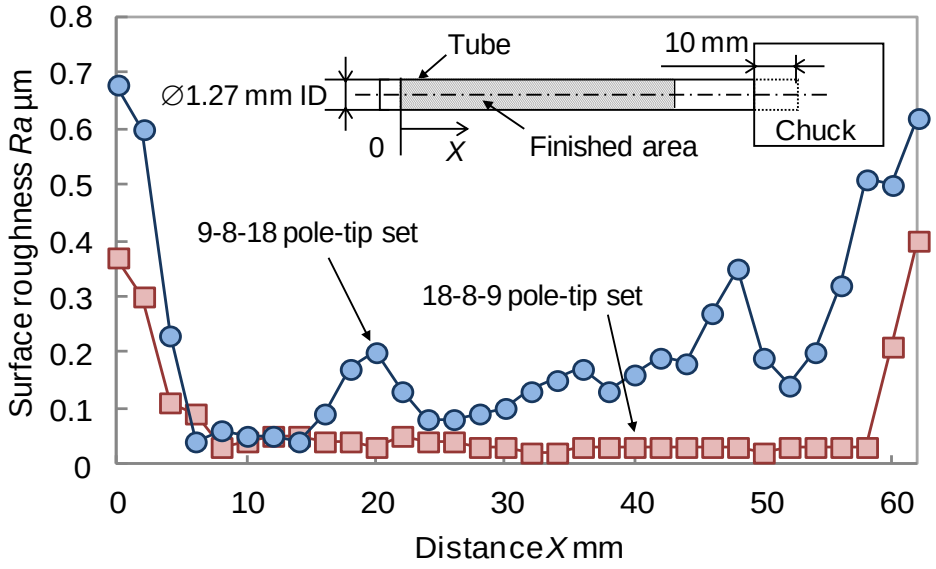

Figure 4-6. Changes in surface roughness with distance *X*

Figure 4-6 shows the changes in surface roughness *Ra* with distance *X*. While the 18-8-9 pole-tip set produced a uniformly finished surface, the roughness increased with the distance *X* in the case of the 9-8-18 pole-tip set. In the 18-8-9 case, the magnetic abrasive is sufficiently distributed by the magnetic field to produce a uniformly finished surface. In the 9-8-18 case, the area corresponding to the chuck-end edge of pole tip A must have the least amount of magnetic abrasive before any pole-tip feed motion. The area beyond *X*=17 mm in the 9-8-18 condition must lack magnetic abrasive from the beginning of the experiments, and the area between *X*=17 and *X*=43 mm must be finished using the magnetic abrasive delivered by the abovementioned mechanism. However, the amount of the magnetic abrasive decreases with increasing distance *X* and must be insufficient for finishing. The experiments confirm that the magnetic abrasive must be sufficiently distributed and that the magnetic field distribution and pole feed length are keys to effectively convey the magnetic abrasive.

4.3.2 Effects of Heat-treated Sections on Internal Deburring of Flexible Capillary Tubes with Multiple Laser-machined Slits

Experiments were conducted using 304 stainless steel flexible capillary tube (1.36 mm OD, 1.02 mm ID, and 100 mm long). Random, irregular burrs and obstacles, 50~70 μm in height, can be seen in Figure 4-7(A), which shows representative micrographs of the as-received surface. The slot pitch (distance between slots) was about 400 μm. In addition to the pole stroke length of 26 mm, a short stroke length of 8 mm was applied for this study. The gap between pole tips is 8 mm, so that is theoretically the shortest stroke that can convey the magnetic abrasive from the inner edge of pole tip A to the adjacent edge of pole tip B. The other conditions are shown in Table 4-1.

In the case of the 8 mm pole stroke, burrs and obstacles remained in the area corresponding to pole tip B (beyond *X*=24 mm, which is slightly shorter than the pole tip width and pole stroke length combined: 18+8 mm). The burrs and obstacles must prevent the introduction of the magnetic abrasive into the area, and the magnetic abrasive must stay at the area corresponding to pole tip A. While the 8 mm stroke causes the inner edge of pole tip A to reach the adjacent edge of pole tip B, the lack of any overlap of these edges makes the stroke too short to adequately convey the abrasive to pole tip B. As a result, the lack of mixed-type magnetic abrasive beyond that point allows burrs and obstacles to remain.

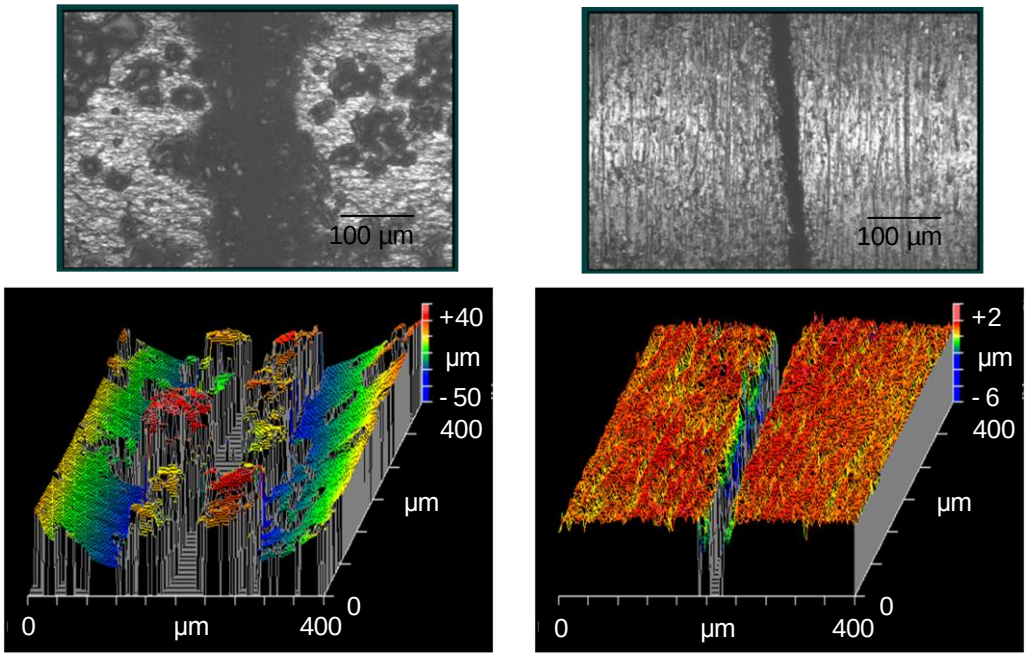

A As-received condition B Finished condition

Figure 4-7. Intensity maps of surface and three-dimensional surface shapes measured by optical profiler

On the other hand, the overlap of the poles with the 26 mm pole stroke must deliver the abrasive more completely (than the 8 mm stroke) to the area corresponding to pole tip B, resulting in the successful machining. Figures 4-7(A) and (B) show the

intensity maps and three-dimensional surface shapes (measured by optical profiler) of the as-received surface and surface finished with the 26 mm pole stroke length conditions respectively. It is seen that both burrs and obstacles were removed by the proposed method and that the surface was uniformly finished from 2.5-3.5 μm *Ra* to 0.3-0.4 μm *R*a. This demonstrates that the proposed abrasive delivery method enables the feasibility of the MAF process for the internal finishing of flexible tubes, regardless of the presence of large burrs and obstacles.

4.3.3 Effects of Heat-treated Sections on Finished Surface and Abrasive Behavior

The effects of the tool behavior in the multiple pole-tip system were experimentally studied using tools with three kinds of magnetic properties. Figure 4-8 shows a photograph of four magnetized 54 mm long tools with iron particles: Tool A is made of carbon steel, Tool B is 304 stainless steel, and Tool C is partially heat-treated 304 stainless steel. In the case of Tool A, the iron particles are more attracted by the tool ends because of the residual magnetism and magnetic shape anisotropy. Tool B exhibits magnetic anisotropy, which was generated during cold work (deformation-induced martensite transformation), and the iron particles are attracted to the tool ends only. In the case of Tool C, the iron particles are attracted to both ends of magnetic regions following the residual magnetism. The center region (18 mm long) of the stainless steel Tool C was heat-treated, and it has a face-centered-cubic structure [35]. This crystal transformation diminishes the magnetism and divides the magnetic section into two regions [35,62,63].

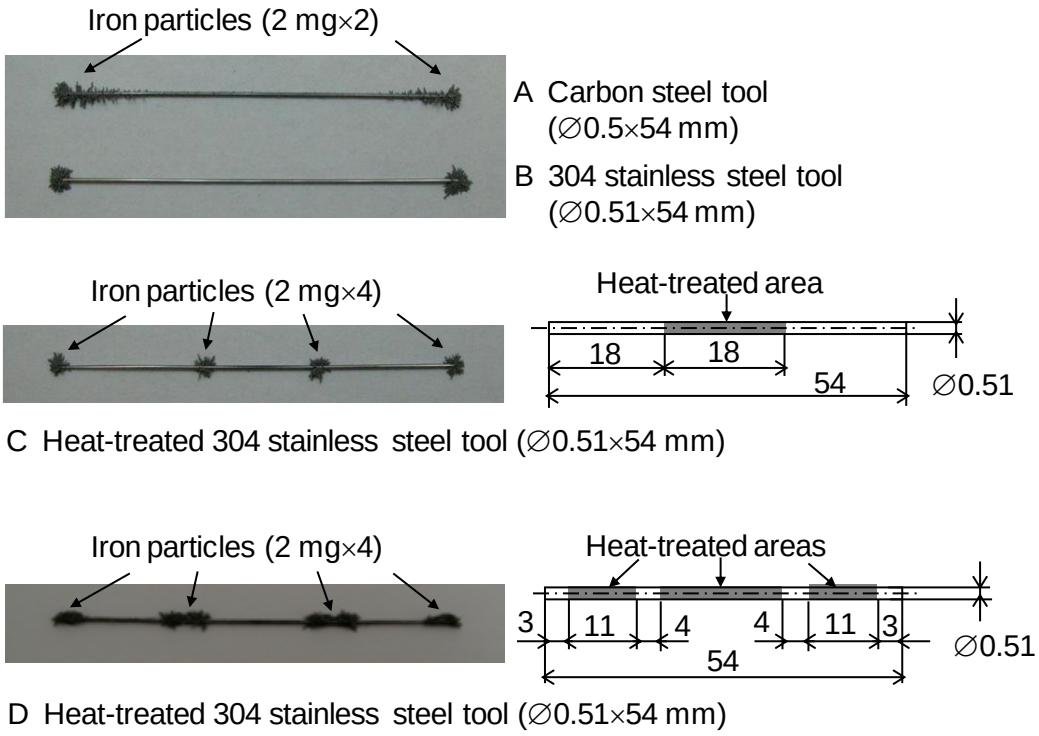

Figure 4-8. Magnetized tools A, B, C and D with iron particles (Photograph courtesy of Junmo Kang)

Figure 4-8(D) shows the configuration of the heat-treated magnetic tool (Tool D) with a photograph of magnetic abrasive with the tool based on that design. The magnetic abrasive is attracted to the borders of the magnetic regions. Compared to Tool C (Figure 4-8(C)), this doubled the number of the places where the magnetic abrasive is held.

Each tool was inserted in a clear polypropylene plastic tube (3 mm outer diameter, 0.7 mm wall thickness), which was set on the machine shown in Figure 4-10. Eight milligrams (8 mg) of a mixture of iron particles and magnetic abrasive was supplied with the magnetic tool. The pole-tip set was fed at 0.59 mm/s, and the feed length was set at 18 mm. The tube was rotated at 200 min^{-1}, and the behavior of the tool, and mixed-type magnetic abrasive inside the tube was observed.

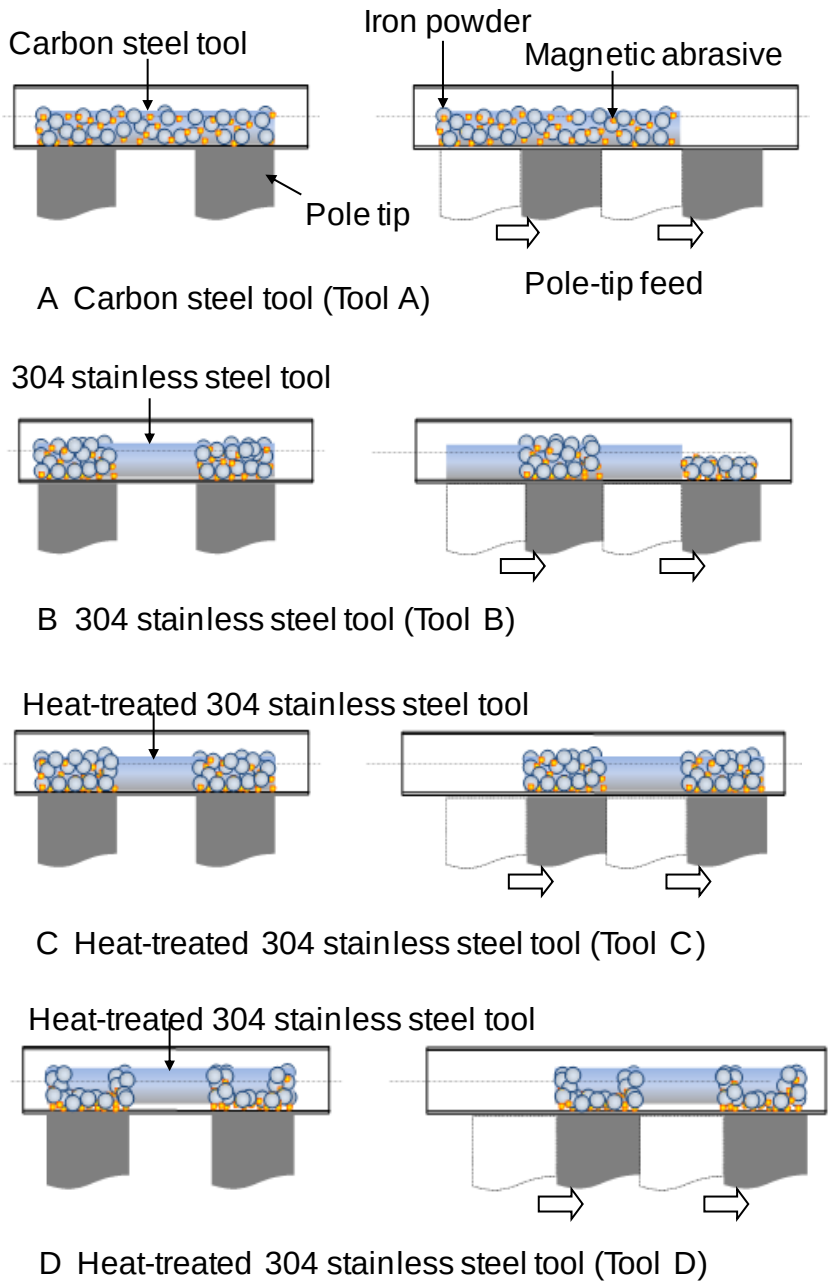

Figure 4-9. Motions of each tool with mixed-type magnetic abrasive for a pole-tip stroke length of 18 mm

Figure 4-9 schematically shows the behavior of the magnetic tools with mixed-type magnetic abrasive while the tube is rotated. Figure 4-9(A) is the case with Tool A. Initially, the mixed-type magnetic abrasive was supplied into two regions corresponding to the pole tips. Once the pole-tip set started moving, some mixed-type magnetic

abrasive stuck to the carbon steel tool surface regardless of the pole-tip motion because of the ferromagnetism of the tool. The carbon steel tool pushes the mixed-type magnetic abrasive against the inner tube surface with a strong magnetic force. This increases the friction force between the tool and inner surface of the tube, and this friction force prevented the tool from following the pole-tip feed in the experiment.

Figure 4-9(B) shows the case of Tool B, which exhibits anisotropic magnetism and lower magnetic susceptibility than the mixed-type magnetic abrasive. The mixed-type magnetic abrasive separated into two finishing sections because it is attracted to the pole tips more than to Tool B. Tool B simply lies on the mass of magnetic abrasive. While the pole tips are moving, the mixed-type magnetic abrasive follows the pole-tip motion. Both ends of Tool B are attracted to the magnetic field according to its anisotropic magnetism; Tool B thereby stays in its initial position regardless of the pole-tip and magnetic abrasive motion.

Figure 4-9(C) shows the case with Tool C. The borders of magnetic regions of the tool correspond to the pole-tip edges and are attracted to the magnetic field. The mixed-type magnetic abrasive is attracted by the pole tips, and once the pole tips are fed along the tube axis; both the mixed-type magnetic abrasives and tool follow the pole-tip motion. As a result, the magnetic abrasive shows smooth relative motion against the tube inner surface needed for internal tube surface finishing. This experimental observation demonstrates the conditions required facilitating the deliverability of the tool and magnetic abrasive in the multiple pole-tip system by conforming to the pole-tip motion, that is, the tool must have alternating magnetic and

non-magnetic regions, and the borders of the magnetic region of tool must correspond to the pole tip edges.

In the multiple pole-tip system using the 54 mm long Tool C, the default finished length is the region corresponding to two 18 mm wide pole tips. If the pole-tip feed is sufficient to cover the gap between two pole tips (18 mm), the 72 mm length should be finished uniformly. In practice, some mixed-type magnetic abrasive adheres to the surface of the tube because the friction between the mixed-type magnetic abrasive and tube surface exceeds the magnetic force acting on the mixed-type magnetic abrasive to follow the pole tip motion. The region corresponding to the chuck-end edge of the pole tip must have the least amount of magnetic abrasive. As a result, the deeper the finishing area was in the tube, the rougher the finished surface was due to the lack of magnetic abrasive. Accordingly, the initial insertion of magnetic abrasive deeper into the tube and the deliverability of the mixed-type magnetic abrasive play important roles in accomplishing the desired finishing performance. The alternating magnetic property and the interval between the magnetic and nonmagnetic regions must be designed to satisfy these matters.

In the case of Tool C (Figure 4-9(C)), magnetic flux flows from one end of the magnetic region to the other end, and the magnetic abrasive is attracted following the flow of magnetic flux. In turn, tube surface finishing is predominantly performed in four places. If the length of the magnetic region is reduced from 18 mm to 3–4 mm, and a region is created on the tool corresponding to each pole-tip edge, the magnetic flux concentrates at the pole-tip edges, doubling the number of borders to attract magnetic abrasive. Finishing is dominantly performed at the four regions where the mixed-type

magnetic abrasive is encouraged to remain by the tool/pole configuration. Visual observation of Tool D with mixed-type magnetic abrasive in a transparent polymeric tube (Figure 4-9(D)) showed that Tool D holds the mixed-type magnetic abrasive at four places and that the pole-tip motion is smoothly followed.

The geometry of pole-tip sets in both single and multiple pole-tip systems used in experiment are shown in Figure 4-10. The width of the pole tip, which defines the default finished length, is 18 mm. The pole-tip set for the single pole-tip system has two magnets. In the case of the multiple pole-tip system, each pole tip has one magnet, and the two magnets are coupled by a steel yoke, which is 54 mm long (parallel to the workpiece axis).

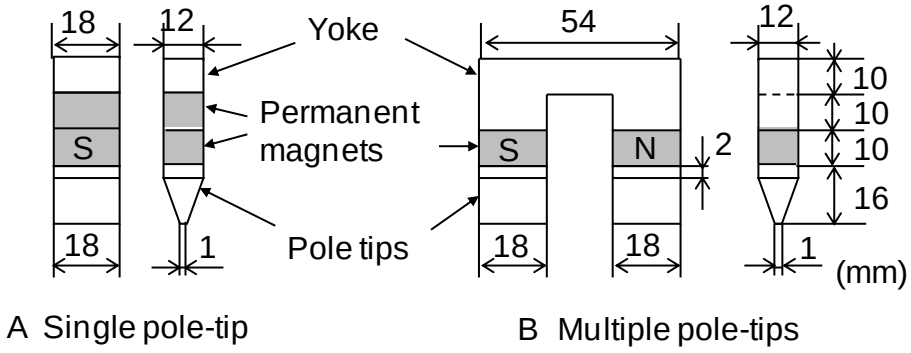

Figure 4-10. Geometry of single and multiple pole-tip sets

Figure 4-11 shows changes in magnetic flux density B_y, measured by a Hall sensor (sensing area: ∅1.0 mm), with distance X in both pole-tip systems. There is no significant difference in the magnetic flux density B_y between the two systems. Both systems show a similar trend: the magnetic flux density and its gradient increase from the center toward the edges of pole tips. The magnetic abrasive is attracted by magnetic force toward the pole-tip edges. Without assistance of a magnetic tool, this

trend encourages the plugging of the magnetic abrasive in the region corresponding to the pole-tip edges when the tube ID is less than 1 mm.

Table 4-2 shows the experimental conditions. Stainless steel tubes (1.27 mm OD, 1.06 mm ID, 100 mm long, initial surface roughness: 2–3 μm *Rz*) were prepared. Ten millimeters at one end of the tube was chucked, and the other end was supported by a flexible jig to reduce run-out during rotation. The tube rotational speed was set at 2500 min^{-1}. The pole-tip feed length and rate were set at 18 mm and 0.59 mm/s, respectively. The finishing experiments began 5 mm from the free tube end. In the case of the single pole-tip system, mixed-type magnetic abrasive 15 mg (80 wt% ferrous particles and 20 wt% magnetic abrasive) was supplied, which took up 45.3 % of the enclosed volume of the finishing area. In the multiple pole-tip system, 47.3 % of the volume at each finishing area was taken up (24.2 % by the mixed-type magnetic abrasive and 23.1 % by the stainless steel tool). In both cases, 90 μL of lubricant was initially supplied into the tube, and 50 μL was added after every 20 pole-tip strokes. For each finishing experiment, the total number of pole-tip strokes was 180. After each experiment, the tube was cleaned using ethanol in an ultrasonic cleaner and sectioned along the tube axis. The inner surface was evaluated using an optical surface profiler and a stereomicroscope. The optical surface profiler has a lateral resolution of 275.7 nm and a vertical resolution of <0.1 nm. The material removal was calculated by comparing the weight (measured using a micro-balance with 10 μg resolution) before and after finishing. The finishing experiment was repeated at least three times under each condition to confirm the representative trends using the finishing equipment shown in Figure 4-12.

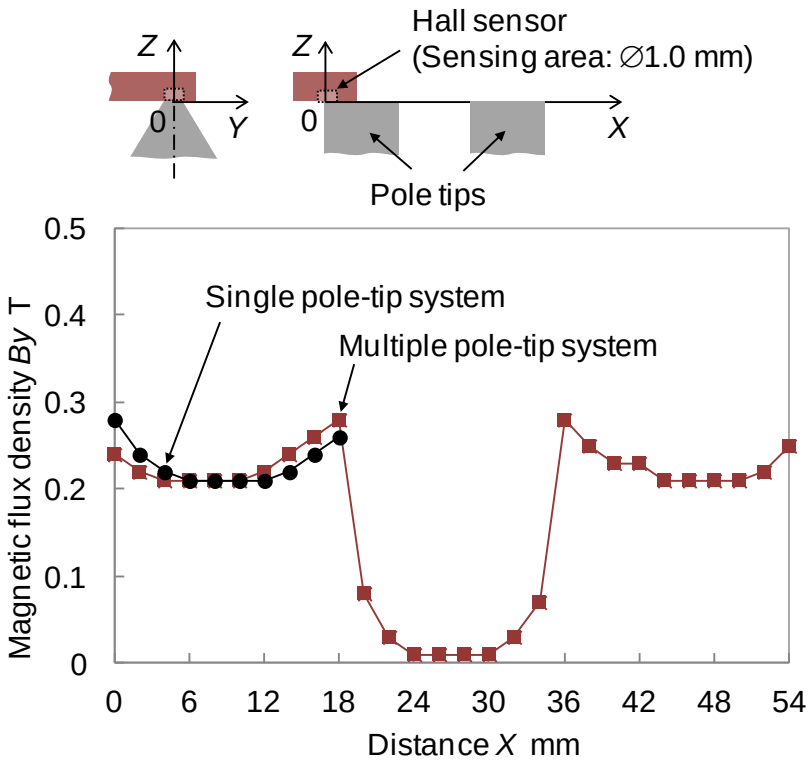

Figure 4-11. Changes in magnetic flux density of single and multiple pole-tip system with distance *X*

Table 4-2. Experimental conditions for 18-18-18 pole-tip set

Workpiece	304 stainless steel tube (∅1.27×∅1.06×100 mm)		
Workpiece revolution	2500 min^{-1}		
Pole-tip feed	Speed: 0.59 mm/s, Number of strokes: 180		
Workpiece-pole-tip clearance	0.3 mm (Polytetrafluoroethylene (PTFE) tape thickness)		
Lubricant	Soluble-type barrel finishing compound (pH: 9.5, Viscosity: 755 mPa·s at 30°C)		
Pole-tip system	Single pole-tip system	Multiple pole-tip system	Multiple pole-tip system
Pole-tip stroke length	18 mm	18 mm	18 mm
Magnetic tool	—	Tool C (Figure 4-8(C))	Tool D (Figure 4-8(D))
Iron particles (150-300 μm dia.) : 80 wt%	12 mg	6.4 mg × 2	6.4 mg × 2
Aluminum oxide (WA) magnetic abrasive (<80 μm mean dia.) : 20 wt%	3 mg	1.6 mg × 2	1.6 mg × 2

Section 4.3.3 will discuss the characteristics of a 72 mm long tube finished using Tool C and Tool D in the multiple pole-tip system. The finishing experiments using the single pole-tip systems will also be discussed for comparison. In the case of single pole-tip system, to finish the same 72 mm length, requires a two-step process with 18 mm pole-tip feed stroke.

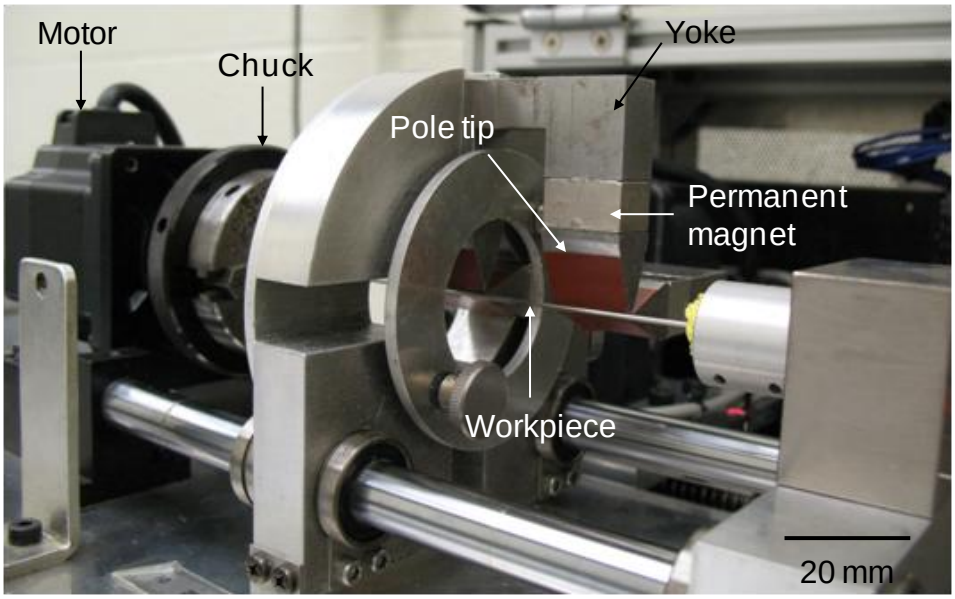

Figure 4-12. External view of multiple pole-tip system (18-18-18 pole-tip set) (Photograph courtesy of Junmo Kang)

Figure 4-13 shows the relationship between surface roughness (the average of ten measurements) and distance *X* in the cases of the multiple pole-tip system using Tool C, multiple pole-tip system using Tool D, and single-pole tip system. No magnetic tool was used in the single pole-tip system (Table 4-2). The roughnesses at *X*=0 and 74 mm are measurements of unfinished surfaces. In the MAF process, the finishing operation is performed by masses of mixed-type magnetic abrasive aligned with the lines of magnetic force. Due to the unstable mixed-type magnetic abrasive motion, the finishing capability generally diminishes at the borders corresponding to the pole tip

edges. As a result, the areas around *X*=0, 36, and 72 mm were less finished, which is more clearly shown by the results from the single pole-tip system.

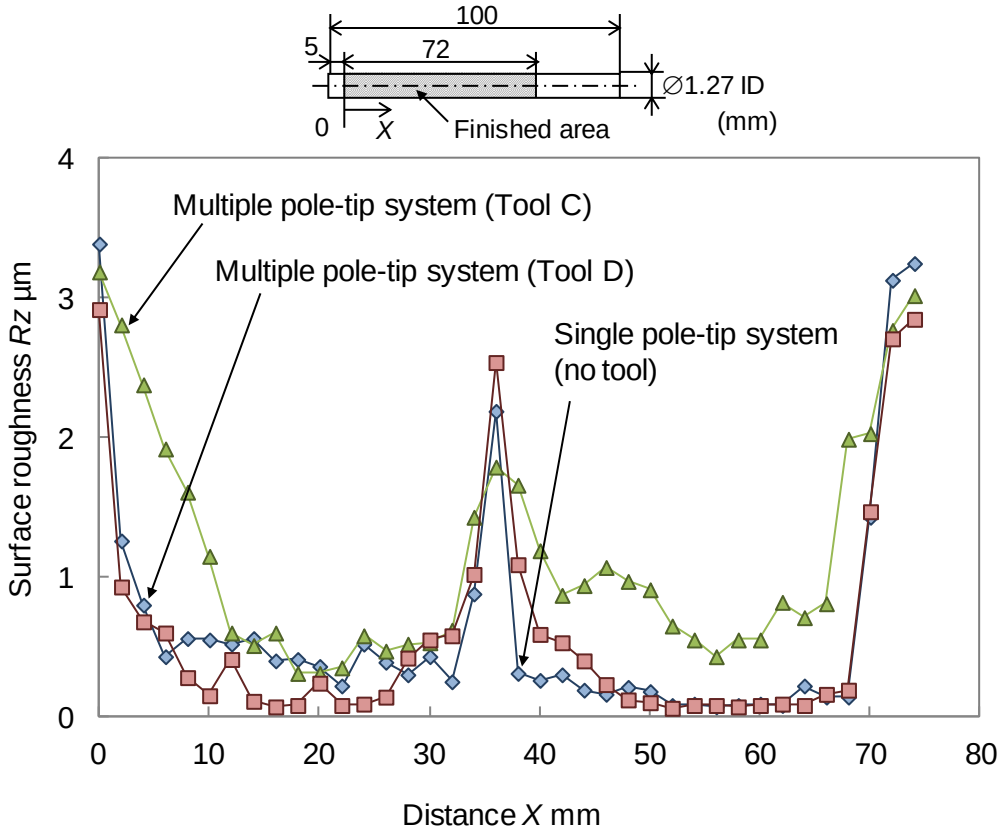

Figure 4-13. Changes in surface roughness with distance *X*

The material removal realized by the multiple pole-tip system using Tool C was 7.85 mg, and it was about one third of that per finishing step of the single pole tip system: 12.98 mg (by the first step) and 11.05 mg (second step). The number of cutting edges active at each finishing area in the Tool C case is estimated to be about half the number in the single pole-tip system. The single pole-tip system does not use a tool, and the mixed-type magnetic abrasive forms chains by magnetic force conforming to the shape of the tube. In turn, the mixed-type magnetic abrasive removes the material not only from the peaks but also the slopes of the surface asperities over the finishing

area, as long as the mixed-type magnetic abrasive enters the valley of the surface asperities. In contrast, the multiple pole-tip system uses a tool (a solid rod), and the mixed-type magnetic abrasive sandwiched between the tube surface and tool at the regions corresponding to the pole-tip edges plays a major role in removing the material.

As mentioned above, in the case using Tool C, some mixed-type magnetic abrasive adheres to the surface of the tube because the friction between the mixed-type magnetic abrasive and tube surface exceeds the magnetic force acting on the magnetic abrasive. The region corresponding to the chuck-end edge of the pole tip must have the least amount of mixed-type magnetic abrasive regardless of the back-and-forth motion of the pole-tip. This lack of abrasive also discouraged the finishing operation. Accordingly, less mixed-type magnetic abrasive is involved in the cutting performance in the multiple pole-tip system using Tool C than that in the single pole-tip system case. The difference in the material removal rates and surface improvement is attributed to these different mechanisms.

The multiple pole-tip system using Tool D smoothly finished the surface in an area deep inside the tube, corresponding to the pole tip located closest to the chuck. A roughness was achieved similar to that in the single pole-tip system case. This resulted from the relative motion of the sufficiently distributed mixed-type magnetic abrasive guided by the tool against the tube surface. After finishing with Tool D, the material removal of 14.2 mg is approximately twice that obtained in the Tool C case, but the material removal per length 0.20 mg/mm is calculated about half of the single pole-tip system (0.36 mg/mm). The use of a solid tool encourages the amount of mixed-type magnetic abrasive participating in the finishing performance and pushes it against the

tube surface more strongly than Tool C. However, since the material is predominantly removed from the peaks of the surface asperities, the material removal rate must be lower than the case with the single pole-tip.

High values of surface roughness, similar to the unfinished surface, are measured at the center of the finished area. They should be eliminated by enhancing the mixed-type magnetic abrasive to contact with the tube surface, which can be achieved by extending the pole-tip feed. Although the finishing result is not shown in this paper, the roughness peak exhibited around X=36 mm in the case of the single pole-tip system was eliminated by lengthening the pole-tip feed to 24 mm in the first phase and 18 mm in the second phase. The 6 mm overlap of the finished area between the first and second phases facilitated the material removal from the center area and improved the uniformity of the finished surface. Analogously, extension of the pole-tip feed length should diminish the unevenness of the roughness in the finished area in the multiple pole-tip system. Section 4.3.4 will find a method to determine sufficient pole-tip feed length by studying the relationship between the pole-tip feed, the overlap of finishing area, and the finished surface roughness.

4.3.4 Pole-tip Feed Length and Surface Uniformity

The relationship between the pole-tip feed length and the finishing characteristics, especially surface roughness, are studied here. The finishing experiment starts with the edge of pole-tip set (at X=0), as shown in Figure 4-15. The pole-tip set moves back and forth according to the feed length. The pole-tip takes 61 s for one 18 mm stroke. In this case, the positions X=18 and 54 mm are covered for the longest duration, while the positions X=0, 36, and 72 mm experience almost no coverage. To cover the center area

(*X*= 36 mm), the stroke length is increased and the effects of stroke length on finished area is calculated and the surface is studied.

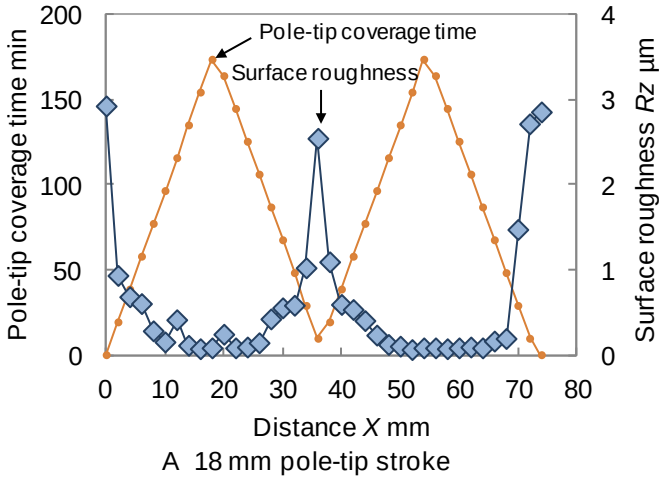

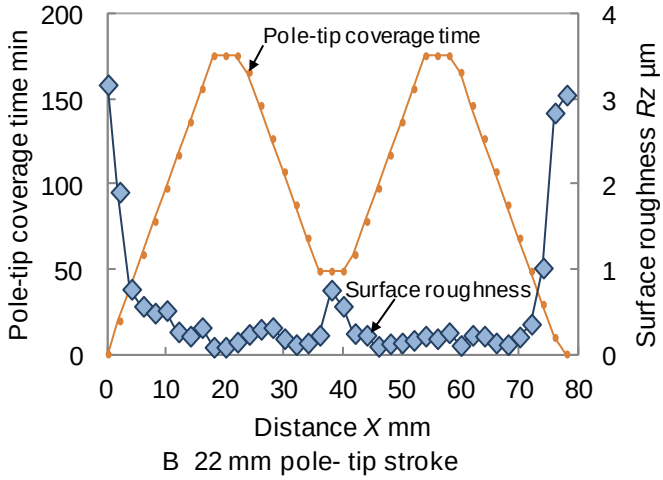

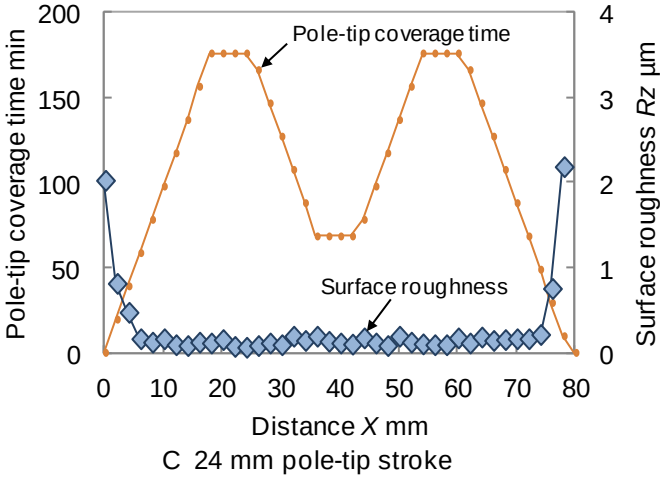

Figure 4-14. Changes in pole-tip coverage times and surface roughness with distance *X*

Figure 4-14 shows the relationship between pole-tip coverage time, roughness of finished surface, and distance *X*. In this study, every 2 mm movement of the pole tip (corresponding to 3.21 s) is plotted as the pole-tip coverage time in the course of one feed. Figure 4-14(A) shows the case with a pole-tip feed of 18 mm. The positions with higher pole-tip coverage times exhibit lower surface roughness. The increase of the pole-tip coverage time increases the contacts between the mixed-type magnetic abrasive and the tube surface and thus facilitates material removal. At *X*=18 and 54 mm, the surface roughness is lower than 0.2 μm *Rz* due to the longest pole-tip- coverage time, 173.4 min, under the conditions. In contrast, the positions *X*=0, 36, and 72 mm exhibit higher roughness due to the lack of contact between the mixed-type magnetic abrasive and tube surface.

The areas between *X*=4 and 32 mm and between *X*=40 and 68 mm have pole-tip coverage times of more than 38.5 min and surface roughness improvement from ~3 μm *Rz* to ~1 μm *Rz*. In other words, to achieve a roughness less than 1 μm *Rz* over the entire finished area, the pole-tip feed length must be set so as to result in a pole-tip coverage time at *X*=36 mm of at least 38.5 min. To prove this concept, a pole-tip feed of 22 mm was chosen for the experiments. The area from *X*=36 to 40 mm is the area covered by both pole tips, and the pole-tip coverage time there is calculated to be 48.6 min. Figure 4-14(B) shows the experimental finishing results and the pole-tip coverage time plotted against the distance *X*. The roughness peak at *X*=38 mm is decreased because of the increased pole-tip coverage. The roughness was improved to less than 0.8 μm *Rz.* If the desired surface is less than 0.5 μm *Rz*, a pole-tip coverage time greater than 60 min is suggested by Figure 4-14(A). To satisfy this condition, a pole-tip

stoke of 24 mm is proposed. The 24 mm pole-tip feed provides the superposed area from *X*=36 to 42 mm with a coverage time of 68.3 min. As seen in Figure 4-14(C), the roughness peak at the center is no longer observed, and the surface roughness is around 0.2 µm *Rz*.

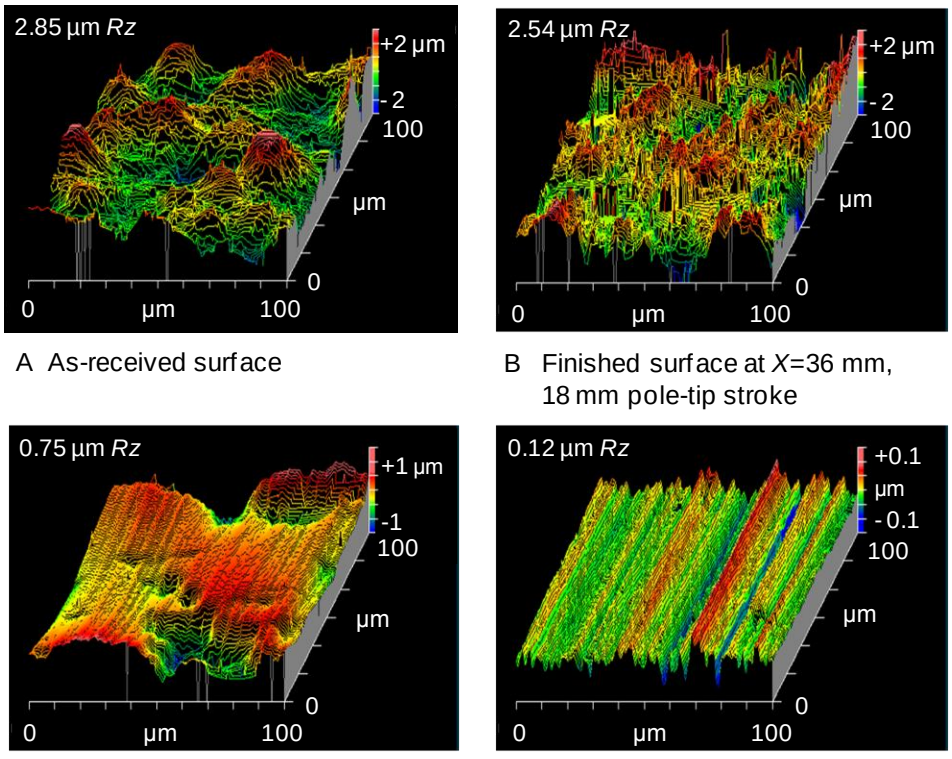

A As-received surface

B Finished surface at *X*=36 mm, 18 mm pole-tip stroke

C Finished surface at *X*=38 mm, 22 mm pole-tip stroke

D Finished surface at *X*=38 mm, 24 mm pole-tip stroke

Figure 4-15. Three-dimensional surface shapes measured by optical profiler

Figure 4-15 shows the three-dimensional shapes (measured by an optical profiler) of the unfinished inner surface and the center of the inner surfaces finished with pole-tip feeds of 18, 22, and 24 mm. The surface finished with the 18 mm pole-tip feed (Figure 4-15(B)) is similar to the unfinished surface (Figure 4-15(A)). Figure 4-15(C), with the 22 mm pole-tip feed, shows some asperities that remained from the initial surface condition. In the surface with the 24 mm pole-tip feed (Figure 4-15(D)) the

asperities from the initial condition are barely observed, and the finished surface consists of cutting marks generated by mixed-type magnetic abrasive.

The pole-tip feed conditions of 22 mm (total finished length: 76 mm) and 24 mm (total finished length: 78 mm) had material removal of 16.83 mg and 18.7 mg, and the material removal per length are calculated to be 0.22 mg/mm and 0.24 mg/mm, respectively. Regardless of the extended pole-tip feed, the material removal rate of the multiple pole-tip system was less than that of the single pole-tip system (0.36 mg/mm). This condition resulted from the differences in the finishing mechanisms with and without the use of the magnetic tool. Moreover, it should be noted that the single pole-tip system took twice the time (6 hr), compared to the multiple pole-tip system, to finish the surface of a 72 mm long tube.

CHAPTER 5
DEVELOPMENT OF HIGH-SPEED FINISHING MACHINE FOR INTERNAL FINSHING OF CAPILLARY TUBES

5.1 Design and Construction of High-speed Finishing Machine

In the internal magnetic abrasive finishing of capillary tubes, the tube rotational speed is a critical factor for efficient finishing. However, as the tube rotational speed increases, stronger centrifugal force affects the magnetic abrasives and lubricant at the finishing area. To clarify the relationship between tube rotational speed and the finishing characteristics, new high-speed finishing equipment, which rotates the tube up to 30000 min^{-1}, has been designed and developed. Previously, the high-speed finishing machine with 30000 min^{-1} successfully finished the inner surface of capillary tube with 0.4 mm ID [34]. However, the multiple pole-tip finishing method has not been applied to a high-speed finishing process. To clarify the finishing characteristics, a new high-speed machine is proposed and constructed.

5.1.1 Proposal of New Finishing Machine

The specifications of the finishing machine used in Chapters 3 and 4 are shown in Table 5-1(A), and the external view of the machine is shown in Figure 5-1 (finishing unit is shown enlarged in Figure 3-4). The maximum main spindle rotation is limited to 3000 min^{-1} and the feed (0-10 mm/s) and vibration (0-5 mm, 0-3 Hz) motion of the pole set are controlled by computer. This rotational speed significantly limits the finishing speed and eventually affects finishing efficiency. This machine can finish tubes which have 0-20 mm OD and are up to 250 mm long. In Chapter 4, the multiple pole-tip system has been applied successfully to this machine for capillary internal finishing. Even though this system shows a relatively reduced processing time, it still requires long processing time (3 hrs for 72 mm finishing) [35, 38].

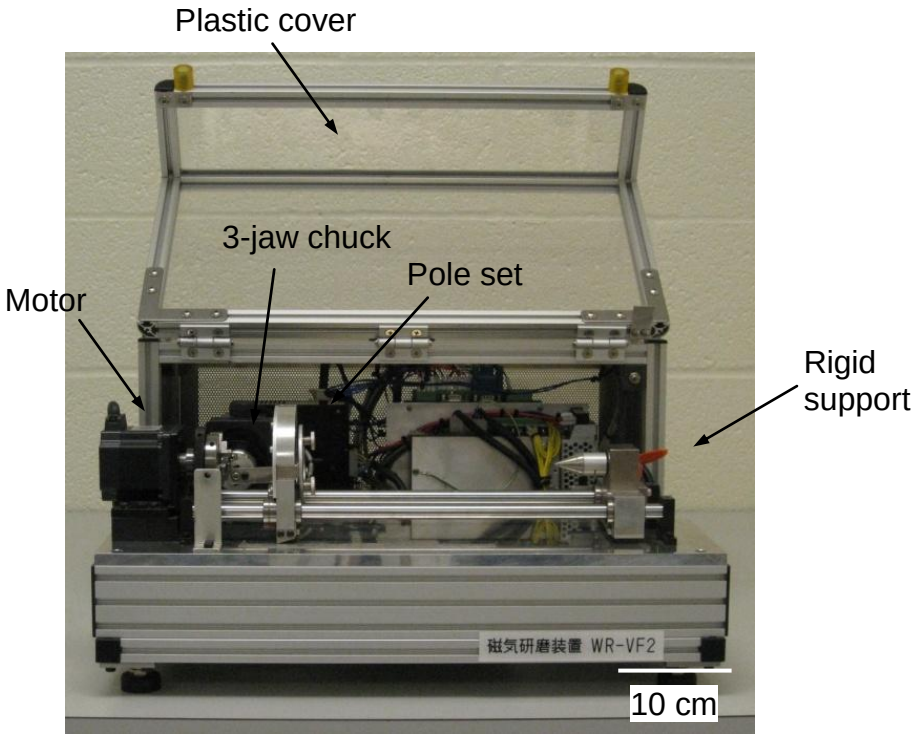

Figure 5-1. External view of the low-speed finishing machine (up to 3000 min^{-1})
(Photograph courtesy of Junmo Kang)

To enhance the finishing efficiency, a high-speed internal finishing machine with spindle speed up to 30000 min^{-1} was developed in Japan in 2004. This machine was capable of finishing an 8 mm length of an internal capillary tube (0.4 mm ID tube) from several micrometers to less than one micrometer in 10 min. Thus, this machine became the model for the newly designed high-speed finishing machine. The specifications of the previously developed high-speed machine are shown in Table 5-1(B). Further improvements of this machine design were considered, and the following two issues were mainly considered to improve the processing performance: (1) the main spindle rotational speed and (2) the control system for positioning the magnetic pole tips.

The main spindle determines the finishing speed and is attached to the workpiece chucking system. In the case of the machine in Figure 5-2, the main spindle rotation

was controlled by a pneumatic gearbox motor, and the rotational speeds (4070, 7653, 30000 min^{-1}) were adjusted by the gear combination. This machine has only three gear combinations, which limits the variation of the workpiece rotational speed. To overcome this limitation, a main spindle with variable rotational speed was desired.

Table 5-1. Specifications of finishing machines; (A) Existing high-speed machine at UF, (B) Existing high-speed machine, (C) Newly proposed high-speed machine

	(A) Existing machine at UF (Low-speed machine)	(B) Existing high-speed machine	(C) Proposed machine (High-speed machine)
Maximum workpiece size	20 mm outer diameter 250 mm length	4 mm outer diameter 150 mm length	3 mm outer diameter 200 mm length
Main spindle rotation	0-3000 min^{-1} Programmably controlled	4070, 7653, 30000 min^{-1}	500, 5000-30000 min^{-1} Programmably controlled
Maximum pole feed rate	10 mm/s	800 mm/s	600 mm/s
Pole vibration	Maximum amplitude: 5 mm Maximum frequency: 3 Hz	-	-
Pole tip positioning	Relative to workpiece surface	Relative to workpiece surface	Absolute position control
Machine dimensions	H270×D460×W510 mm	H200×D250×W450 mm	H270×D350×W500 mm
Weight	15 kg	10 kg	13 kg
Power supply	110 VAC, 50/60 Hz	110 VAC, 50/60 Hz	110 VAC, 50/60 Hz

In capillary tube finishing, the magnetic field is a key parameter to control the magnetic force, which generates the finishing force in the process. In the machine in Figure 5-2, the magnetic field is generated by permanent magnets, and the positional relationship between the finishing area and pole tips must be critically controlled to within an order of 10 μm in order to obtain the desired magnetic field intensity. This is more important and difficult as the tube diameter becomes smaller. The clearance between the pole tip and pole position was practically determined by using a spacer of known thickness (e.g., polytetrafluoroethylene (PTFE) tape). Because the roundness

and cylindricity of the workpiece were not critically controlled in the original manufacturing process, finding the center of the workpiece was difficult. Moreover, misalignment of the pole tips would result in the instability of the abrasive motion and the nonuniformity of the finished surface. In the existing low-speed machine (Figure 5-1), it is difficult to adjust the pole-tip distance because the positioning work has to be done by manually and once the pole tip is stuck together, every set up has to be done again. To overcome this issue, the new machine was desired to have a precision pole-tip positioning system.

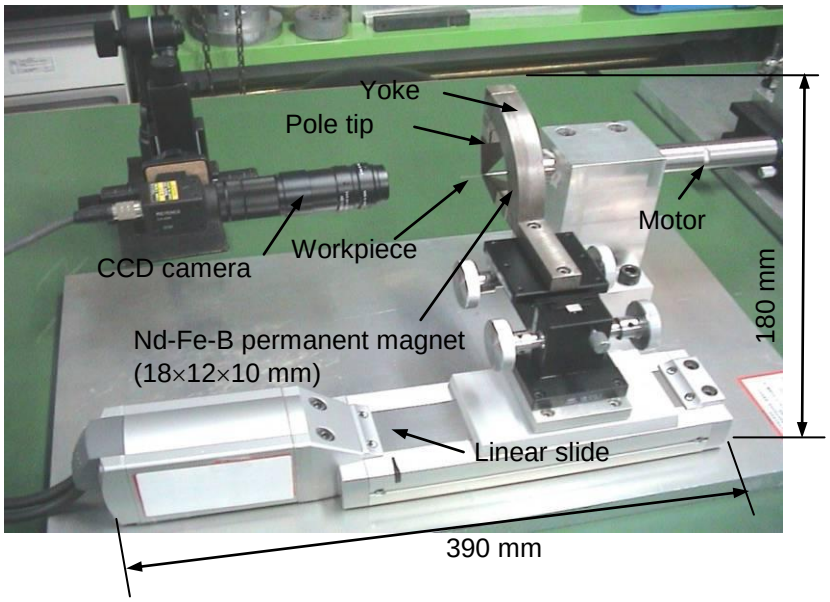

Figure 5-2. External view of existing high-speed finishing machine [34]

Based on these concepts, the design specifications were determined as shown in Table 5-1(C). The electric motor to control the main spindle was selected because it has high torque to accommodate the larger and heavier chucks required for larger workpieces, and tasks ranging from simple rinsing to heavy duty cleaning (including deburring) can be performed on various diameter workpieces. The rotational speeds of the motor are in the range of 5000–30000 min^{-1} and 500 min^{-1}. To simplify the machine,

the pole vibration system was not considered. To allow the pole tips to be positioned to within 10 μm with respect to the tube in radial direction, the permanent magnet and pole tips are mounted on a precision single-axis micrometer stage.

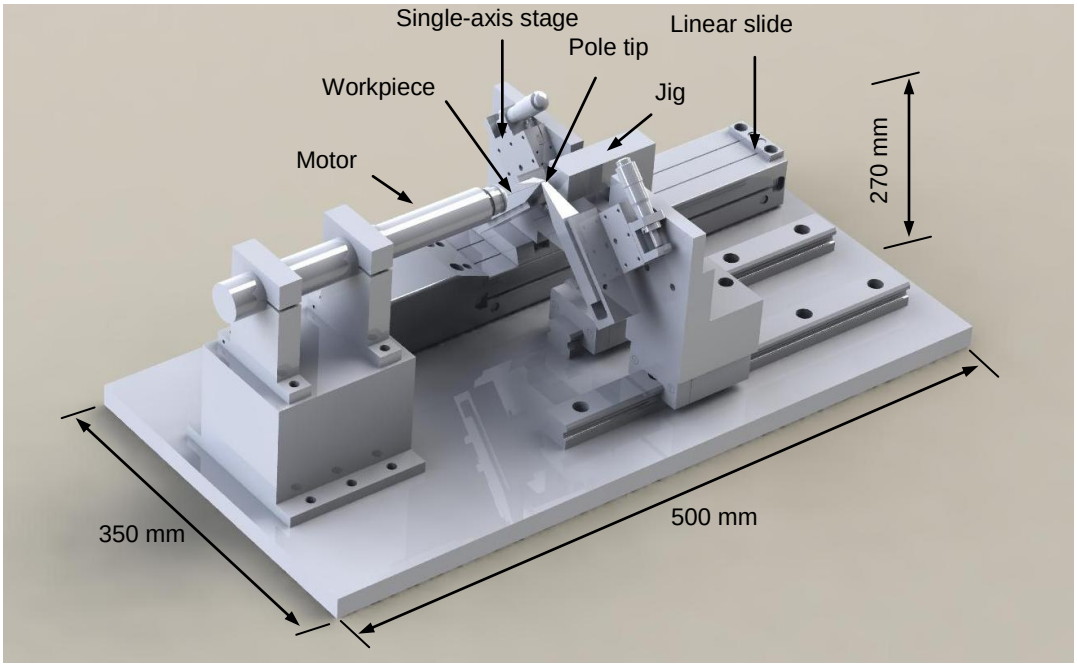

Figure 5-3. Schematic of the proposed high-speed finishing machine

Figure 5-3 shows the schematic of the proposed high-speed machine. It was designed using Solidworks to avoid interference between the parts. The main spindle rotation and the pole-tip motion are controlled through software, and the pole-tip geometry can be modified depending on the workpiece size.

5.1.2 Description of New High-speed Finishing Machine

Based on the prototype in Figure 5-3, the new high-speed finishing machine is developed. Figure 5-4(A) shows overview of the machine developed. The machine consists of a finishing unit (Figure 5-4(B)) and a separate control unit (Figure 5-4(C)), which are located beneath transparent covers for safety reasons. The control unit is connected to the finishing unit to control the main spindle and pole motions. The

necessary motion is programmed in advance using the computer, which is connected to linear guide controller, and it is transferred through the control unit to the finishing unit. The air line kit keeps the main spindle clean during operation by providing a continuous flow of air (0.15–0.25 MPa), which prevents the accumulation of dust in the small clearance between the main spindle and spindle holder. Moreover, the compressed air cools the spindle assembly and machine during operation.

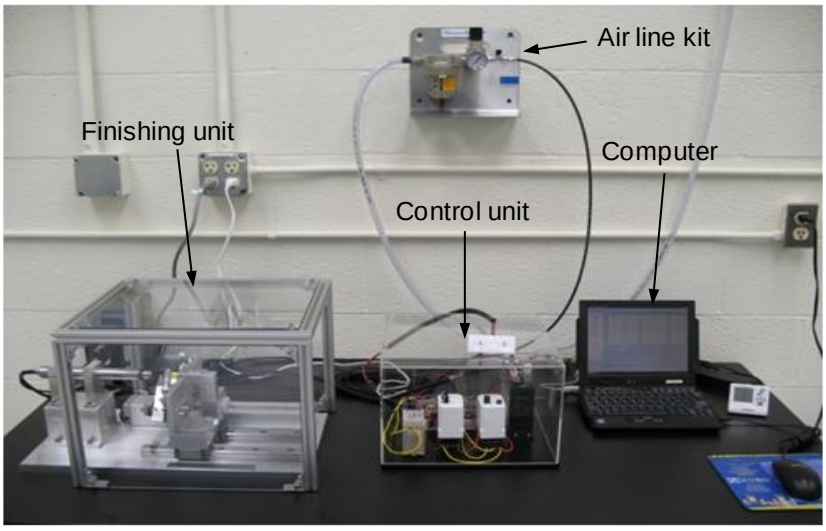

A Overview of developed machine

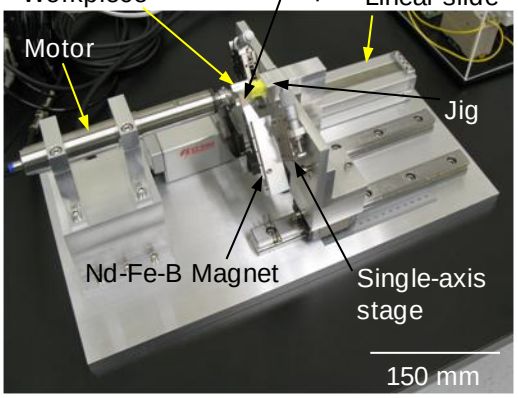

B Finishing unit

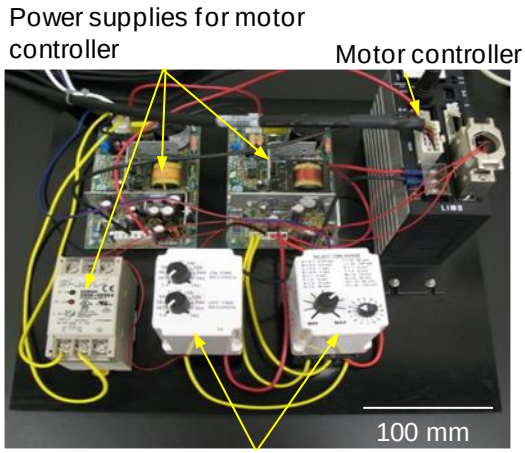

C Control unit

Figure 5-4. Photographs of developed machine overview, finishing unit, and control unit (Photograph courtesy of Junmo Kang)

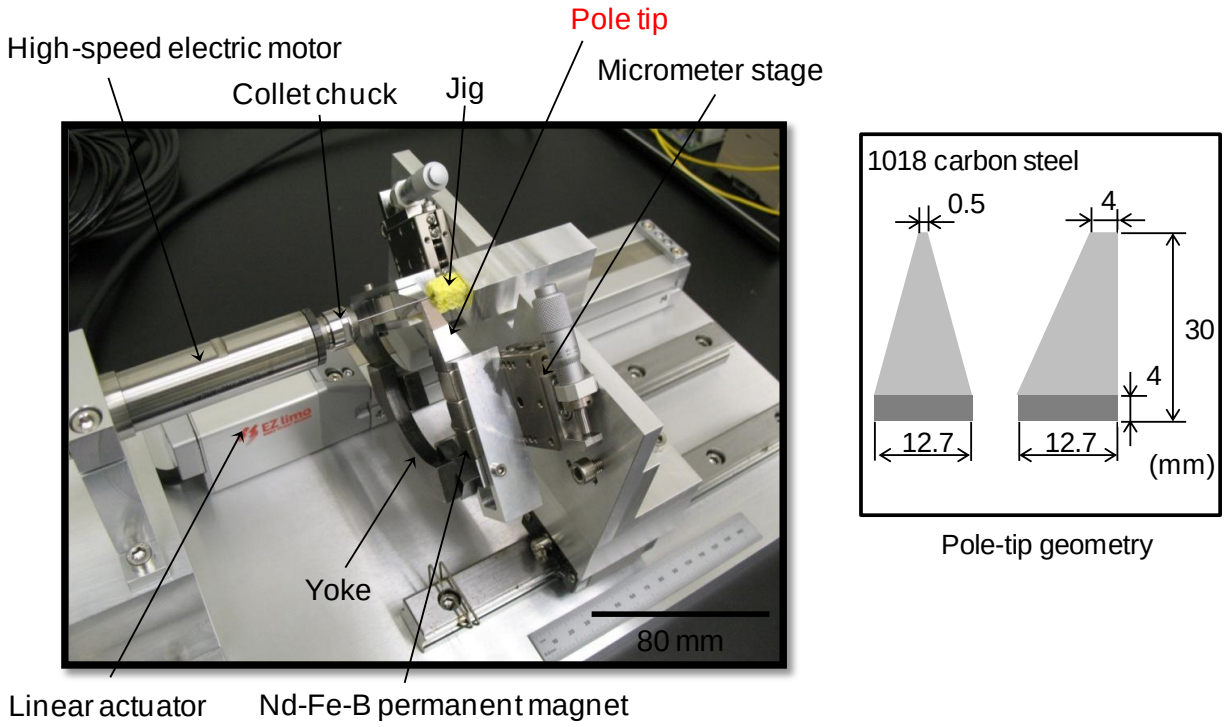

Figure 5-5. Photograph of finishing unit and pole-tip geometry (Photograph courtesy of Junmo Kang)

The finishing machine is just like the schematic shown in Figure 5-3. The neodymium-iron-boron permanent magnets (Grade N42, 0.5×0.5×0.5 in (12.7×12.7×12.7 mm)) are used to generate the magnetic field [67]. The magnetic flux density of 0.42 T was measured with a Hall sensor at the center of the magnet surface. The pole-tip geometry shown in Figure 5-5 was designed to generate a magnetic field strong enough to generate relative motion between the magnetic abrasive and the workpiece inner surface. Practically, the pole-tip geometry is determined by the workpiece size. For capillary finishing, each pole tip was attached to three magnets, and the magnetic flux density of 0.14–0.15 T was measured at the pole tip end. Since the detecting area of the Hall sensor (1.0 mm diameter) exceeded the pole tip end area

(0.5×4 mm), the Hall sensor showed less magnetic flux density. The magnetic flux density at the pole tip end is estimated theoretically to be over 1 T [34].

The magnet and pole-tip subassemblies can be manually moved in the tube radial direction, and they are manipulated in the tube axial direction by a linear slide. The motor controller and timer relays shown in Figure 5-4(C) control the reciprocation of the pole tips: the pole feed rate and the start and end positions.

5.2 Finishing Characteristics of High-speed Machine

Finishing experiments of stainless steel capillary tubes (0.64 mm OD, 0.48 mm ID) were executed with the newly developed machine (Figure 5-5, single pole-tip system) at a spindle speed of 30000 min^{-1} to confirm the machine's finishing performance. Table 5-2 shows the experimental conditions of existing low-speed and developed high-speed finishing machines. In the case of the new machine, the finishing experiments with various times have been executed to produce the finely finished surface (~0.1 μm *Rz*). Since the experiments did not require significant material removal from the workpiece, diamond abrasive was not considered. A mixture of magnetic abrasive and ferrous particles was supplied as a cutting tool. Finishing experiments with the existing low-speed machine (Figure 5-2) were also conducted to compare the finishing performance of the two machines.

Theoretically, the finishing time for high-speed machine can be roughly estimated using the previous experiment conducted using the existing machine. The number of strokes is 180 at 2500 min^{-1}. However, the rotational speed has increased with developed machine twelve times so the number of strokes has been considered twelve times less than the previous result.

Figure 5-6 shows the microscopy of the tube interior of the unfinished and finished surfaces. In both cases, the roughly drawn surfaces were modified to ones covered with unidirectional scratches generated by the magnetic abrasive during finishing. The vertical direction is the circumferential direction of the tube. It was confirmed that the developed high-speed machine was capable of finishing the inner surface of the capillary tube at 30000 min^{-1} in less than one fifth the time needed for low-speed finishing.

Table 5-2. Experimental conditions for finishing performance between existing low-speed machine and newly developed high-speed finishing machine

Machine	Existing machine (Low-speed machine)	Developed machine (High-speed machine)
Workpiece	304 stainless steel tube: ∅0.64×∅0.48×60 mm	
Workpiece revolution	2500 min^{-1}	30000 min^{-1}
Mixed-type magnetic abrasive	Iron particles (-50/+100 mesh, 150-300 μm dia.): 0.4 mg + Aluminum oxide (WA) particles (80 μm mean dia.) in magnetic abrasive (<10 μm): 0.1 mg	
Workpiece-Pole clearance	0.11 mm	
Pole feed	Feed length: 4 mm; Feed rate: 0.5 mm/s	
Lubricant	Soluble-type barrel finishing compound	
Processing time	54 min	10 min

Close observation of the finished surfaces show that the cutting marks in the 2500 min^{-1} tube rotation case (Figure 5-6(A-ii)) are more uniform than the ones in the 30000 min^{-1} case (Figure 5-6(B-ii)). The high-speed rotation is twelve times faster than the low-speed case. Due to the higher centrifugal force in the high-speed case, the lubricant mixed with the mixed-type magnetic abrasive spun off easily. The higher the tube rotational speed, the easier the ejection of the lubricant from the finishing area. The lubricant plays an important role by (1) encouraging the mass of mixed-type magnetic abrasive to conform to the inner surface of the tube at the beginning of the process and

(2) maintaining smooth relative motion against the tube surface. The lack of the lubrication deteriorates the smooth relative motion between the magnetic abrasive and the tube inner surface, resulting in irregular cutting marks. In addition, lubricant can cool down the temperature during the cutting process, so the lack of lubrication may cause the adherence of particles onto the surface due to the friction.

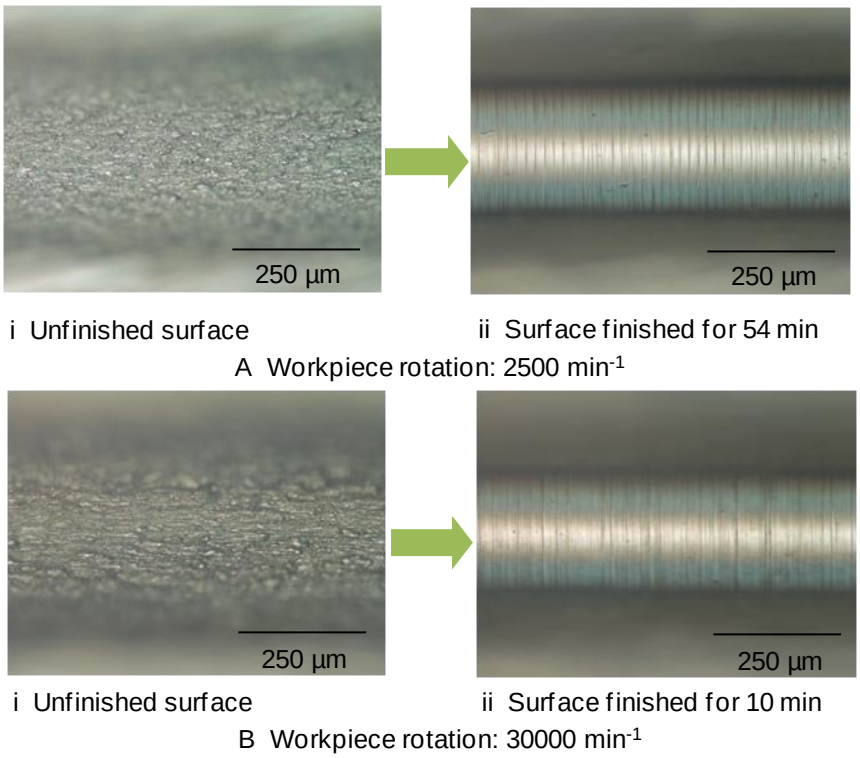

Figure 5-6. Microscopy of tube interiors before and after finishing at the rotational speeds of 2500 min^{-1} and 30000 min^{-1}

Figure 5-7 shows representative three-dimensional shapes of the inner surface of tubes. The finished surfaces are typical in the MAF process, and the irregular micro-asperities are more visible in the case of high-speed finishing than with low-speed finishing. As mentioned above, this must be due to the mixed-type magnetic abrasive behavior as well as the lack of lubricant at the finishing area.

Figure 5-8 shows measured surface roughness of unfinished and finished surfaces in both conditions (Table 5-2). The initial surface conditions of the stainless steel tubes depend on the tube manufacturing processes, and the roughness of drawn 304 stainless steel tubes is typically around 7 µm *Rz*. After 54 min in the case of low-speed conditions, and 10 min in the case of high-speed conditions, respectively, the tube surfaces were smoothly finished to 0.1–0.3 µm *Rz*. It is seen that the surface finished with high-speed conditions shows slightly higher roughness than the one with low-speed conditions.

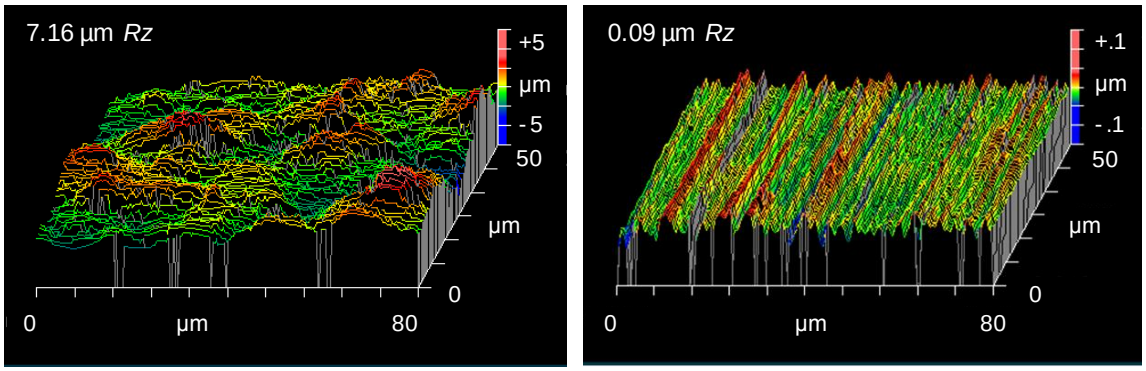

i Unfinished surface ii Surface finished for 54 min

A Workpiece rotation: 2500 min^{-1}

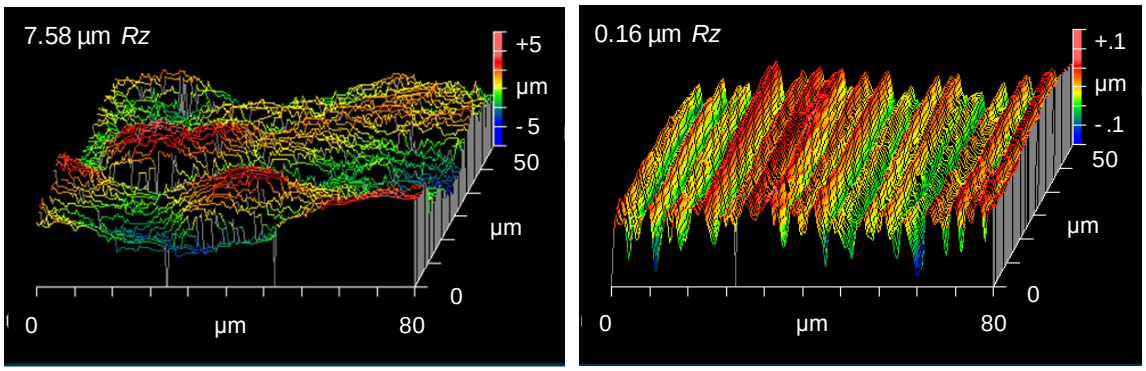

i Unfinished surface ii Surface finished for 10 min

B Workpiece rotation: 30000 min^{-1}

Figure 5-7. Three-dimensional surfaces of tube interiors before and after finishing at the rotational speeds of 2500 min^{-1} and 30000 min^{-1} measured by optical profilometer

Consequently, the finishing experiments demonstrated the applicability of the developed machine for high-speed internal finishing of capillary tubes. The results shown demonstrated that the developed high-speed machine exhibits improved finishing efficiency over 5 times compared to the existing low-speed machine. As mentioned above, the previously developed high-speed machine in Japan required 8 min to improve the surface roughness of 304 stainless steel tubes (0.5 mm OD, 0.4 mm ID) from 2 μm *Rz* to 0.15 μm *Rz* [34]. Although the tube size is slightly different, it can be confirmed that the newly developed machine can perform the internal finishing with superior speed. This is a result of the precision pole-tip position control, which achieves precision control of magnetic field at the finishing area.

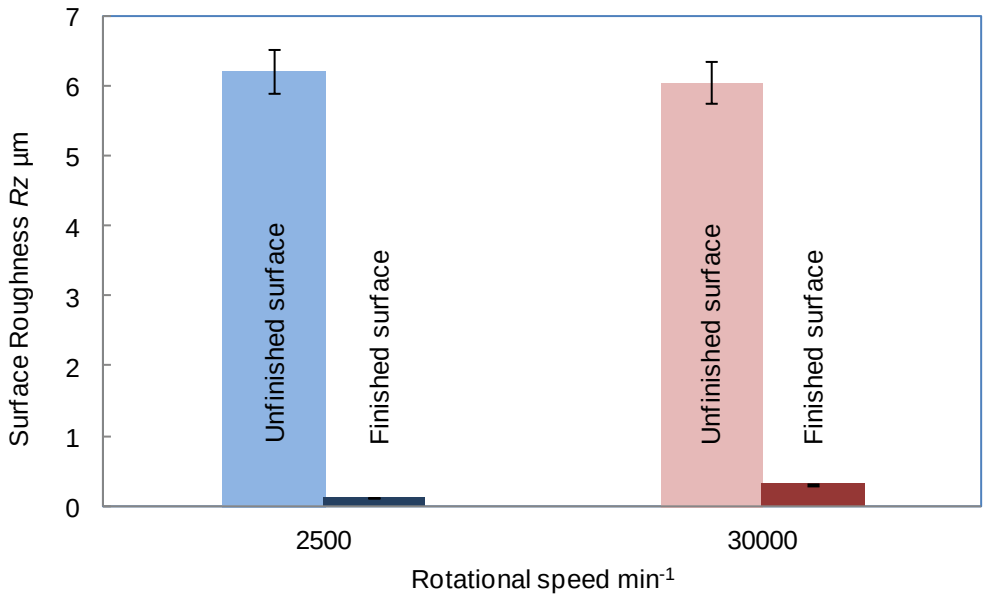

Figure 5-8. Surface roughness of unfinished and finished surfaces in rotational speed 2500 and 30000 min^{-1}

CHAPTER 6
HIGH-SPEED INTERNAL FINISHING OF CAPILLARY TUBES BY MULTIPLE POLE-TIP SYSTEM

6.1 Internal Finishing of Capillary Tubes by High-speed Multiple Pole-tip System

In order to improve the finishing efficiency, a multiple pole-tip system has been proposed and applied to the internal finishing process. The development of a multiple pole-tip system using a partially heat-treated magnetic tool allows the finishing of multiple regions simultaneously in capillary tubes. Moreover, the high-speed finishing machine has also been developed to improve finishing efficiency and demonstrate its finishing performance. Although an increase in finishing efficiency in multiple pole-tip system has been observed, the finishing characteristics of general straight capillary tubes in the newly developed high-speed machine has not been studied yet. Therefore, high-speed internal finishing of capillary tubes using a multiple pole-tip system has been developed and the respective finishing experiments have been executed.

Firstly, finishing equipment with double pole-tip sets is developed, which enables a tube to rotate up to 30000 min^{-1}. Secondly, the effects of tube revolution on abrasive motion are investigated through the tube finishing experiments. The behaviors of the tool and magnetic abrasive as a function of tube rotational speed are studied. In addition, the finishing characteristics and mechanism are studied using the straight capillary tubes. Finally, the flexible capillaries are applied to the high-speed multiple pole-tip finishing method and studied its finishing characteristics and mechanism.

Figure 6-1 shows a schematic for a method using double pole-tip sets, which generates magnetic fields in two finishing areas, and a photograph of the equipment developed to realize the method. The finishing area is doubled as magnetic abrasive is introduced and pushes against two regions of the tube surface. As the pole-tip sets

move along the tube axis, the finished area is extended. The number of pole-tip sets can be increased if needed. For a constant pole-tip width, the finishing area will be a function of the total number of pole-tip sets. The doubled pole-tip sets require the introduction of a magnetic tool with the mixed-type magnetic abrasive. The tool guides the magnetic abrasive deep into the tube and increases the magnetic force acting on the magnetic abrasive as mentioned in Chapter 4.

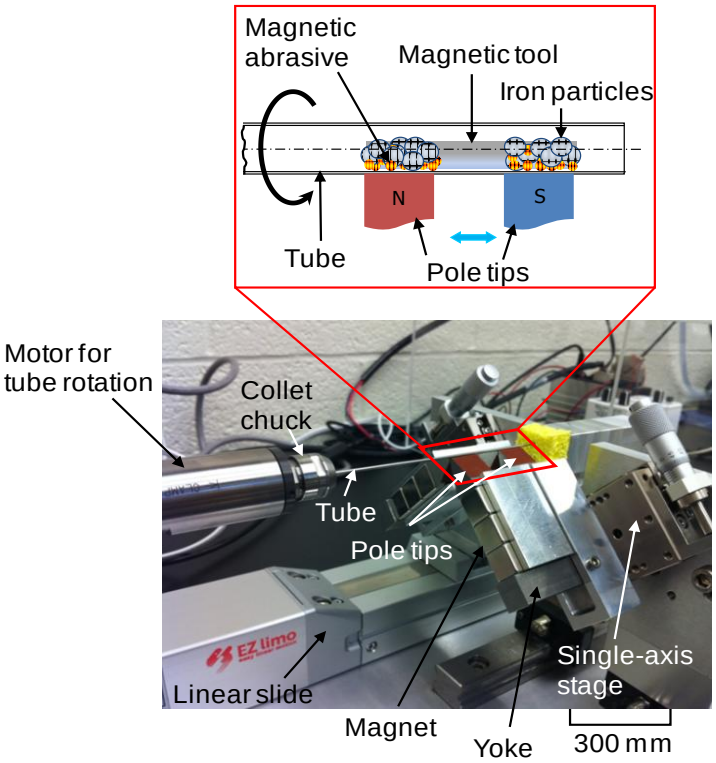

Figure 6-1. Schematic of the processing principle for internal finishing by multiple pole-tip system (Photograph courtesy of Junmo Kang)

The workpiece (straight capillary tube) is chucked to a motor (speed range: 500 min^{-1}, 5000–30000 min^{-1}). Two pole-tip sets consisting of six neodymium permanent magnets (12.7×12.7×12.7 mm; residual flux density 1.26–1.29 T; coercive force >875 AT/m) are mounted in right angle configuration on a single-axis micrometer stage, and their position is adjustable in the tube radial direction. To avoid collision between the rotating tube and pole tips, the pole-tip surfaces are covered by 0.3 mm thick

polytetrafluoroethylene (PTFE) tape. The pole-tip sets are mounted on a linear slide so that they can be fed in the tube axial direction. The feed length and speed are adjustable to maximums of 150 mm and 600 mm/s, respectively.

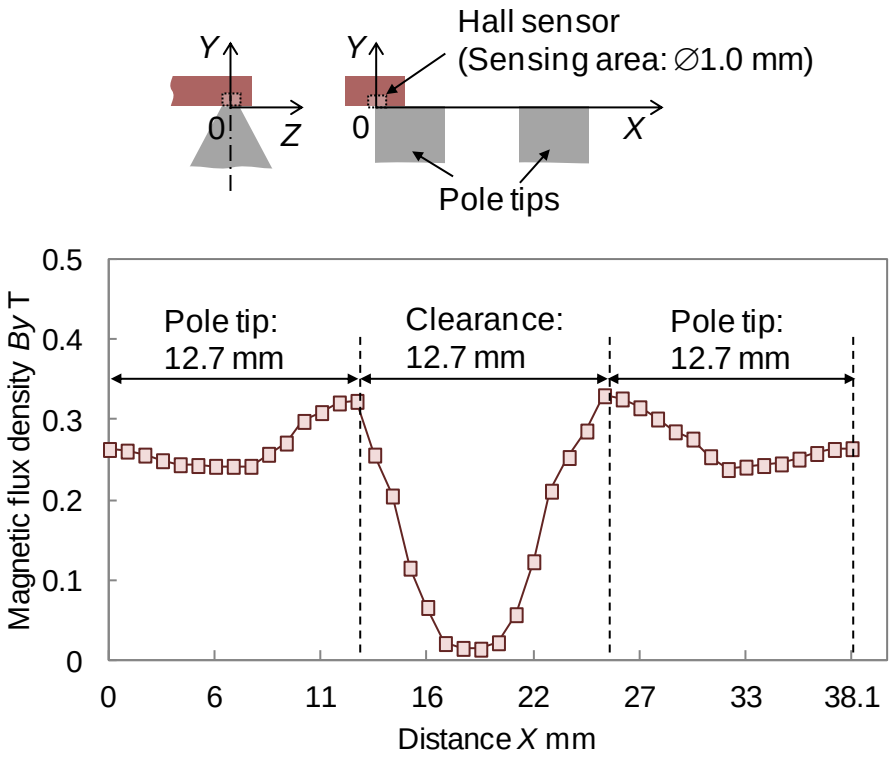

Figure 6-2. Changes in magnetic flux density in multiple pole- tip sets at *Y*=0 mm

Figure 6-2 shows changes in magnetic flux density B_y, measured by a Hall sensor (sensing area: ∅1.0 mm), with distance *X* for double pole-tip sets. The magnetic flux density and gradient increases from the center toward the edges of pole tip. A particle in the magnetic field is attracted to the pole-tip edges where the magnetic force is higher.

Table 6-1 shows the experimental conditions. Austenitic stainless steel tubes (304 stainless steel, ∅1.27×∅1.06×100 mm; 2–3 μm *Rz* initial surface roughness) were prepared as workpieces for this experiment. A 304 stainless steel tool with three heat-

treated regions was used as a magnetic tool (Figure 6-3). The heat-treated regions became non-magnetic as a result of the treatment while the four untreated sections remained magnetic. The mixed-type magnetic abrasive separates as it is attracted to the ends of the four magnetic sections. The magnetic regions correspond to the two sets of magnetic pole-tips. The pole-tip feed length was set to 12.7 mm, and the feed rate was set to 0.59 mm/s.

Table 6-1. Experimental conditions for the high-speed internal finishing of straight capillary tubes

Workpiece	304 Stainless steel tube (∅1.27×∅1.06×100 mm)
Workpiece revolution	500, 5000, 10000, 20000 and 30000 min^{-1}
Mixed-type magnetic abrasive	Iron particles (-50/+100 mesh, 150-300 μm dia.): 4 mg + Aluminum oxide (WA) particles (80 μm mean dia.) in magnetic abrasive (<10 μm): 1 mg
Magnetic tool	Figure 6-3
Pole-tip feed	0.59 mm/s
Pole-tip feed length	12.7 mm and 16 mm
Workpiece-pole-tip clearance	0.3 mm (Polytetrafluoroethylene (PTFE) tape thickness)
Lubricant	Soluble-type barrel finishing compound (pH: 9.5, Viscosity: 755 mPa·s at 30°C)
Processing time	10 and 20 min

For the experiments, 5 mg of mixed-type magnetic abrasive (80 wt% iron particles and 20 wt% magnetic abrasive) was introduced with the magnetic tool. The mixed-type magnetic abrasive and magnetic tool filled 21.4 vol%, and 23.1 vol% inside the tube, respectively. The tube rotational speeds were varied between 5000, 10000, 20000, and 30000 min^{-1}. To encourage the mixed-type magnetic abrasive to uniformly cover the tube surface prior to high-speed finishing, the tube was rotated at 500 min^{-1} with a single pole-tip stroke before finishing.

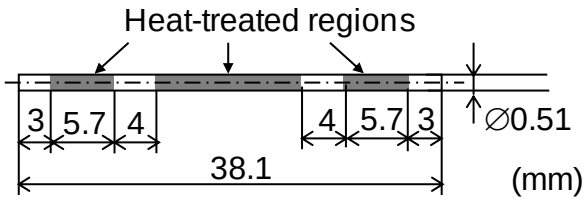

A Geometry of heat-treated magnetic tool

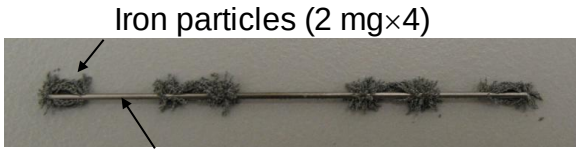

B Magnetized tool with iron particles

Figure 6-3. Tool geometry and magnetized tool with iron particles (Photograph courtesy of Junmo Kang)

6.2 Effects of Lubrication on Finishing Characteristics

In high-speed finishing, centrifugal force tends to cause displacement of the lubricant from the finishing area, which, in turn, causes the mixed-type magnetic abrasive to adhere to the tube surface as a result of friction and heat. Adhered material noticeably covered the surface in Figure 6-4(B), which shows the surface finished continuously for 10 min at a tube revolution rate of 30000 min^{-1}. No adhered material is observed in Figure 6-4(C), which shows the surface finished for 10 min with lubricant added after 5 min.

During the finishing process, the presence of lubricant is crucial to encourage the smooth relative motion between the mixed-type magnetic abrasive and the tube surface that facilitates finishing performance of the abrasive. Accordingly, in the cases of 20000 and 30000 min^{-1} tube revolution, the finishing experiments were interrupted to inject fresh lubricant every 5 min.

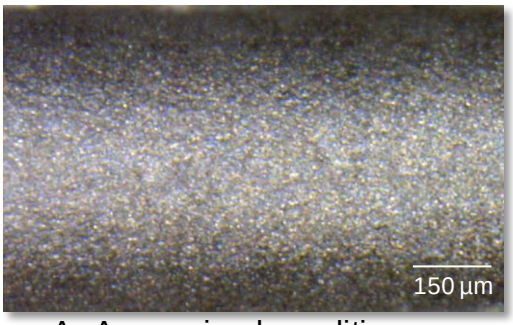

A As-received condition

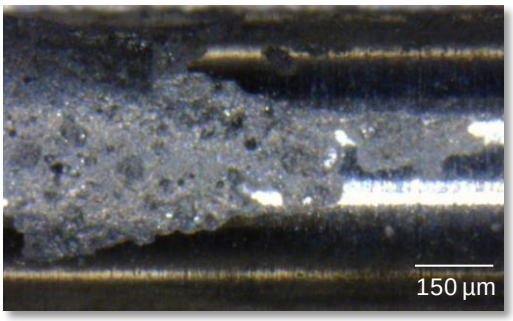

B One-step (10 min)

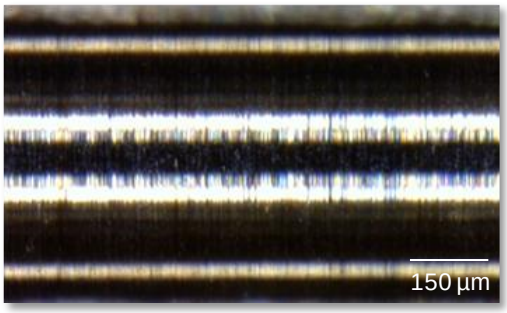

C Two-step (5 min + 5 min)

Figure 6-4. Microscopy of the initial and finished surface for 10 min at 30000 min^{-1}: Initial surface, finished for 10 min continuously, and finished for 5 min and another 5 min with fresh lubricant

For the cases of 5000 and 10000 min^{-1} tube revolution, the finishing experiments were performed continuously for 10 min without additional lubricant injection. Each experiment was repeated at least three times to ensure the repeatability of the results. Before and after the finishing experiments, the tube was rinsed with ethanol in an ultrasonic cleaner for 1 hr to measure the material removal rate.

6.3 Effects of Tube Rotational Speed on Finishing Characteristics

Figure 6-5 and 6-6 show intensity maps and oblique plots—measured by an optical profiler at *X*=13 mm—of the unfinished surface and surfaces finished for 10 and 20 min, respectively. Figure 6-8 shows changes in material removal with tube revolution and finishing time. The surface finished for 10 min at a tube revolution of 5000 min^{-1} (Figure 6-5(B)) has a roughness of 0.15 μm *Rz*, but multiple irregular asperities from the initial surface remained. However, an extension of the finishing time for another 10 min allowed the abrasive to remove the irregular asperities. The material removal after 20 min was more than twice the removal after 10 min. Although the magnetic abrasive was not exchanged during the interruptions to inject lubricant, the reconfiguration of the magnetic abrasive during these breaks encouraged the relocation of sharp abrasive cutting edges. The sharp cutting edges and newly added lubricant seemed to refresh the finishing performance after each interruption.

At a tube revolution rate of 10000 min^{-1}, the surface was smoothly finished (0.1 μm *Rz*) after 10 min, and the roughness value remained constant after 10 min of extra finishing time despite the additional material removal (Figure 6-8). Compared to 10 min at a tube revolution rate of 10000 min^{-1}, the material removal is drastically increased after finishing for 20 min. Analogous to the case of finishing for 20 min at 5000 min^{-1}, the pauses to add lubricant after 10 min aided the finishing performance.

It was confirmed that the increase in the tube revolution (i.e., cutting speed) improves the material removal rate and finishing efficiency. However, due to the high centrifugal force, the high-speed tube rotation creates more opportunities for the mixed-type magnetic abrasive and magnetic tool to lapse into unstable conditions. The lack of a uniform magnetic abrasive distribution under an unstable rotating magnetic tool may

lead to the deep, irregular scratches on the surface. This trend was observed in the case of 20000 min^{-1} (Figure 6-5(D)), the finished surface has deep scratches and surface distortions (Figure 6-5(E)). Extending the finishing time slightly increased the material removal due to the longer duration contact of the magnetic abrasive cutting edges against the tube surface and removed the relatively short-wavelength surface asperities (Figure 6-6(C)); however, the deep scratches produced by the irregular motion of the magnetic tool and mixed-type magnetic abrasive remained on the surface.

In Figure 6-7, irregular surface asperities were observed at the rotational speeds between 20000 and 30000 min^{-1}. Especially, in the case of 30000 min^{-1}, after 10 min finishing, the surface roughness is almost 10 times higher (1.12 μm *Rz*, 5.52 mg) than the cases of 5000 (0.15 μm *Rz*, 1.5 mg) and 10000 min^{-1} (0.10 μm *Rz*, 2.02 mg); despite a few times material removal (Figure 6-8). The finished surface with irregular surface asperities, in spite of higher material removal, must be related with instability of magnetic tool and abrasive behavior due to higher centrifugal and friction force. Moreover, after 100000 times of tube rotation at 5000 and 10000 min^{-1}, surface finished at 10000 min^{-1} produced the smoother surface (0.10 μm *Rz*) with less material removal (2.02 mg) compared with slower rotation case (0.12 μm *Rz*, 4.52 mg). On the other hand, after 200000 times of tube rotation in each rotational speed, the surfaces finished at 5000 and 10000 min^{-1} have similar material removal (8.2 and 7.69 mg respectively). Conversely the irregular asperities were remained the surface finished at 20000 min^{-1} with less material removal (0.36 μm *Rz*, 5.38 mg). This indicates the material removal per tube rotation is decreased with increasing tube rotational speed.

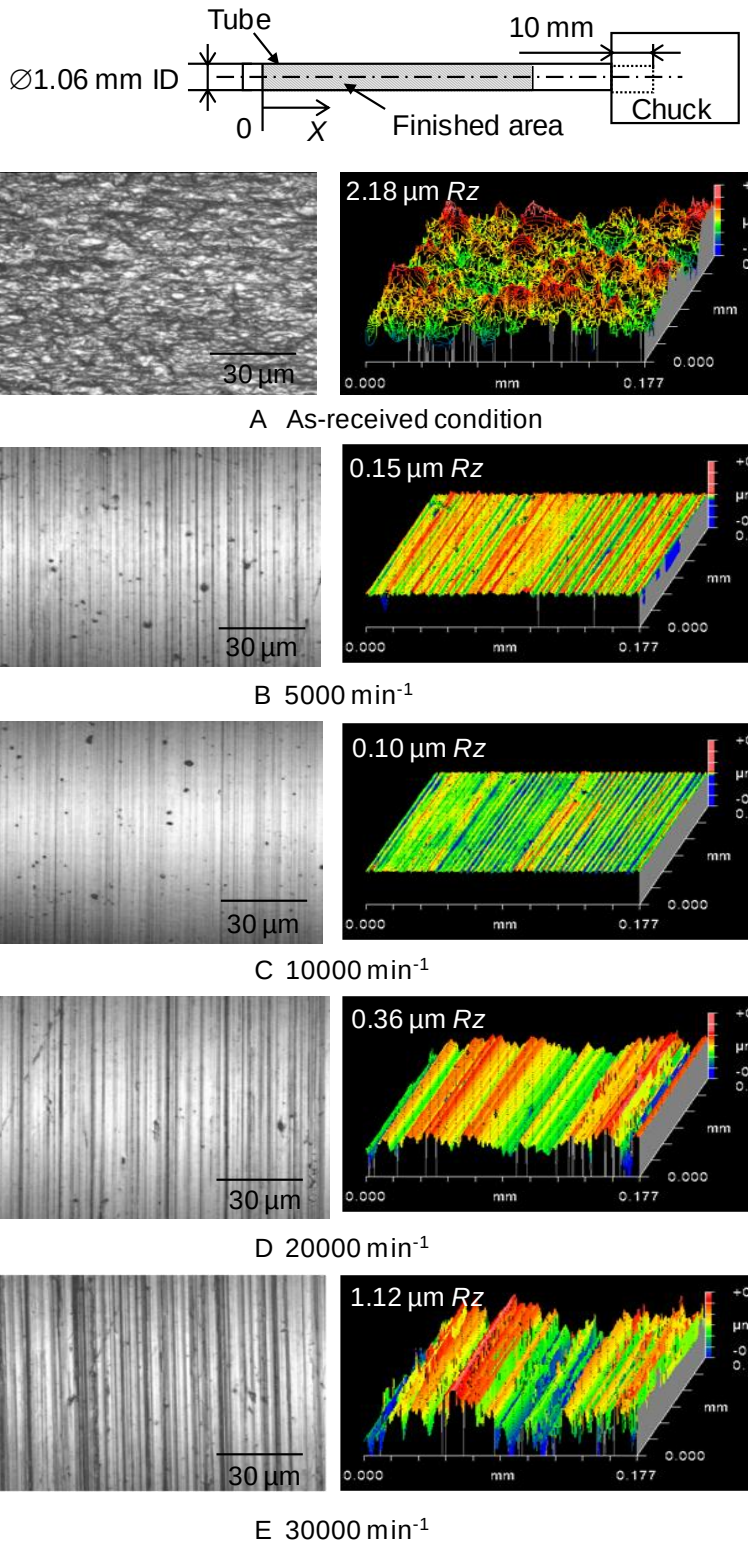

Figure 6-5. Intensity maps and oblique plots of the initial surface and the surface finished for 10 min at 5000 min^{-1}, 10000 min^{-1}, 20000 min^{-1}, 30000 min^{-1}

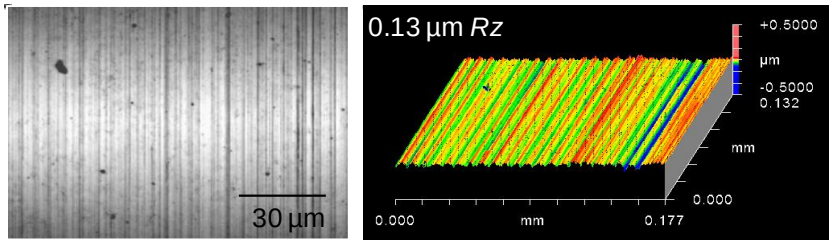

A 5000 min^{-1}

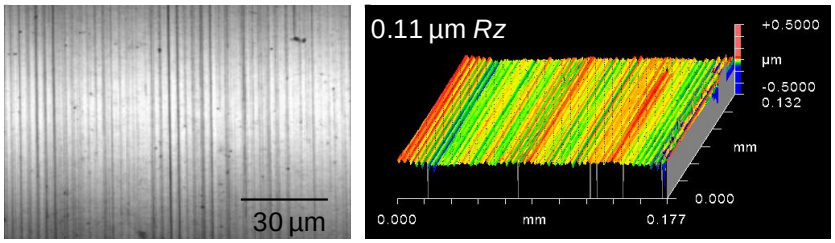

B 10000 min^{-1}

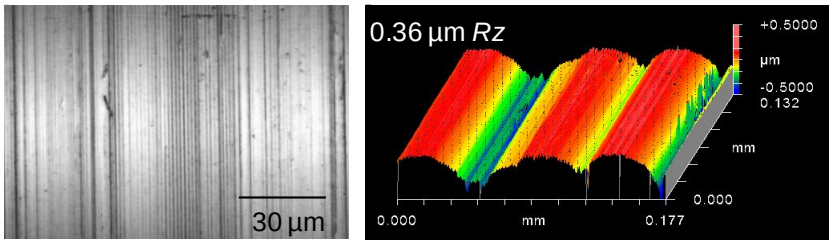

C 20000 min^{-1}

Figure 6-6. Intensity maps and oblique plots of the surface finished for 20 min at 5000 min^{-1}, 10000 min^{-1}, 20000 min^{-1}

Use of the previously developed multiple pole-tip finishing system produced a uniformly finished surface (from 2–3 µm *Rz* to ~0.2 µm *Rz*) 72 mm long—four times the pole-tip width—in 180 min (at 2500 min^{-1}). The high-speed finishing system proposed in this research can produce a finished surface 50.8 mm long (four times the pole-tip width) in 10 min with a roughness of about 0.1 µm *Rz*. Thus the newly developed high-speed finishing system is twelve times more efficient than its predecessor. Internal machining of flexible capillaries with laser-machined slits were performed using the high-speed finishing machine. The processing characteristics will be presented in Section 6.4.

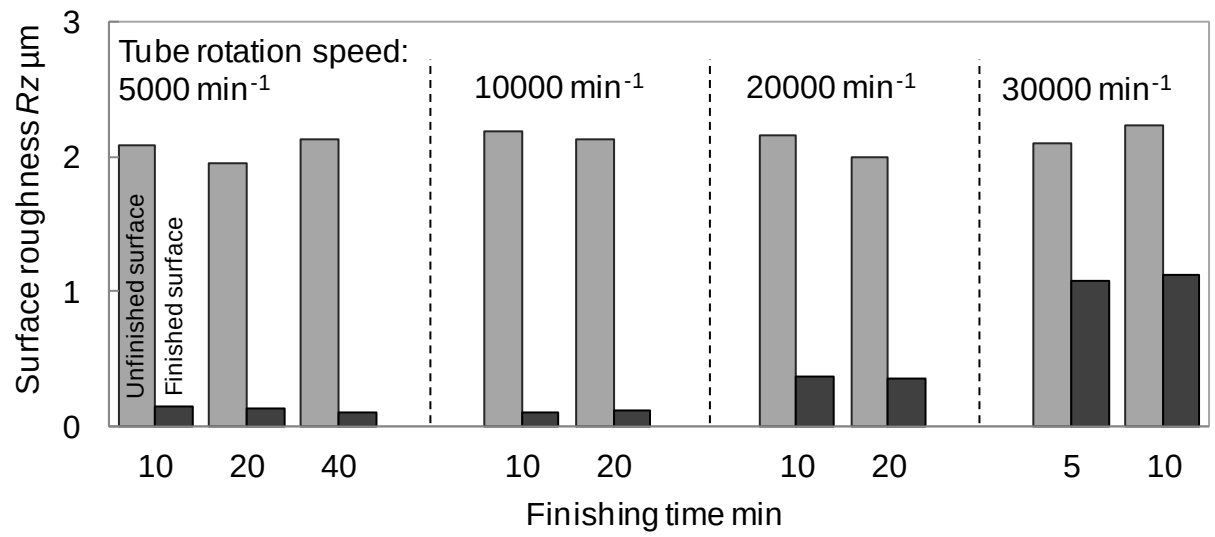

Figure 6-7. Changes in surface roughness with tube revolution observed in multiple pole-tip system

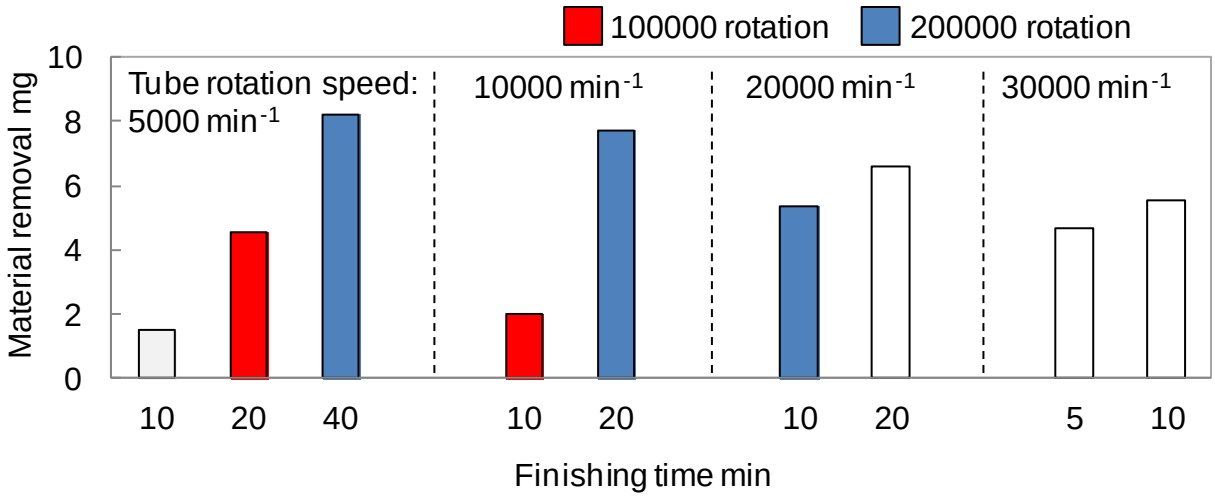

Figure 6-8. Changes in material removal with tube revolution in multiple pole-tip system

6.4 Flexible Capillary Tube Finishing

6.4.1 Finishing Characteristics

Figure 6-9 shows a schematic of processing principle for internal finishing of flexible capillary tube by multiple pole-tip finishing system. The partially heat-treated austenitic stainless steel tool and mixed-type magnetic abrasives are introduced into the tube. Under effects of magnetic field, both tool and abrasives are attracted into the inner

surface of the tube. When the tube rotates with reciprocating motion of the pole tips, the surface and edges inside the tube can be finished gradually.

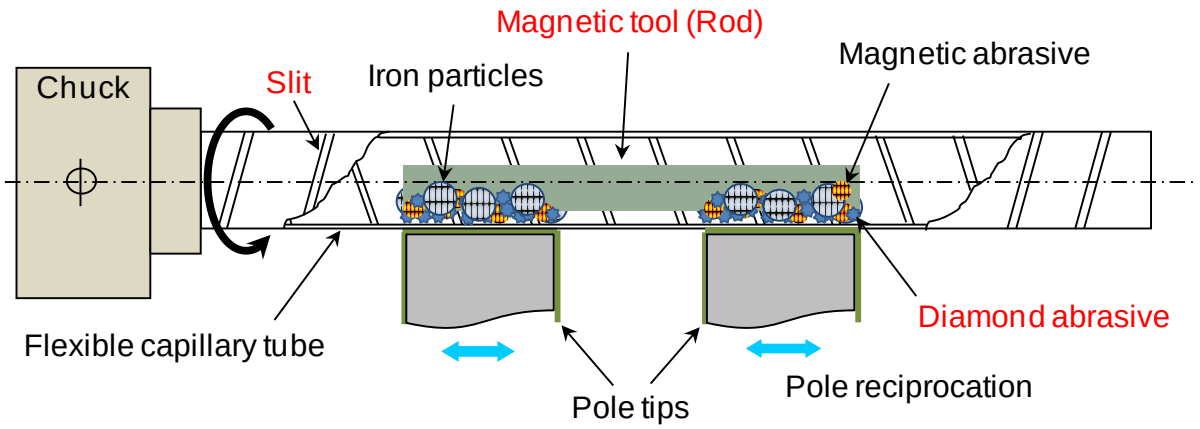

Figure 6-9. Schematics of the processing principle for the internal finishing of flexible capillary tubes by a multiple pole-tip system

Two differently heat-treated tools (Tool C and D, Figure 6-10(A) and (B) respectively) are prepared for the finishing experiments. A photograph of the equipment is shown in Figure 6-11 for the internal finishing using double pole-tip sets. The flexible capillary tubes with laser-machined slits were prepared. In order to prevent the irregular tube rotation, the free end of the flexible capillary tube is wrapped with PTFE tape and held by the jig.

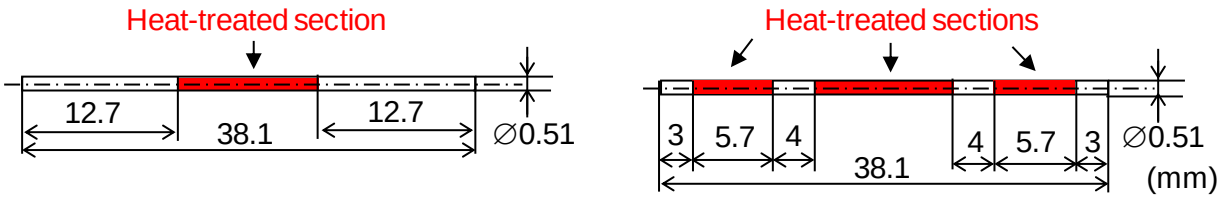

A Tool C B Tool D

Figure 6-10. Schematics of the partially heat-treated metastable austenitic stainless steel tools: Tool C and Tool D

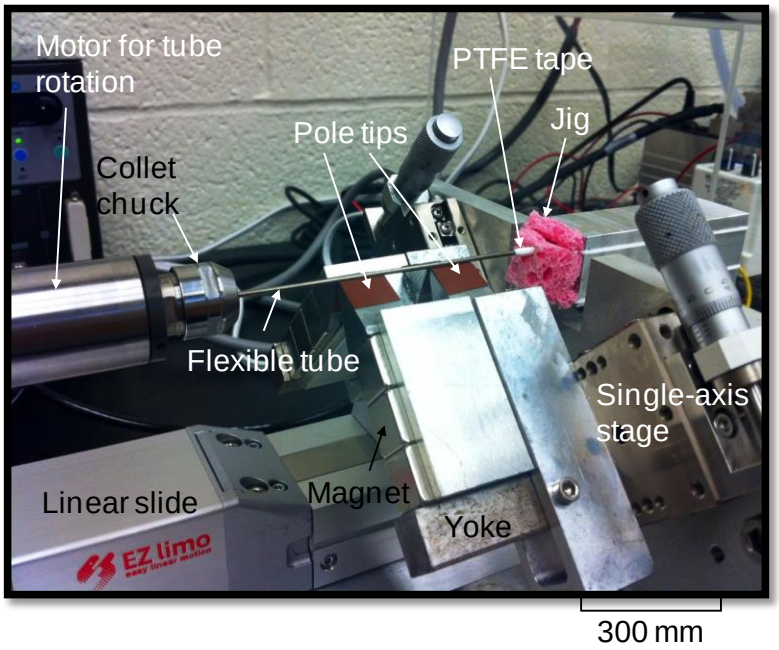

Figure 6-11. External view of high-speed multiple pole- tip finishing system for flexible capillary tube finishing (Photograph courtesy of Junmo Kang)

Table 6-2. Experimental conditions for the high-speed internal finishing of flexible capillary tubes: Tube B

Workpiece	Flexible stainless steel tube (∅1.36×∅1.02×100 mm)
Workpiece revolution	10000 min^{-1}
Pole reciprocating motion	Speed: 0.5 mm/s, Stroke length: 16 mm
Lubricant	Soluble-type barrel finishing compound (pH: 9.5, Viscosity: 755 mPa·s at 30°C): Fresh lubricant addition every 6.5 min (6 stroke times)
Mixed-type magnetic abrasive	Iron particles (-50/+100 mesh, 150-300 μm dia.): 80 wt% + Aluminum oxide (WA) particles (80 μm mean dia.) in magnetic abrasive (<10 μm): 20 wt% ; 5 mg
Diamond abrasive	50-70 μm diamond paste
Magnetic tool	Figure 6-10

To increase the pole-tip coverage time at the center of finishing area, the stroke length was set to 16 mm. The overlap covers the less finished surface due to friction between abrasive and inner surface. In the case of internal deburring process with

flexible capillaries, the lubricant easily escapes through the slits during tube rotation, and higher material removal rate is required compared with surface finishing of straight capillary tube. For encouragement of the material removal, lubricant mixed with diamond abrasives (50-70 μm) was added every 6 times of pole stroke (Table 6-2).

After the micro-laser machining process, the re-solidified material adhered on the edge and surface inside the tube. The initial surface has burrs on the edges which have a height up to 90 μm (Figure 6-12(A)). This is slightly bigger than the size of the magnetic abrasive. These burrs obstruct the magnetic abrasive to follow the pole reciprocating motion. In order to make the abrasives go over the burrs, the heat-treated magnetic tool is introduced to increase the magnetic force acting on the abrasives. Figures 6-12(B) and 6-12(C) represent the surfaces finished by Tool C and Tool D for 26 min, respectively. The burrs on the edges and re-solidified material on the surface were completely removed from the surface finished by Tool C. Conversely, the burrs on the edge and the re-solidified material remained on the surface finished by Tool D.

Figure 6-13 shows the spectrum plots of as-received surface and surfaces finished by Tool C and Tool D. The surface roughness indicated in the each plot is measured in the average of 10 measurements with 100 μm length surface profiles. As shown in Figure 6-13(A), the initial surface roughness between slits is measured in 2.5-3.5 μm *Ra*. The surface finished by Tool C (0.3-0.4 μm *Ra*) is rougher than the case finished by tool D (0.2-0.3 μm *Ra*). This trend was observed in previous result in Section 3.3.3. This demonstrates that the developed high-speed multiple pole-tip finishing system delivers the magnetic abrasive inside the flexible capillary tubes.

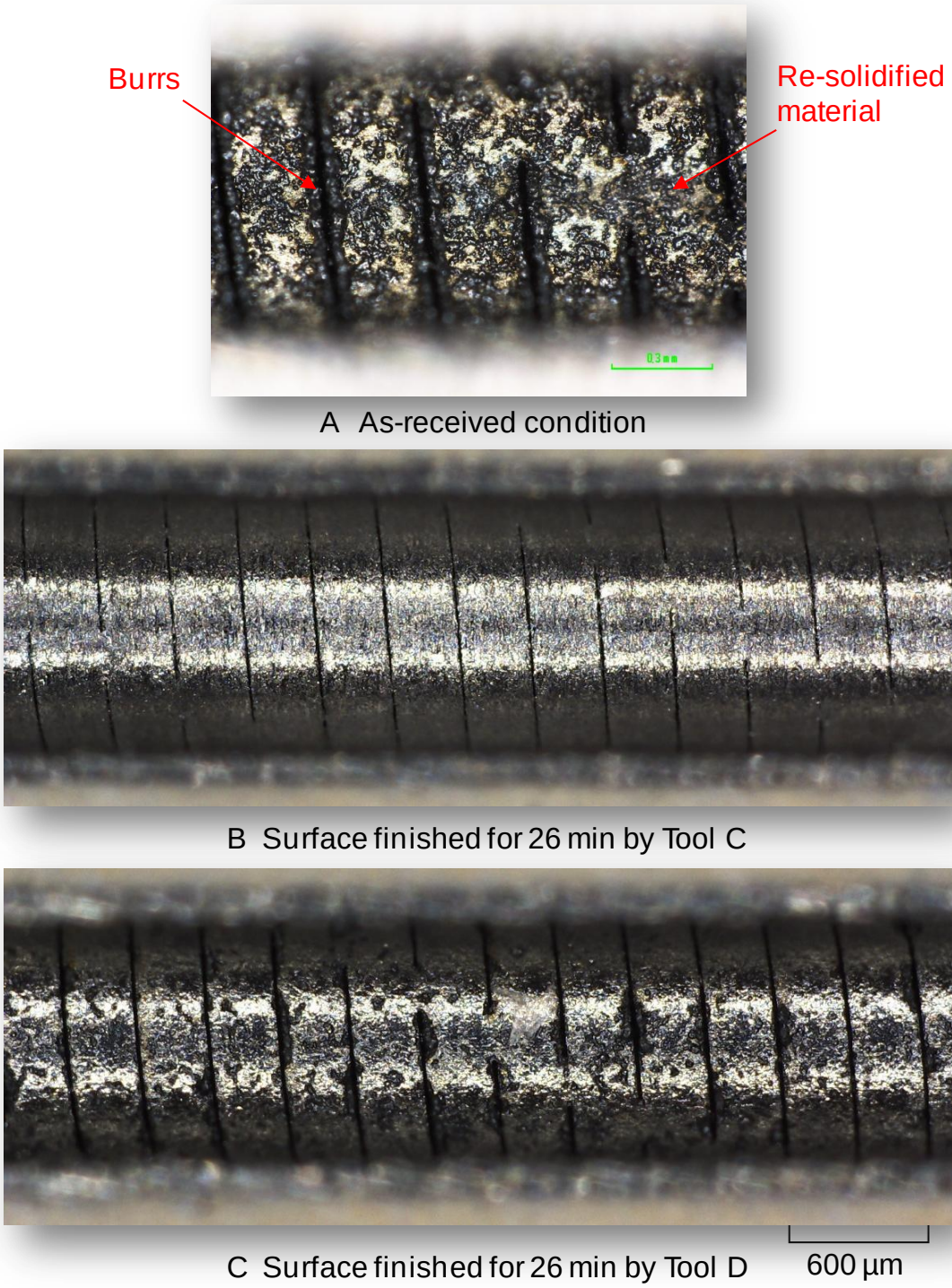

Figure 6-12. Microscopy of tube interiors: As-received condition and surface finished for 26 min by Tool C and Tool D

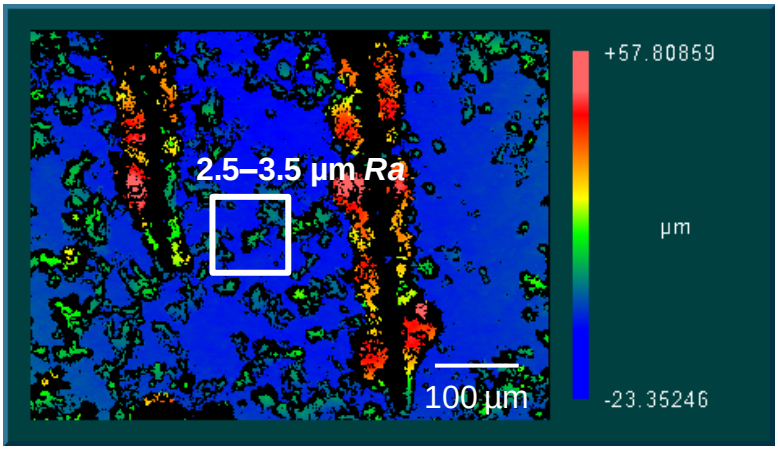

A As-received condition

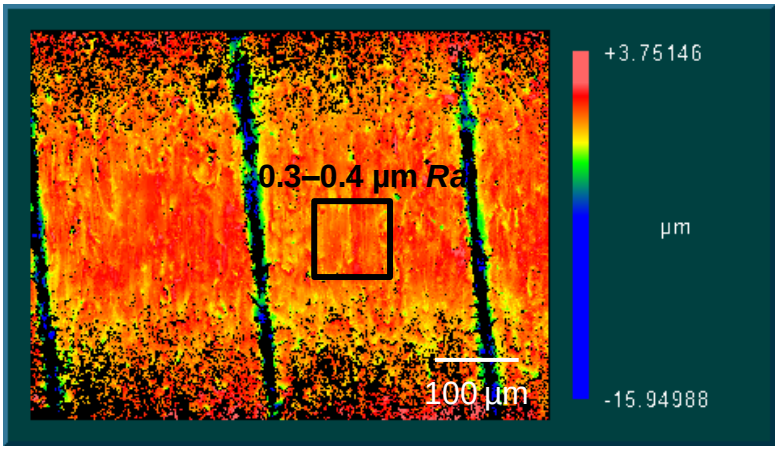

B Surface finished by Tool C

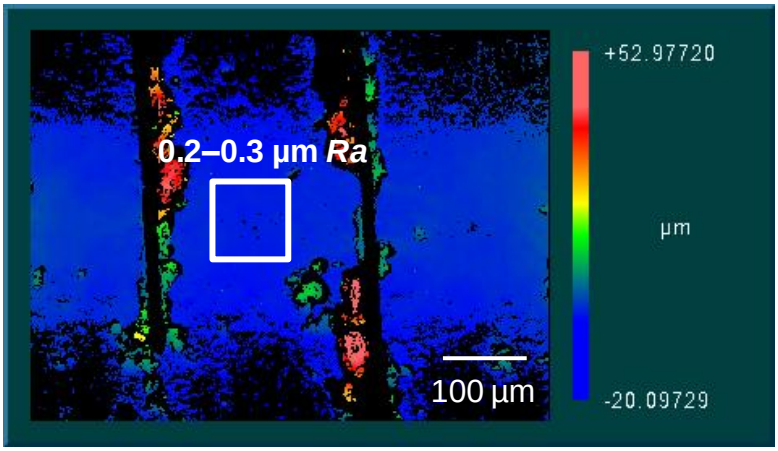

C Surface finished by Tool D

Figure 6-13. Spectrum plots of the tube interiors: As-received condition, surface finished by Tool C and Tool D

According to the previous experimental results (2.3 mg, 8 mm finished length) described in Section 3.3.3, 0.29 mg/mm of material removal was expected for 54.1 mm finished length. In the high-speed finishing system, the case of Tool C, it achieved 0.24 mg/mm, which is close to the desired removal rate. However, the case of Tool D showed only 0.15 mg/mm. This implies that Tool C is more appropriate for high material removal in a shorter time period while the Tool D is slower in material removal but producing smoother surface.

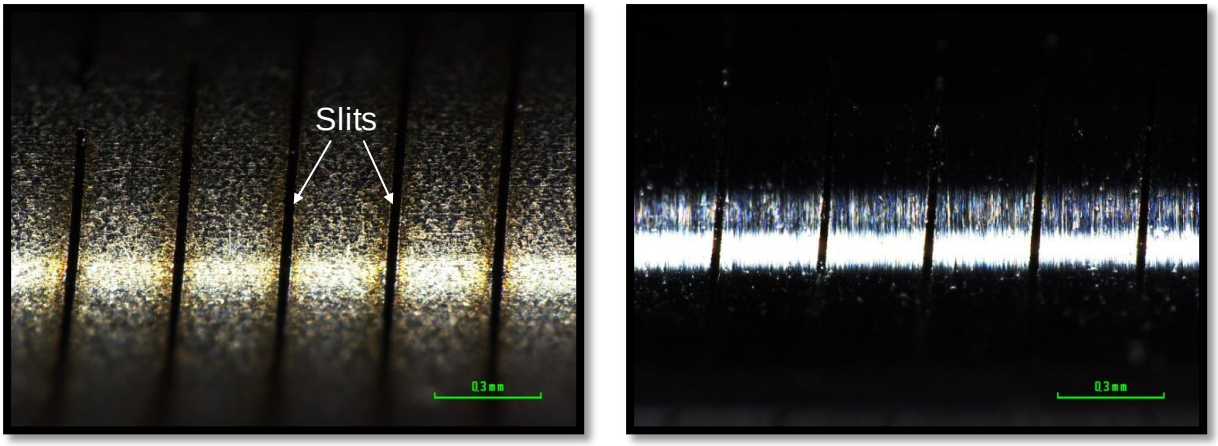

A As-received condition B Finished for 26 min

Figure 6-14. Microscopy of tube exteriors: As-received condition and surface finished for 26 min

Figures 6-14 shows the external view of flexible capillary tubes before and after finishing process for 26 min respectively. Even though the gaps between the slits were smaller (~12 µm) than the abrasive diameter, the abrasives were crushed and finished debris could be leaked out from slits under the effect of finishing pressure. The leaked particles come into contact with outer surface during finishing process and cause the material removal on the outer surface along the tube axis.

The Tool C has achieved internal finishing of flexible capillary tubes in timely manner but failed to internal finishing of straight capillary tubes. On the contrary to this,

Tool D has produced smoothly finished surface in straight capillary tubes but not internal finishing of flexible capillary tubes. The only difference between the tools is heat-treated regions (non-magnetic areas). This causes different tool behaviors, particle distribution, and magnetic forces acting on magnetic abrasive, and these factors affect on the finishing characteristics critically. Section 6.4.2 discusses the tool behavior and particle distribution.

6.4.2 Tool Behaviors and Particle Distribution

In order to observe the behaviors of each magnetic tool with ferrous particles, the tool and particles are introduced into the transparent glass tube (∅6.9×∅5.0×75 mm). In Figure 6-15(A), due to the uniform magnetic field on the pole tip, the particles are distributed along the pole-tip width, and the tool is strongly attracted against the inner surface. On the other hand, in Figure 6-15(B), the particles are mostly divided into four sections, which are magnetic regions of magnetic tool, and are attracted to these sections while barely distributing around the central area of each pole tip. Moreover, most particles are attracted on the surface stronger than the tool and pushed by the tool.

Using the smaller glass tube (∅2.75×∅2.11×90 mm), the tool and particle behaviors were introduced into the tube and observed during the tube rotation between 5000 and 10000 min^{-1}. In the case of Tool C (Figure 6-16(a)), the tool and particles were unstable even though the rotational speed was low (5000 min^{-1}). The tool was periodically vibrated along the tube axis and rotated itself while the pole set remains in same position. The tool rotation might be caused by friction force between the tool and inner surface during tube rotation. The tool is strongly attracted to the inner surface and the particles are attracted to the surface around the tool through the line of magnetic

field. However, in high-speed tube rotation (10000 min^{-1}), the tool lapsed into unstable condition (e.g. vibration and rotation), the particles circumvent the tool, and the majority resituate to the area behind the tool. During the process, the tool pushes a few of magnetic abrasives strongly and this makes deep scratches on the surface.

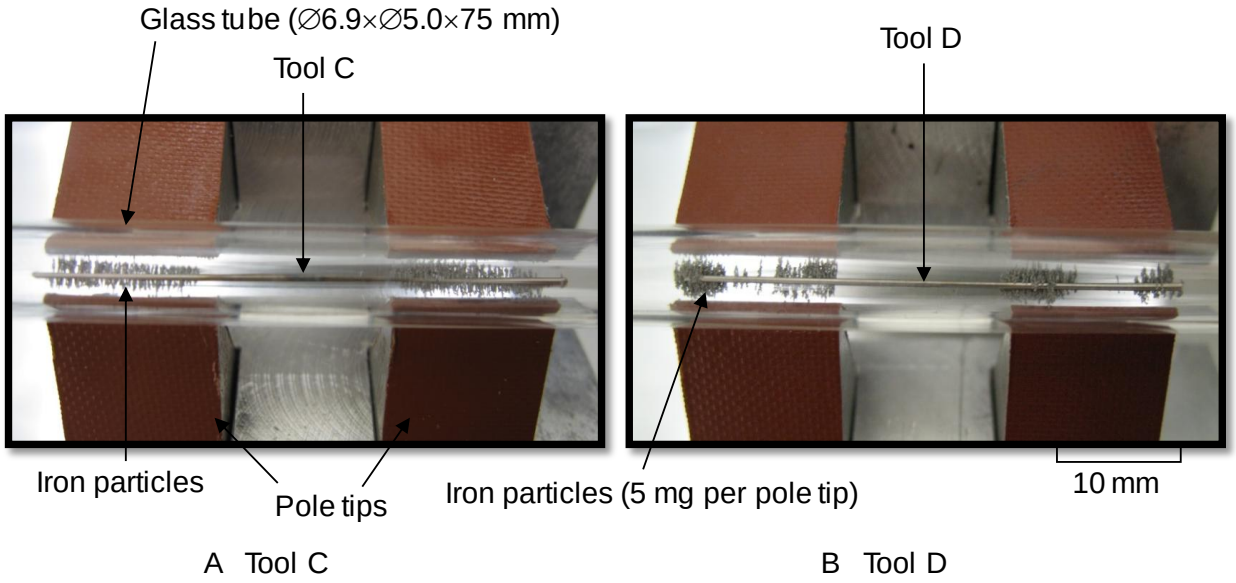

Figure 6-15. Powder distribution with differently heat-treated magnetic tools: Tool C and Tool D (Photograph courtesy of Junmo Kang)

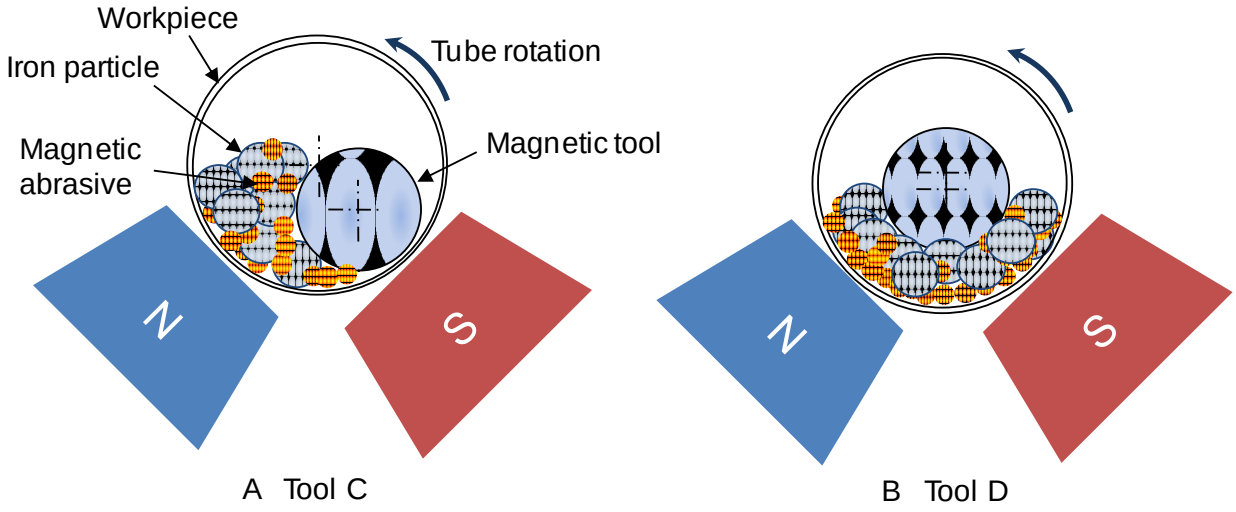

Figure 6-16. Schematics of the powder distribution with differently heat-treated magnetic tools: Tool C and Tool D

In the case of Tool D (Figure 6-16(B)), both tool and particles shows stable at the rotational speed of 5000 min^{-1}. The particles are attracted to the inner surface strongly and the tool pushes the particles in a stable motion neither vibration nor rotation. Moreover, even though the tube rotated at the speed of 10000 min^{-1}; both the tool and particles retain rigidly and smoothly follows the pole-tip motion.

6.4.3 Relationship between Finishing Force and Magnetic Tools

The heat treatment alters the magnetic properties of the 304 stainless steel tool, and the magnetic properties of the tool determine the abrasive behavior and distribution and tool behavior. To clarify the finishing mechanism of flexible capillary tubes using the heat-treated magnetic tools in a multiple pole-tip finishing system, the measurement of the magnetic force acting on the magnetic abrasive is indispensable.

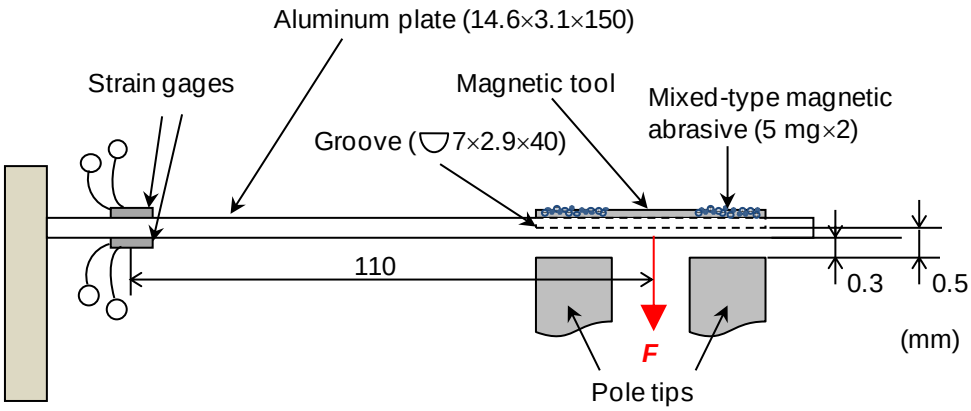

Figure 6-17. Schematics of magnetic force measurement system

The system for magnetic force measurement using strain gauges was designed (Figure 6-17) and implemented (Figure 6-18). Strain gages (gage factor: 2.09±1.0%, gage resistance (at 24°C, 50% RH): 119.8±0.2Ω) were attached in a half-bridge arrangement to the aluminum plate (14.6×3.1×150 mm), and the plate was located on a three-axis micrometer stage. In order to avoid physical contact between the bottom of plate and the top of pole tips, a clearance of 0.3 mm was selected. The heat-treated tool

with particles (mixed-type magnetic abrasive) was located in the groove on the plate to prevent dispersion of the particles. As shown in Figure 6-18, the particles were distributed with both Tool C and D. The magnetic force *F* acting on the tool with and without particles was measured by two strain gages, and each measurement was conducted three times.

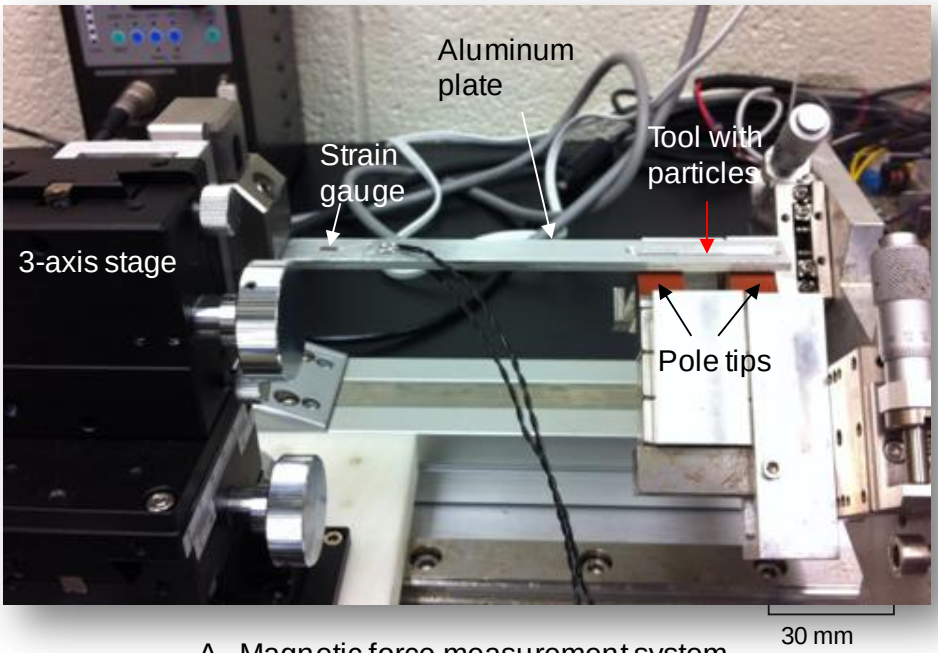

A Magnetic force measurement system

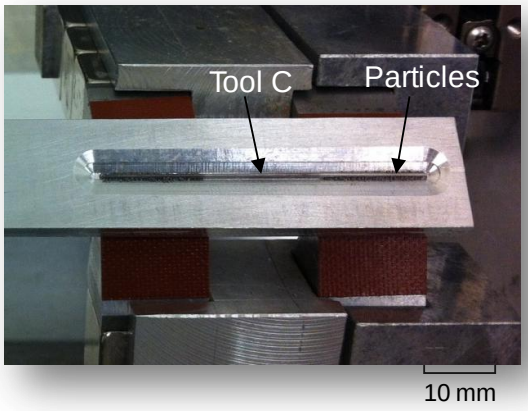

B Tool C with particles

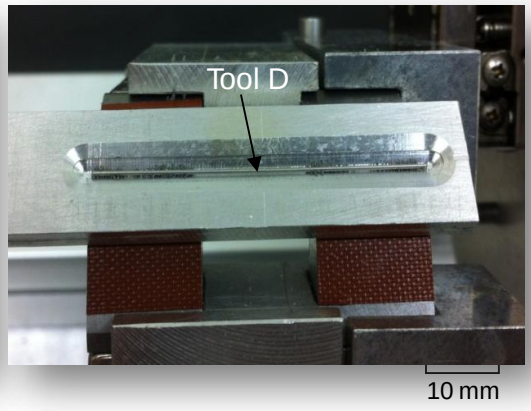

C Tool D with particles

Figure 6-18. Photograph of magnetic force measurement system for multiple pole-tip finishing machine, Tool C with particles, and Tool D with particles (Photograph courtesy of Junmo Kang)

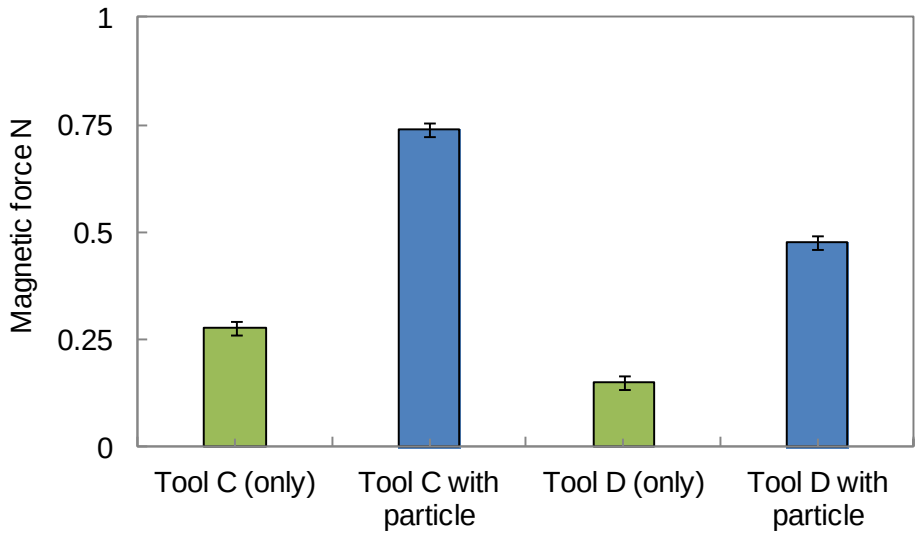

Figure 6-19. Relationship between magnetic force and ferrous tool

Figure 6-19 shows that the magnetic force acting on Tool C without particles is 1.8 times stronger than that of Tool D without particles. The magnetic area of Tool C is 1.8 times longer than the area in Tool D (Figure 6-10). Increasing the magnetic area increases its volume, resulting in greater magnetic force in Tool C than Tool D. Adding the particles (5 mg per pole tip, total: 10 mg, Figures 6-18(B) and (C)), the magnetic force acting on the tool and particles was increased by factors of 2.7 and 3.2, respectively, when compared with the cases of Tool C or Tool D only. In the case of Tool D, the particles were attracted by the smaller areas. This increased the particles per area, influenced the magnetic field intensity and its gradient, and increased the magnetic force in the case of Tool D more than the case of Tool C.

Figure 6-20 shows the relationship between finishing force per area (pressure) and magnetic tools. The contact area was determined by the visual observation as shown in Figure 6-16. The pressures of Tools C and D without particles were similar, but Tool D with particles showed higher pressure than Tool C with particles. This might be attributed to the differences in particle distribution. The stronger pressure led to the

stable motion of Tool D, delivered the particles deep into the straight capillary tubes, and achieved the surface finishing over the entire finished area. On the other hand, the lower pressure of Tool C caused instability of the tool behavior and difficulties in delivering the particles deep into the finishing area. As a result, Tool C could not finish the inner surface the tube.

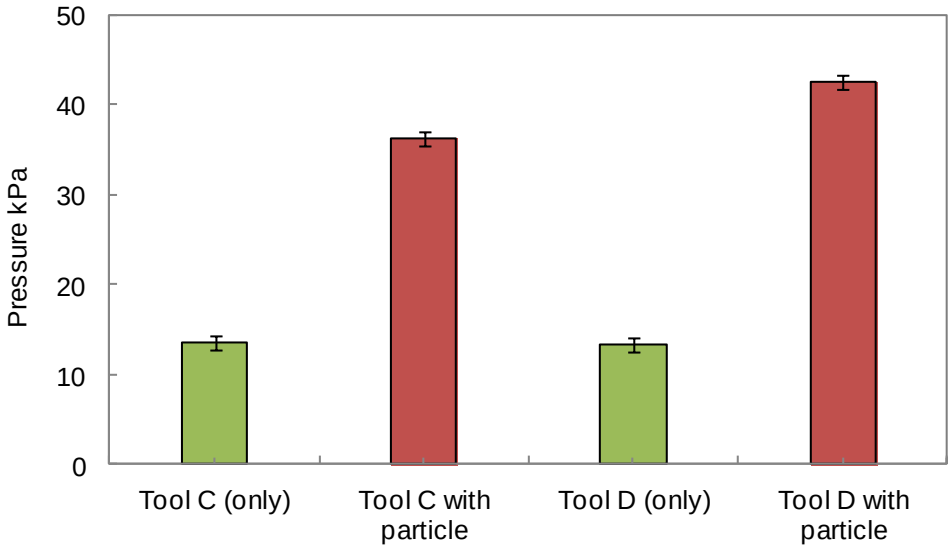

Figure 6-20. Relationship between finishing pressure and heat-treated tools

In the case of flexible capillary tube finishing, Tool D showed a lower material removal rate (0.29 mg/min) when compared to Tool C (0.50 mg/min). Moreover, Tool D partially left burrs on the edges while Tool C removed burrs and re-solidified material completely. The total material removal in 26 min was 7.54 mg and 13.03 mg, respectively, in the cases of Tools D and C. As mentioned above, Tool D had more particles per magnetic areas of the tool. This might have increased the probability of particles clogging inside the tube and retarded the relative motion between the particles in flexible capillary tubes for surface finishing and deburring due to the existence of

burrs. In contrast, Tool C successfully removed material, including burrs, and finished the surface despite the low pressure.

Some other parameters must have influenced the finishing performance in the case of Tool C, which needs to be clarified to understand the finishing mechanism. The straight capillary tubes used in the experiments were most likely magnetized during the cold-working production process. Section 6.4.4 will discuss the effects magnetic properties of the tubes on the finishing characteristics, and the finishing mechanism of Tool C will be clarified.

6.4.4 Effects of Tube Magnetism on Finishing Characteristics

Generally, internal finishing of nonmagnetic tubes by MAF is performed in magnetic fields with 0.2-1 T. If a magnetic tube is placed instead of nonmagnetic tube for internal finishing, magnetic fluxes tend to flow into magnetic tube in a magnetic field due to the higher permeability of magnetic objective when compared to air. The magnetic abrasive adheres to the inner surface of the tube and rotates with the tube when the tube rotates: No finishing action is performed. However, if the magnetic field intensity is increased to magnetically saturate the tube (magnetic flux density above 1 T), the magnetic flux leaks from the tube. If the magnetic field inside the magnetic tube becomes strong enough to hold the magnetic abrasive at the finishing area while the tube rotates, the inner surface of magnetic tube can be finished. A previous report showed that MAF enabled the internal finishing of 0.4 mm thick carbon steel tube [68]. The straight and flexible capillary tubes used in this study have thinner walls (0.105 mm and 0.26 mm, respectively).

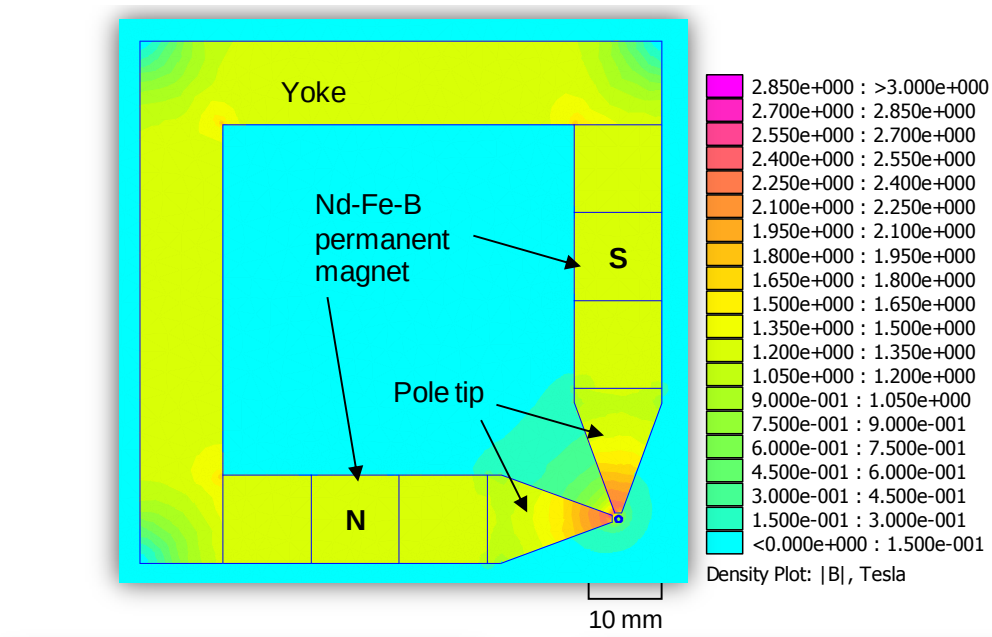

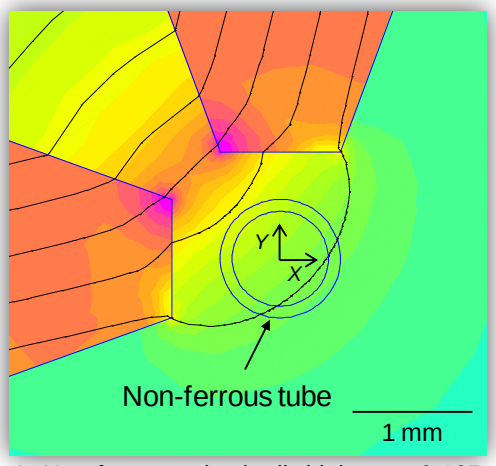

A Non-ferrous tube (wall thickness: 0.105 mm)

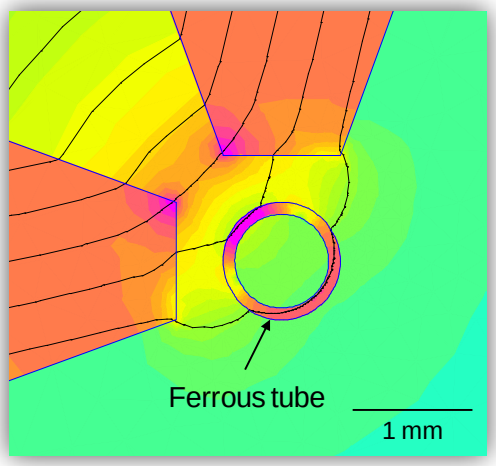

B Ferrous tube (wall thickness: 0.105 mm)

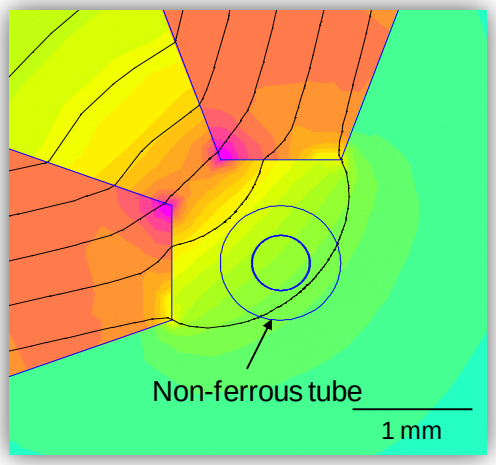

C Non-ferrous tube (wall thickness: 0.26 mm)

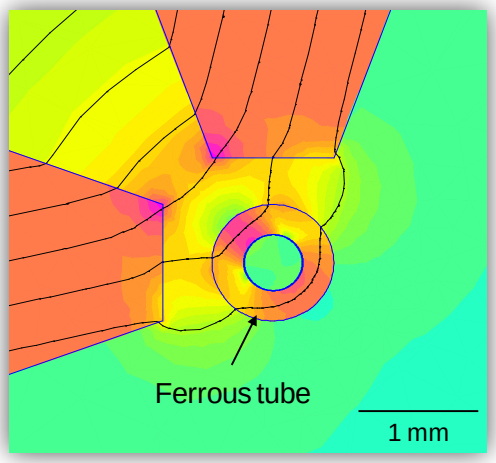

D Ferrous tube (wall thickness: 0.26 mm)

Figure 6-21. 2-D magnetic field analysis by FEM with non-ferrous and ferrous tubes

In order to estimate the magnetic flux density at the finishing area, a two-dimensional finite element method (FEM) was applied. The magnetic properties of 1018 carbon steel were used in place of those of a magnetized 304 stainless steel. Figure 6-21 shows the FEM result of magnetic flux density in nonmagnetic 304 stainless steel tube and magnetic 1018 carbon steel tubes of 0.105 and 0.26 mm tube wall thickness. The lines in each figure indicate the magnetic flux flow. In the case of nonmagnetic tube with 0.105 mm tube thickness (Figure 6-21(A)), the magnetic flux density at the finishing area is calculated to be 1.23 T. In the case of magnetic tube with 0.105 mm wall thickness (straight capillary tube, Figure 6-21(B)); the magnetic flux density is lower: 1.10 T. This means the tube is almost magnetically saturated, and some magnetic flux leak inside the tube. Assume a magnetic tool and particles are introduced into the magnetic tube. If the magnetic tool and particles have magnetic permeability high enough to generate magnetic force to overcome the friction between the particles and inner tube surface, finishing action is performed. If not, some particles adhere to the tube surface and rotate with the tube, resulting in unstable finishing. Accordingly, the condition with Tool D, which produced higher pressure, more successfully demonstrated tube finishing than the condition with Tool C.

In the case of flexible capillary tubes (Figure 6-21(C) and (D)), the lower magnetic flux density in the finishing area was calculated in the magnetic tube (0.61 T, Figure 6-21(D)). The thicker the tube wall, the weaker the magnetic field inside the tube (at the finishing area).

The flexible capillary tube was manufactured by a combination of cold working and laser machining processes. To create multiple slots, some sections of tube were melted

by the laser machining process. Under the condition above Curie temperature, the structures previously transformed from austenitic to martensitic by cold-working were transformed back to austenitic structures, and the tube partially lost its magnetism. The pressure of Tool C with particles was strong enough to remove the nonmagnetic burrs from the slot without clogging the tube and to finish the surfaces between the slots of the flexible tube. In order to confirm the differences in the tube magnetism between the straight and flexible capillary tubes, the following experiments were performed.

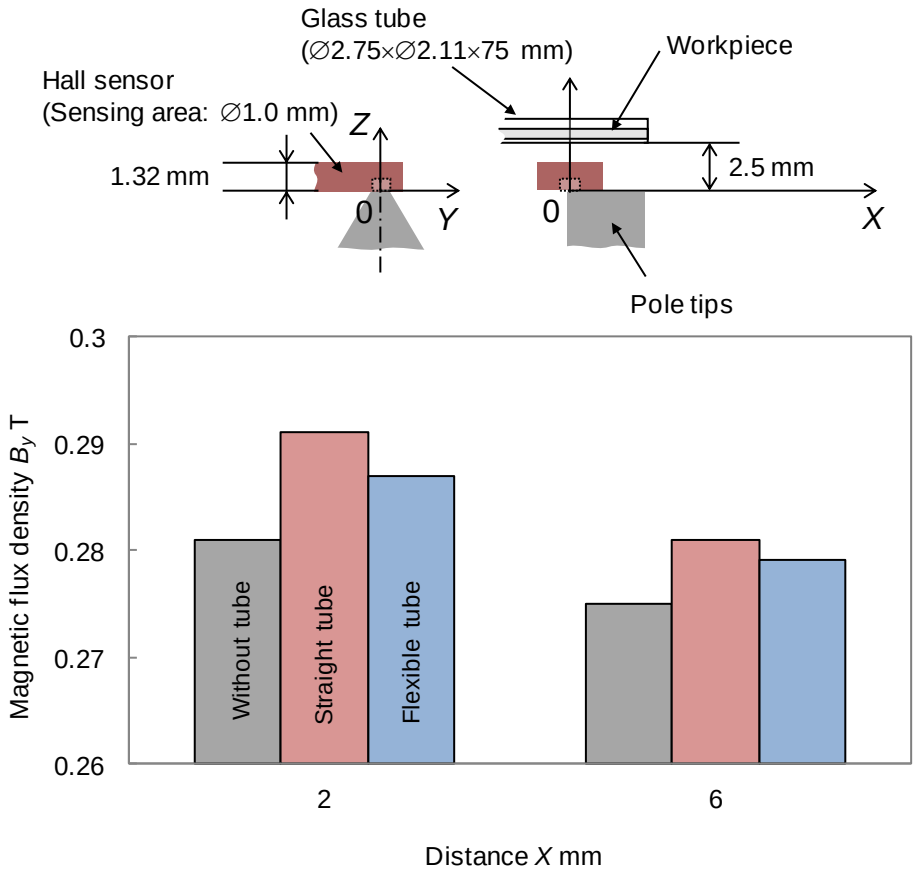

Figure 6-22. Relationship between magnetic flux density and both capillary tubes at distance *X*

It was hypothesized that the magnetic flux density between the tube and magnet could be higher if the tube showed higher magnetic permeability. Figure 6-22 shows the

schematic of magnetic flux measurement system and the changes of magnetic flux density with straight and flexible capillary tubes. To prevent bending, the tubes were put into a glass tube (∅2.75×∅2.11×90 mm) and the glass tube was chucked. The clearance between the glass tube and pole tip was set at 2.5 mm (*z*-axis). The hall sensor was located on the pole tip (underneath the glass tube), and the magnetic flux density was measured in each case: without the tube, and with straight and flexible capillary tubes at *X*=2 and 6 mm, corresponded to the areas close to the pole tip edge and center of pole tip respectively.

The strongest magnetic flux density was detected with the straight capillary tube at both locations. It implies that the straight capillary tube has higher magnetic permeability than the flexible capillary tube. The pressure of Tool C might have not been high enough to show the relative motion against the tube surface needed for finishing in the case of straight tubes but sufficient for the flexible tubes.

CHAPTER 7
DISCUSSIONS AND CONCLUSIONS

7.1 Fundamental Finishing Characteristics of Flexible Capillary Tubes

The application of magnetic abrasive finishing to the deburring of flexible capillary tubes with multiple laser-machined slits has been examined and the conditions to achieve the internal deburring based on the finishing experiments have been studied. The finishing experiments showed the feasibility of magnetic abrasive finishing for both surface and edge finishing of the flexible capillary tubes.

Hard, sharp cutting edges such as those of diamond abrasive are necessary for removing laser-machined burrs. Maintaining the presence of nonferrous diamond abrasive at the finishing area is a key factor to deburring the inside of the flexible capillary tubes. In order to keep the nonferrous abrasive at the finishing area, the ferrous particles must have microasperities on their surfaces. Additionally, the diamond abrasive should be larger than the slit width to avoid losing the abrasive cutting edges from the finishing area. The viscosity of the lubricant should be high enough to avoid leaking through the slits and to encourage the lubrication between the abrasive cutting edges and target surface but low enough to be introduced into the capillary tube.

The role of the large ferrous tools mixed with the magnetic abrasive is to enhance the finishing force by increasing the magnetic force acting on the magnetic abrasive inside the capillary tube and thereby achieving the desired finishing behavior. In particular, the iron particles are able to form chains that conform to the tube interior like a flexible brush. The flexibility of the chains facilitates surface fine finishing. The ferromagnetic rod (carbon steel rod) generates superior magnetic force because of its high susceptibility and large volume. This pushes magnetic abrasive rigidly against the

target surface, enhancing the material removal for deburring. The ferromagnetic rod with magnetic anisotropy (304 stainless steel rod) develops weaker magnetic force and pushes the magnetic abrasive with only one end. This causes unstable rod motion and reduces the finishing capability. The shape of the ferrous rod maintains the straightness of the flexible tube during internal finishing and its increased volume enhances the magnetic force acting on the magnetic abrasive.

The combination of the rod and iron particles in a hybrid method was considered, and it was successful in achieving fine finishing of both surface and edges. In the case of internal deburring of flexible capillary tubes with slits, the burrs are obstacles for the ferrous particles mixed with diamond abrasive when the particles follow the pole movement in the axial direction; this limited the increase of the axial feed rate. As a result, the processing speed can be rather low. In order to improve the processing rate, a new method is proposed to have multiple finishing locations in a single tube to finish multiple regions simultaneously.

7.2 A New Finishing Method: Multiple Pole-tip Finishing System

New finishing method called a multiple pole-tip finishing system has been designed. A condition required to realize the multiple-pole tip system is the use of a special metastable austenitic stainless steel tool with alternating magnetic and non-magnetic regions. This unique magnetic property facilitates simultaneous finishing of multiple sections with a short pole stroke.

The unique tool can be simply fabricated by the partial heat treatment of 304 stainless steel tool. The XRD analysis of the tool surface revealed that the untreated section has both bcc (due to pre-finishing process) and fcc structures while the heat-treated section has fcc structure only.

The length of the magnetic region of the tool must be such that the borders of the magnetic region of the tool correspond to the pole-tip edges. Generating a short magnetic region on the tool with edges corresponding to the pole-tip edges concentrates the magnetic flux at the pole-tip edges, which doubles the number of borders of the magnetic regions to attract the magnetic abrasive. The use of this method attracts the magnetic abrasive more strongly to the tool by magnetic force and improves the deliverability of the magnetic abrasive to desired areas deeper in the tube. This achieves the uniform surface finishing in the entire finishing area.

The insertion of a magnetic tool with magnetic abrasive facilitates the removal of material from the peaks of the surface asperities by the magnetic abrasive when lodged in between the tool and target surface. This results in a smoothly finished surface with less material removal than the use of iron particles only (used in the single pole-tip system). Moreover, a method was proposed to define the pole-tip feed length that sufficiently achieves a uniform desired surface roughness on the entire target surface by calculating pole-tip coverage time over the target surface.

7.3 Development of High-speed Internal Finishing Machine

In order to improve the processing rate, a high-speed finishing system has been developed for finishing capillary tubes, and finishing experiments have been performed with tube revolutions up to 30000 min^{-1}. The machine demonstrates its finishing performance successfully in comparison with the previous high-speed machine in Japan and existing low-speed machine. This machine improved the processing rate by a factor of 5.4 when compared to the low-speed finishing machine with single pole-tip system.

7.4 Internal Finishing of Capillary Tubes by High-speed Multiple Pole-tip System: Straight Capillaries

A multiple pole-tip system has been applied to the high-speed finishing machine for finishing capillary tubes, and finishing experiments have been performed with tube revolutions up to 30000 min^{-1}.

In the single pole-tip system, the magnetic abrasive is stable and performs efficient surface finishing up to 30000 min^{-1}. Conversely, the magnetic abrasive and tool lapse into unstable conditions in the multiple pole-tip system at high speed due to high centrifugal force. This causes deep scratches and irregular asperities on the finished surface. Moreover, lack of lubricant disturbs the relative motion of abrasives against the inner surface and makes the abrasives adhere on the surface due to heat generation. Increased machining rate in the system consumes more lubricant and requires fresh lubrication more frequently.

The high-speed multiple pole-tip system has been constructed and successfully achieves surface finishing up to a tube revolution of 10000 min^{-1}. It produces a smoothly finished surface (≈0.1 μm *Rz*) and is twelve times more efficient than the previous single pole-tip finishing system. The increase of the tube rotational speed facilitates the removal of material from the peaks of surface asperities. The material removal per tube rotation is decreased with increasing tube rotational speed.

7.5 Internal Finishing of Capillary Tubes by High-speed Multiple Pole-tip System: Flexible Capillaries

Based on the results from straight capillary tube finishing, the flexible capillary tubes have been applied for internal deburring process using each partially heat-treated magnetic tool, Tool C and D.

Although the Tool C has instability during the tube rotation, with stronger magnetic field, this condition assisted the tool and particles to follow the pole reciprocating motion and keep the abrasives at the finishing area. Stronger magnetic force of the Tool C and its powder distribution allow the successful internal surface and edge finishing of flexible capillary tube.

Conversely, even though the Tool D achieves successful internal finishing in straight capillary tubes, this tool retains the burrs and re-solidified material after finishing process in flexible capillary tubes because of weak magnetic field in the finishing area. The powder distribution in Tool D increases the chance for particles clogging and particle loss during the pole reciprocation motion due to its weaker magnetic force. This condition results in a slower processing rate when compared with Tool C.

Effects of tube magnetism have been studied with finite element method and magnetic flux density measurement. Thinner tube (straight capillary) is almost magnetically saturated and has stronger magnetic field in the finishing area. In the other hand, in the case of thicker tube (flexible capillary), the magnetic flux flows into the tube and has weaker magnetic field in the finishing area.

CHAPTER 8
REMAINING WORK

8.1 Development of Higher Numbered Pole-tip System

The development of a multiple pole-tip system using a partially heat-treated magnetic tool allows the finishing of multiple regions simultaneously in capillary tubes and improves the finishing efficiency. Although the increase of finishing efficiency in double pole-tip system has been achieved, more number of pole-tip in system will be required for longer capillary tubes (length of catheter shaft: up to 1 m). Increase of pole-tip set will enhance the finishing efficiency in capillary tube finishing and allows the longer tube finishing. The configuration of pole tip affects the intensity of magnetic field at the finishing area, therefore the effects of this geometry and arrangement on the magnetic field should be studied.

As the tube length is getting longer, it is difficult to introduce the abrasive deep into the capillary tube. To avoid that situation, a long tool embedded abrasives on the ferrous area needs to be fabricated. Even though the lubricant can be easily leaked through the slits during the workpiece rotation, increased tube rotational speed and the number of finishing spots will consume the injected lubricant more quickly, which entails the magnetic abrasive to have a higher tendency to adhere on the surface due to the heat generation from frictional forces. This occurrence critically affects the behavior of the magnetic tool and magnetic abrasives in high-speed multiple pole-tip finishing system. The method related to lubrication circulating system for capillary tube is required for further study.

8.2 Pole Rotation System for Flexible Capillary Tubes

Due to the long length of flexible capillary tubes (up to 1 m); it is difficult to rotate the tube at high speed because of the torsion acting on the tube even though multi-numbered pole-tips support the tube. A pole-rotation system might be alternated to solve this problem. In this case, the lubrication circulating system should be easily considerable when compared with workpiece rotation system.

8.2 Magnetic Field Analysis of Multiple Pole-tip System

Since the magnetic property is not clearly determined in plastically deformed 304 stainless steel, the magnetic field analysis has not been accomplished. This study should be a key to help clarify each characteristic of tool behavior in multiple pole-tip system.

LIST OF REFERENCES

1. S. Lin, P. A. Kew, K. Cornwell, 2001, Two-phase Heat Transfer to a Refrigerant in a 1 mm diameter Tube, International Journal of Refrigeration, Vol. 24:51-56.

2. R. Ankur, C. Animesh, E. Chhaya, K. Devesh, 2004, Development and Assessment of 316LVM Cardiovascular Stents, Material Science and Engineering:A, Vol. 386(1-2):331-343.

3. K. Nagayoshi, K. Tsuneo, 2012, Laser and Electrochemical Complex Machining of Micro-stent with On-machine Three-dimensional Measurement, Optics and Laser in Engineering, Vol. 30(3):354-358

4. E. A. Trillo, L. E. Murr, 1998, Effects of Carbon Content, Deformation, and Interfacial Energetic on Carbide Precipitation and Corrosion Sensitization in 304 Stainless Steel, Acta Materialia, Vol. 47(1):235-245.

5. N. B. Dahotre, S. P. Harimkar, 2008, Laser Fabrication and Machining of Materials, Springer, NY.

6. J. Meijer, K. Du, A. Gillner, D. Hoffmann, V. S. Kovalenko, T. Masuzawa, A. Ostendorf, R. Poprawe, W. Schulz, 2002, Laser Machining by Short and Ultrashort Pulses, State of the Art and New Opportunities in the Age of the Photons, CIRP Annals – Manufacturing Technology, Vol. 51(2):531-550.

7. K. Enda, G. Vlado, 2009, Catheter and Specialty Needle Alloy, Materials & Processes for Medical Devices Conference & Exposition, Minneapolis, August 10-12.

8. Y. P. Kathuria, 2005, Laser Microprocessing of Metallic Stents for Medical Therapy, Journal of Materials Processing Technology, Vol. 170(3):545-550.

9. Y. P. Kathuria, 1997, Laser Precision Processing in Microtechnology. Part1 Nd-YAG laser processing Proceedings of LANE 97, Germany, 272.

10. K. D. Avanish, Y. Vinod, 2008, Experimental Study of Nd:YAG Laser Beam Machining – An Overview, Journal of Materials Processing Technology, Vol. 195(1-3):15-26.

11. T. Whelan, S. Parmelee, 2009, Micro Abrasive Blasting Delivers 21st Century Stents, Medical Device Technologies, Vol. 20(5):30-1.

12. H. Zhao, J. V. Humbeeck, S. Jürgen, I. D. Scheerder, 2002, Electrochemical Polishing of 316L Stainless Steel Slotted Tube Coronary Stents, Journal of Materials Science, Materials in Medicine, Vol. 13(10):911-916.

13. J. Shih, 2008, Biomedical Manufacturing: A New Frontier of Manufacturing Research, Journal of Manufacturing Science and Engineering, Vol. 130(2):919-926.

14. H. Yamaguchi, J. Kang, 2010, Study of Internal Deburring of Capillary Tubes with Multiple Laser-machined Slits, Burrs-Analysis, Control and Removal, Part 7: 205-212.

15. E. S. Lee, 2000, Machining Characteristics of the Electropolishing of Stainless Steel (STS316L), Journal of Advanced Manufacturing Technology, Vol. 16(8):591-599.

16. Z. E. Geller, K. Albrecht, J. Dobranszky, 2008, Electropolishing of Coronary Stents, Material Science Forum, Vol. 589:367-372.

17. W. C. Elmore, 1939, Electrolytic Polishing, Journal of Applied Physics, Vol. 10(10):724-727.

18. L. K. Gillespie, 2006, Mass Finishing Handbook, Industrial Press, Inc., New York.

19. J. P. Caire, E. B. Chainet, N. P. Valenti, 1993, Study of A New Stainless Steel Electropolishing Process, Proceedings of the 80th AESF Annual Technical Conference in USA, 149-156.

20. S. Mohan, D. Kanagraraj, R. Sindhuja, S. Vijayalakshmi, N. G. Renganathan, 2001, Electropolishing of Stainless Steel: A Review, Transactions of the Institute of Metal Finishing, Vol. 79(4):140-142.

20 K. M. D. Silva, H. S. J. Altena, J. A. McGeough, 2003, Influence of Electrolyte Concentration on Copying Accuracy of Precision-ECM, CIRP Annals – Manufacturing Technology, Vol. 52(1):65-168.

21 H. Z. Choi, S. W. Lee, Y. J. Choi, G. H. Kim, 2004, Micro Deburring Technology using Ultrasonic Vibration with Abrasive, Proceedings of the 7th International Conference on Deburring and Surface Finishing, 231-238.

22 H. Z. Choi, S. W. Lee, Y. J. Choi, S. L. Ko, 2003, Micro Deburring Technology using Ultrasonic Cavitation, Proceedings of International Conference on Leading Edge Manufacturing In 21st Century: LEM21, 1013-1018.

23 Thermal Deburring Apparatus and Method, US Patent 4561839.

24 T. K. Brockbank, 2004, Thermal Energy Deburring, Proceedings of the 7th International Conference on Deburring and Surface Finishing, 225-230.

25 D. P. DeLo, J. M. Greenslet, G. Munko, 2007, Improved Microhole Precision and Performance by MicroFlow Abrasive Flow Machining, Proceedings of the 15th International Symposium on Electromachining, 399-403.

26 S. Sehijpal, H. S. Shan, 2002, Development of Magnetic Abrasive Flow Machining Process, International Journal of Machine Tools and Manufacture, Vol. 42(8):953-959.

27 J. D. Kim, Y. H. Kang, Y. H. Bae, S. W. Lee, 1997, Development of A Magnetic Abrasive Jet Machining System for Precision Internal Polishing of Circular Tubes, Journal of Materials Processing Technology, Vol. 71(3):384-393.

28 S. H. Lee, D. A. Dornfeld, 2001, Precision Laser Deburring, ASME Journal of Manufacturing Science and Engineering, Vol. 123:601-608.

29 O. Sugiura, N. Imahashi, M. Mizuguchi, 1997, Development of A Cylindrical Type Magnetic Barrel Finishing Machine, Journal of the Japan Society for Precision Engineering, Vol. 63(3):399-403.

30 S.L. Ko, Y.M. Baron, J.I. Park, 2007, Micro Deburring for Precision Parts using Magnetic Abrasive Finishing Method, Journal of Materials Processing Technology, Vol. 187-188:19-25.

31 T. Shinmura, 1990, Study on Magnetic Abrasive Finishing, CIRP Annals – Manufacturing Technology, Vol. 39(1): 325-328.

32 S. Yin, T. Shinmura, 2004, Vertical Vibration-assisted Magnetic Abrasive Finishing and Deburring for Magnesium Alloy, International Journal of Machine Tools & Manufacture, Vol. 44(12-13):1297-1303.

33 H. Yamaguchi, J. Kang, 2010, Study of Ferrous Tools in Internal Surface and Edge Finishing of Flexible Capillary Tubes by Magnetic Abrasive Finishing, Transactions of NAMRI/SME, Vol. 38:177-184.

34 H. Yamaguchi, T. Shinmura, R. Ikeda, 2007, Study of Internal Finishing of Austenitic Stainless Steel Capillary Tubes by Magnetic Abrasive Finishing. ASME Journal of Manufacturing Science and Engineering. Vol. 129(5):885–892.

35 J. Kang, H. Yamaguchi, 2010, Internal Finishing of Capillary Tubes by Magnetic Abrasive Finishing using a Metastable Austenitic Stainless Steel Tool. Proceedings of the Twenty-fourth Annual ASPE Meeting, 1-4.

36 J. Svoboda, 2004, Magnetic Techniques for the Treatment of Materials, Kluwer Academic.

37 H. Yamaguchi, J. Kang, F. Hashimoto, 2011, Metastable Austenitic Stainless Steel Tool for Magnetic Abrasive Finishing. CIRP Annals-Manufacturing Technology, Vol. 60(1):339-342.

38 J. Kang, H. Yamaguchi, 2012, Internal Finishing of Capillary Tubes by Magnetic Abrasive Finishing using a Multiple Pole-tip System, Precision Engineering, Vol. 36(3):510-516.

39 F. W. Preston, 1927, The Theory and Design of Plate Glass Polishing Machines, Journal of the Society of Glass Technology, Vol. 11, 214–256.

40 Y. M. Baron, 1975, Technology of Abrasive Finishing in Magnetic Field, Mashinostroenie, Leningrad.

41 H. Yamaguchi, T. Shinmura, T. Kaneko, 1996, Development of A New Internal Finishing Process Applying Magnetic Abrasive Finishing by Use of Pole Rotation System, International Journal of the Japan. Society for Precision Engineering, Vol. 30(4):317–322.

42 T. Shinmura, Y. Hamano, H. Yamaguchi, 1998, A New Precision Deburring Process for Inside Tubes by the Application of Magnetic Abrasive Machining, 1st Report, On the Process Principle and a Few Deburring Characteristics (in Japanese), Transaction of the Japan Society of Mechanical Engineers., Vol. 64(620), Series C, 1428–1434.

43 S. L. Ko, Y. M. Baron, J. W. Chae, V. S. Polishuk, 2003, Development of Deburring Technology for Drilling Burrs Using Magnetic Abrasive Finishing Method. Proceedings of International Conference on Leading Edge Manufacturing in 21st Century, Japan Society of Mechanical Engineers, 367-372.

44 K. Suzuki, H. Takahashi, H. Ohashi, T. Yonemura, E. Miyasaki, T. Uematsu, 1990, The Research on Magnetic Grinding Method using Short Fiber Magnetic Abrasives –1st Report, The Effect of the Metal Short Fiber Contamination to Magnetic Abrasives. Proceedings of the JSPE Spring Annual Meeting, 307-308 [in Japanese].

45 T. Sato, H. Yamaguchi, T. Shinmura, T. Okazaki, 2006, Study of Surface Finishing Process using Magneto-rheological Fluid (MRF) –2nd report: Effects of the Finishing Behavior of MRF-based Slurry on Finishing Characteristics–. Journal of Japan Society for Precision Engineering, Vol. 72(11):1402-1406 [in Japanese].

46 T. Mori, K. Hikota, Y. Kawashima, 2003, Clarification of Magnetic Abrasive Finishing Mechanism, Journal of Material Processing Technology. Vol. 143-144(20):682-686.

47 H. Yamaguchi, T. Shinmura, M. Takenaga, 2003, Development of a New Precision Internal Machining Process Using an Alternating Magnetic Field, Precision Engineering, Vol. 27(1): 51-58.

48 H. Yamaguchi, T. Shinmura, M. Sekine, 2005, Uniform Internal Finishing of SUS304 Stainless Steel Bent Tube Using a Magnetic Abrasive Finishing Process, ASME Journal of Manufacturing Science and Engineering, Vol. 127(3):605-611.

49 H. Yamaguchi, T. Shinmura, 1995, Study on a New Internal Finishing Process by the Application of Magnetic Abrasive Machining –4th Report, Effects of Diameter of Magnetic Abrasives on Finishing Characteristics–. Transactions of the Japan Society of Mechanical Engineers Series C, Vol. 61(591):4470-4475 [in Japanese].

50 H. Yamaguchi, K. Hanada, 2008, Development of Spherical Magnetic Abrasive Made by plasma Spray, ASME Journal of Manufacturing Science and Engineering, Vol. 130(3):999-1008.

51 T. Shinmura, H. Yamaguchi, 1995, Study on a New Internal Finishing Process by the Application of Magnetic Abrasive Machining –Internal Finishing of Stainless Steel Tube and Clean Gas Bomb, International Journal of Japan Society of Mechanical Engineering Series C, Vol. 38(4):798-804.

52 T. Shinmura, H. Yamaguchi, T. Aizawa, 1993, A New Internal Finishing Process of Non-ferromagnetic Tubing by the Application of a Magnetic Field –The Development of a Unit Type Finishing Apparatus using Permanent Magnets, International Journal of Japan Society for Precision Engineering, Vol. 27(2):132-137.

53 Y. H. Zou, T. Shinmura, 2009, A New Internal Magnetic Field Assisted Machining Process using a Magnetic Machining Jig –Machining Characteristics of Inside Finishing of a SUS304 Stainless Steel Tube, Advanced Material Research, Vol. 69-70:143–147.

54 H. Kawakubo, K. Tsuchiya, T. Shinmura, 2003, Consideration on Mechanism of Polishing Force in Magnetic Polishing Method using Loose Abrasive, Journal of Japan Society for Abrasive Technologies, Vol. 47(12):672-676 [in Japanese].

55 H. Nishida, K. Shimada, Y. Ido, 2008, Fluid Dynamic Investigation of Polishing the Inner Wall of a Tube Utilizing a Magnetic Compound Fluid (MCF), Proceedings of the 7th JFPS International Symposium on Fluid Power, TOYAMA, 837-840.

56 W. Kordonski, D. Golini, 2002, Multiple Application of Magnetorheological Effect in High Precision Finishing, Journal of Intelligent Material Systems and Structures, Vol. 13:401-404.

57 H. Yamaguchi, T. Shinmura, S. Watanabe, 2001, Study of a Magnetic Field Assisted Internal Finishing Process using Abrasive Slurry Circulation System – Effects of Geometrical and Magnetic Properties of Magnetic Particles on the Finishing Characteristics–, Journal of the Japan Society for Precision Engineering, Vol. 67(3):444-449[in Japanese].

58 H. Yamaguchi, T. Shinmura, N. Horiuchi, 2001, Study of Magnetic Tool Behavior and Its Relationship to the Processing Characteristics in a Magnetic Field Assisted Barrel Finishing Process, Transactions of NAMRI/SME, Vol. 29:197-204.

59 K. Mumtaz, S. Takahashi, J. Echigoya, Y. Kamada, L. F. Zhang, H. Kikuchi, K. Ara, M. Sato, 2004, Magnetic Measurements of Martensitic Transformation in Austenitic Stainless Steel after Room Temperature Rolling, Journal of Materials Science, Vol. 39:85-97.

60 S. Takahashi, J. Echigoya, T. Ueda, X. Li, H. Hatafuku, 2001, Martensitic transformation due to plastic deformation and magnetic properties in SUS 304 stainless steel, Journal of Materials Processing Technology, Vol. 108:213-216.

61 P. L. Mangonon, G. Thomas, 1970, The martensite phases in 304 stainless steel, Metallurgical and Materials Transactions B, Vol. 1(6):1577-1586.

62 J. Childress, S. H. Liou, C. L. Chien, 1988, Magnetic Properties of Metastable 304 Stainless Steel with BCC Structure. Journal de Physique Colloques, Vol. 49(C8):113–114.

63 S.S.M. Tavares, D. Fruchart, S. Miraglia, 2000, A magnetic study of the reversion of martensite α′ in a 304 stainless steel, Journal of Alloys and Compounds Vol. 307:311-317.

64 K&J Magnetics. Inc. catalog. http://www.kjmagnetics.com/proddetail.asp?prod=B888, November 18, 2012(Accessed date), Tel.1-215-766-8055

65 H. Yamaguchi, T. Shinmura, 1994, Study on a New Internal Finishing Process by the Application of Magnetic Abrasive Machining (2nd Report, Effects of Magnetic Field Distribution on Magnetic Force Acting on Magnetic Abrasives), Transactions of the Japan Society of Mechanical Engineers Series C, Vol. 60(578):3539-3545. [in Japanese]

66 T. Sato, H. Yamaguchi, T. Shinmura, T. Okazaki, 2009, Study of Internal Finishing Process for Capillary using Magneto-rheological Fluid, Journal of Japan Society of Precision Engineering, Vol. 75(5): 612-616. [in Japanese]

67 J. Kang, A. George, H. Yamaguchi, 2012, High-speed Internal Finishing of Capillary Tubes by Magnetic Abrasive Finishing, Proceeding of CIRP, Vol. 1: 414-418.

68 H. Yamaguchi, T. Shinmura, 1995, Magnetic Abrasive Finishing of Inner Surface of Tubes, Proceedings of International Symposium for Eletromachining, 963-976.

BIOGRAPHICAL SKETCH

Junmo was born in Guri-si, Gyeonggi-do, South Korea in 1980. He obtained a B.S. degree in mechanical engineering from the Sungkyunkwan University (SKKU) in South Korea in 2006. He served in the military service (Korean Army) for 26 months from 2000 to 2003 as a field service technician. At SKKU, he received a scholarship and a few prizes for designing the new concept tiller. After graduation, he came to United States for his Ph.D. study and joined Dr. Hitomi Greenslet's group in the Department of Mechanical and Aerospace Engineering at the University of Florida (UF) in 2008. He received an Academic Achievement Award from UF in 2007. During his Ph.D. studies, he was sponsored by the UF Research Foundation (Gatorade) to fabricate the finishing machine, and received an E. Wayne Kay Graduate Scholarship from the Society of Manufacturing Engineers (SME) Education Foundation. He wishes to continue his career as a researcher.